EVALUATION OF A MECHANICAL FOAM MITIGATION DEVICE

BY

GILBERT TURNER IV

THESIS

Submitted in partial fulfillment of the requirements
for the degree of Master of Science in Technical Systems Management
in the Graduate College of the
University of Illinois at Urbana-Champaign, 2013

Advisor:

Professor Richard S. Gates

ABSTRACT

Foam production in deep-pit swine manure storages has become a significant problem for the swine industry in recent years. Foaming creates management and safety issues for swine producers, including increased risk of flash fires or explosions and reduced manure storage capacity. Due to these concerns, a means of quickly and safely mitigating foam produced in these facilities was sought. The objective of this study was to assess the efficacy of a purpose-built mechanical foam mitigation device to destroy foam in foaming swine deep-pit manure storages and to evaluate the difference, if any, of continuous versus episodic device operation and device installation location. A swine production facility in central Illinois, with a history of extensive foam production, was selected to evaluate the mechanical foam mitigation device. The device was tested in three barns and various foam depths for both continuous and episodic operation. Results show that the device was capable of destroying foam at rates ranging from 3% to 6% of initial foam volume destroyed per hour. Although operating the device episodically produced superior results in terms of foam destruction rate in foam depths greater than 0.2 m when the device was installed in a pump-out port, the improvement did not offset the time the device was inactive. Therefore, it is recommended that the device be operated continuously. When installed in a pump-out port and operated continuously, the device was capable of mitigating foam over a radial distance of at least 21 m.

ACKNOWLEDGEMENTS

I would like to thank my advisor, Dr. Richard Gates, for allowing me to work on this project and for his patient guidance in pursuing this research and in crafting my thesis. I could not ask for a more patient, thoughtful, and insightful guide. Thanks are also due to Dr. Ted Funk for serving on my graduate committee and for his hands-on assistance in pursuing this project. I also wish to thank Dr. Joe Harper for serving on my graduate committee. Special thanks are due to Laura Pepple for her help in editing my thesis and for her guidance with the analysis of my data. Her insights and knowledge were indispensible and I cannot thank her enough for the time she spent working with me on this project. I would also like to thank Brad Eversole, Tom Fleshner, and GSI® for building the mechanical foam mitigation device. Without them and the support of GSI® this project would not have been possible. Finally, thanks are owed to Rachel, my wife, for the sacrifices she has made so I could pursue this research and for her unconditional support throughout this process. She selflessly attended to the details of life so I could focus on this project.

Table of Contents

Chapter 1: Introduction

1.1 Summary

The United States' pork industry consists of more than 65 million head of swine distributed among nearly 69,100 operations (USDA-NASS, 2012a, 2012b). Of these operations, 8,800 of them have more than 2,000 head and account for 87% of the pigs in the United States (USDA-NASS, 2012a). A typical pork operation of this scale in the United States grows swine in a confinement environment and must address such issues as building maintenance, animal management, environmental control, and manure management. Many confinement finishing operations are located in the Midwest and deep-pit manure storages are a common feature of that region.

For reasons not fully understood, deep-pit manure storages (DPMS) have recently experienced unpredictable foaming. Foaming can potentially lead to flash fires or explosions during pit agitation, reduce usable pit storage capacity, and negatively impact animal welfare if foam enters the animal living space. Furthermore, in recent years there has been an increase in the number of reported cases of pit foaming (Moody *et al*, 2009). For these reasons, a reliable means of safely mitigating foam is needed. Mechanical mitigation is one possible solution. Mechanical mitigation has the potential to be a simple, reliable solution, and its efficacy could be quickly evaluated.

An effective mechanical foam mitigation device (MFMD) must also be cost-competitive with other available foam control products. GVC Chemical (GVC Chemical Corporation, East Rockaway, NY) and ProfitPro (ProfitPro, LLC, Albert Lea, MN) both offer products intended to

reduce or prevent foaming. Elanco (Elanco, Greenfield, IN) markets Rumensin 90®, which the University of Minnesota Extension (UMN) has recommended as a foam control agent (Clanton *et al.*, 2012). As tested, the calculated operating cost per day for the MFMD was $0.96/day (Table 1.1). This cost assumes that the device operates for twelve out of every twenty-four hours. When the estimated purchase price is included, the total cost per day for the MFMD over 180 days is $20.41/day. Farm Digestant® (GVC Chemical Corporation, East Rockaway, NY) has an estimated operating cost per day over 180 days of $1.39 to $2.04, depending on application rate. Profit Pro products were estimated to have operating costs of $1.26 to $3.79/day over 180 days and total costs of $2.64 to $4.31 per day over the same time period. Rumensin 90® (Elanco, Greenfield, IN), used according to UMN guidelines, is estimated to have an operating cost of $1.92/day over 180 days and a total cost of $5.88/day over the same period. Estimated operating costs per day were calculated based upon manufacturers' or UMN recommended application rates and using retail prices current in January, 2013. Total costs per day were calculated upon manufacturers' or UMN recommended application rates and minimum purchase amounts. These estimates provide a sense of what producers are currently paying to control foam in swine DPMSs.

1.2 Description of Project

In 2011, Dr. Ted Funk and Ms. Laura Pepple, extension specialists at the University of Illinois, developed the idea of mitigating foam in swine DPMS's using a MFMD. In 2012, four prototype devices were constructed in collaboration with an agricultural equipment company for evaluation. This study details the initial evaluation of the purpose-built MFMD at a swine DPMS site. The questions that this study sought to address were:

- Is the purpose-built MFMD capable of mitigating foam in a swine DPMS?
- How effective is a MFMD at mitigating foam?
- Is there a difference in effectiveness when operating a MFMD continuously versus episodically?
- Does the installation location in the barn impact device performance?

To answer these questions, it was necessary to develop a method to accurately measure the initial foam volume in the manure storage, as well as measure the change in foam height over time as the MFMD operated. The change in foam volume over time and total foam volume destroyed were the primary metrics used to assess the effectiveness of the MFMD.

In addition to answering questions about a purpose-built MFMD's efficacy, this study seeks to establish an empirical framework for future testing of the MFMD and potentially for other foam mitigation technology applied to swine DPMS.

1.3 Tables

Table 1.1 – Cost comparison of various foam mitigation products. Costs were calculated based on treating a single deep-pit manure storage with dimensions of 60.9 m x 12.2 m x 3 m with initial treatment occurring when the pit was filled to a depth of 1.2 m. Costs were calculated using manufacturer recommended application rates. Mechanical foam mitigation device electrical usage was calculated using an electrical consumption rate of 0.943 Kw at a price of $0.085/kWh.

Product	Mechanical Foam Mitigation Device	GVC Chemical Farm Digestant			Profit Pro		Elanco Rumensin 90
		High (est.)	-	Low (est.)	Manure Master FoamAway	Manure Master Microbial + FoamAway	
Operating Cost per Day (90 days)	$0.96	$3.57	-	$2.45	$2.53	$5.44	$1.28
Operating Cost per Day (180 days)	$0.96	$2.04	-	$1.39	$1.26	$3.79	$1.92
Total Cost per Day (90 days)[1]	$39.85				$5.28	$8.61	$5.88
Total Cost per Day (180 days)[1]	$20.41				$2.64	$4.31	$2.94
Operating Cost per 90 Days	$86.57	$321.30	-	$220.54	$227.33	$489.41	$115.08
Operating Cost per 180 Days	$173.13	$367.11		$251.07	$227.33	$682.27	$345.24
Start Up Cost	$3,500.00[2]				$475.00[3]	$775.00[3]	$529.00[3]

[1] Total cost equals start up costs plus operating costs for the device and minimum purchase amounts for other products

[2] Estimated retail purchase price for a single device. Freight costs not included.

[3] Cost reflects minimum purchase amount. Freight costs not included.

Chapter 2: Literature Review

Foam production in swine DPMS is a significant problem facing today's swine industry. Foaming reduces usable pit storage capacity by entraining gases produced during anaerobic digestion and results in a high volume, low density slurry that creates a significant management problem for farmers (Robert *et al*., 2011). The foaming also creates a serious safety issue as one of the primary gases entrained within the foam is methane (Moody *et al*., 2009; Rehberger *et al*., 2010). Swine production facilities have exploded when large quantities of methane were released due to the rapid destruction of foam which then came into contact with an ignition source (Choiniere, 2004; Kinsey, 2009; Moody *et al*., 2009). This issue is of such concern that the National Pork Board listed it as an area for targeted research in its 2012 operating budget (National Pork Board, 2012). In light of these concerns, a means to safely mitigate foam build up in swine DPMS's is needed.

2.1 Theory of Foam Stability and Destruction

Before discussing mitigation strategies, it is instructive to have a basic understanding of the theory of foam formation and destruction. Put in the simplest terms, foam is defined as the dispersion of gas in a liquid in which the distance between bubbles is small and the proportion, by volume, of gas to liquid is large (>95% gas) (Vardar-Sukan, 1998; Varley *et al.*, 2004). Foams can be either metastable, with a bubble lifetime measured in hours or days, or transient, with a bubble lifetime of seconds to a few minutes (Pugh, 1996). For foaming to occur, surface active agents, gas movement through the liquid, and hydrophobic material must all be present in solution (Barber, 2005). A DPMS possesses these three prerequisites for foaming in that volatile fatty acids (VFAs), proteins, and other surface active compounds are present (Masse *et al*. 1997;

Rehberger *et al*., 2010); gas flow can be present in the form of methane produced as a result of anaerobic processes (Donham *et al*., 1982, Moody *et al,* 2009); and hydrophobic materials are present in the form of lipids (Rehberger *et al.*, 2010). For stable foam to develop, gas bubbles must remain separated by thin liquid walls called lamella and a specific geometry of lamella to lamella contact must be reached (Junker, 2007). In stable foam, three lamellae meet at a common edge and are equally inclined to each other at 120 degrees. At a point four edges meet and are inclined to each other 109 degrees (Figure 2.1) (Pelton, 2002). To destroy stable foam, the lamella must be destabilized either by chemical means, such as an antifoaming agent, or by mechanical stress that disrupts the stable geometry of the foam. From these definitions, foams produced in DPMS can be classified as metastable foams that require intervention to be reduced in a timely manner.

Natural processes that lead to foam deterioration occur through liquid drainage, bubble rupture, and bubble coalescence (Pelton, 2002). Drainage is the flow of liquid from foam that is induced by gravity and complex pressure gradients. Drainage leads to drying and destabilization of the foam matrix, resulting in collapse. Bubble rupture is the bursting of a bubble, resulting in a reduction in the volume of foam (Pelton, 2002). Bubble coalescence is the merging of two bubbles to form a single larger bubble and thus has no effect of the total volume of foam although it can change the foam stability. These processes are largely governed by the type or types of surfactants present and by the physical properties of films (Pugh, 1996; Vardar-Sukan, 1998). A mechanical foam mitigation device should maximize bubble rupture in order to reduce foam volume.

2.2 Mitigation Strategies

Foam mitigation strategies come in many forms and can be classified as biological, chemical or mechanical in approach (Moody *et al.*, 2009). Limited research is available on foam mitigation within swine DPMS. However, there are similarities between DPMS and anaerobic digesters in that both are anaerobic environments. This literature review will examine documented foam mitigation strategies that have been used in swine DPMS and anaerobic digesters, as well as other applicable industries.

2.2.1 Biological Mitigation

Biological mitigation involves introducing a non-foam forming, competitive species of microbe into the system to compete with the foam-causing species. It can also involve introducing one or more microbial species that metabolize the foam forming compounds produced by the offending microbes (Vardar-Sukan, 1998; Barber, 2005). Adjusting slurry operational parameters such as temperature, pH, or new material loading rate so that non-foam generating species have a competitive advantage over less desirable species of microbes is another possible solution (Barber, 2005).

Tsang *et. al*. (2008) illustrated the potential of adjusting operational parameters, such as the influx of microbial substrates, to control foam caused by filamentous microorganisms. In this study, the authors examined the growth requirements of *N. amarae*,[1] a filamentous microorganism responsible for foaming issues in activated sludge treatment, and compared its growth requirements to those of desirable, floc-forming microbes. Using this information, they then devised what they termed a "feast-fast operation program" to provide a competitive

[1] *N. amarae* has been reclassified as *G. amarae* (Klatte *et al.*, 1994)

disadvantage for *N. amarae* and thereby control foaming in an activated sludge treatment system. The feast-fast operation program exposed the microbial communities in the waste treatment system's aeration columns to alternating conditions of high substrate availability followed by prolonged, near-starvation conditions. Their results indicated that in the scope of an activated sludge treatment system, *N. amarae* and foaming caused by it could be controlled using this strategy while still achieving waste treatment targets (Tsang *et al*., 2008).

While the results of Tsang *et al* (2008) indicate that under certain circumstances foaming can be controlled through environmental manipulation, their results are not directly applicable to swine DPMS. In typical slatted floor DPMS, control of the influx of microbial substrates is not possible. Additionally, it has been demonstrated that *G. amarae* (formerly *N. amarae*) is an obligate aerobe that enters anaerobic digesters with the waste inflow from activated sludge treatment streams (Niekerk *et al*., 1987; Ganidi *et al*., 2009). Since swine DPMSs are primarily anaerobic systems, it is unlikely that *G. amarae* is the cause of foaming and management strategies that inhibit the growth of *G. amarae* would likely be ineffective in controlling foaming in DPMSs.

In 2012, University of Minnesota (UMN) Extension personnel conducted a preliminary study to investigate the effectiveness of an additive (monensin) as a foam control agent in DPMS (Clanton *et al*., 2012). Monensin, commonly marketed as Rumensin 90® (Elanco, Greenfield, IN), is a product that is commonly fed to beef cattle to alter the microbial population in the rumen to control foamy bloat. In the rumen, monensin causes an increase in the production of propionic acid leading to a decrease in the production of acetic acid. Acetic acid is a precursor for methane and this shift in VFA production helps reduce the incidence of foamy bloat by

ultimately reducing methane production in the rumen. Three sites of four barns each were chosen to ensure similarity of management, genetics, diet, and building age at each test location. At the outset of the study, all barns at all sites were experiencing foaming and foam depths ranged from 6 inches to 21 inches. At each site, randomly assigned treatments of 0 (control), 2.5, 5.0 or 10 lbs of Rumensin 90® per 100,000 gallons of pit slurry were assigned to each of the four barns. The results of this study indicated that the addition of monensin to foaming DPMS could reduce foam depth. After six weeks, all the pits that were treated with monensin experienced reductions in the amount of foam present and the barns treated with the two higher rates of 5 and 10 lbs of monensin per 100,000 gallons of manure experienced an average foam reduction of 99%. It should be noted that significant reductions in foam were also observed in the control pits of site 1 (100% reduction) and site 2 (71% reduction). The foam reduction observed in two of the control DPMSs begs the question "Was the foam reduction observed in the treated barns due to the treatment, or to some unknown factor?" Based on these results, the UMN Extension issued a recommendation of 5 lbs Rumensin 90® per 100,000 gallons of manure in a DPMS to control foaming (Clanton *et al*., 2012).

While monensin addition may hold some promise for foam control in DPMS, more research must be conducted to further quantify its effectiveness. Use of Rumensin 90® as a foam control agent in DPMSs is not an approved use of the product by the FDA (Elanco, 2013) and no research has been conducted on the environmental effects of monensin added directly to manure. Furthermore, care must be taken so that the pit is not overdosed because this can reduce biological activity in the pit to zero (Clanton *et al*., 2012) increasing solids build up. Clanton *et al*. (2012) also indicated that the addition of monensin may take up to 2 weeks to observe a reduction in foam, depending on the method of application.

The difficulty in using competitive microbial species as a control measure is illustrated in a study by Rahman *et al*. (2011). The efficacy of Digest3+3©, a microbial pit additive, was evaluated for its ability to reduce odor and pollutant gas emissions from a swine gestation-farrowing operation in North Dakota. The test site consisted of four barns; two with deep-pits and two with shallow pits. Digest3+3© was added per the manufacture's recommendations to one of the deep-pits and one of the shallow pits and air samples were collected from all four barns for eight months. It was found that the use of the microbial additive had no statistically significant effect on odor, ammonia, or hydrogen sulfide concentrations and emissions when comparing the treated barns to the control barns' emissions. No information was given on the cost of the product and no information was provided on the application method (Rahman *et al*., 2011). When used according to the manufacture's recommendations, this product failed to influence gas and odor emissions from the pits, indicating the organisms being introduced were not competing with the microbes researches hoped to control.

Recent research has indicated that differences exist between the microbial populations of foaming and non-foaming manure storages (Rehberger *et al.*, 2009; Rehberger *et al*., 2010; Pepple *et al*., 2012). However, it is not yet clear if these differences in microbial population are the cause of, or the result of manure foaming (Pepple *et al*., 2012). Assuming that swine DPMS foaming is caused by some microbial species, that species has yet to be identified. Without an identification of any (assumed) microbial culprit or culprits, selecting a competitive species is not possible. For the same reasons, adjusting operational parameters to control microbial growth is currently not a viable option. Treatment with monensin has been successfully tested on a limited scale, but further testing is needed to validate the findings of Clanton *et.al.*(2012) and to

assess its downstream effects. Monensin treatment is not appropriate for emergency treatment of acutely foaming pits as it is effective only after a significant amount of time.

2.2.2 Chemical Mitigation

Chemical mitigation works by changing the interfacial properties of the fluid, either preventing foam formation or causing foam collapse (Barber, 2005). Chemicals used for foam mitigation can be described as defoamers and antifoamers, depending on their use. Defoamers are added to foaming systems and act on the foam via surface action, leading to collapse. Defoamers compete for the surface layer, thereby displacing other foam-causing surface active agents (Junker, 2007). Antifoams, on the other hand, are added prior to the onset of foaming. Antifoams change the surface properties of the liquid so that foam formation is prevented (Pugh, 1996). Since the mechanism for foam formation and collapse is poorly understood, and according to one author, there does not appear to be a method for predicting an antifoam's performance based upon its chemical make-up (Junker, 2007), the correct antifoam and its rate of application is usually found via trial and error (Barber, 2005).

Vardar-Sukan (1988) found that natural oils exhibited some foam suppression ability, but that ability varied with foaming media type and the natural oil in question. Castor, corn, cotton-seed, linseed, olive, poppy seed, sesame, soybean, and sunflower oils were tested in four different foaming media (sterilized or unsterilized solutions of soybean flour and sterilized or unsterilized solutions of sugar beet cosette). The author sought to correlate foam-suppression ability with the physical and chemical properties of the natural oils; however, no clear correlation was evident. It was concluded that the effectiveness of natural oils as antifoaming agents varied with media type and that further study was required (Vardar-Sukan, 1988).

In a follow up study, Vardar-Sukan (1991) investigated the efficacy of natural oils in facilitating foam collapse in different foaming media. In this study, castor, corn, linseed, poppy seed, and soybean oil were tested for their ability to act as de-foaming agents in 4 different simulated foaming fermentation broths. The author found that all five natural oils accelerated foam collapse, but did so at different rates depending on the oil type, concentration, and simulated fermentation broth (Vardar-Sukan,1991).

Etoc *et al.* (2006) compared the efficacy and efficiency of three different types of commercially available antifoam agents. In this study, an organic antifoam agent, a silicone-based emulsion containing *in situ* treated silica, and a silicone/organic blend antifoam were evaluated for their ability to control foaming in fermentation media of *Yarrowia lipolytica*. The different antifoam agents were tested in fermentation media of varying age from 0 hours to 24 hours. It was found that as the fermentation broth increased in age, the stability of the foam generated in the media also increased. The authors suspected that this increase in foam stability was due to the increased presence of proteins on the surface of the broth. Furthermore, as foam stability increased, the ability of the different antifoam agents to control the media foam decreased, requiring more antifoam agent to achieve control. The authors were able to determine that in the limited scope of the study, the silicone/organic blend antifoam had the highest efficacy and efficiency across all ages of fermentation broth (Etoc *et al*., 2006).

Robert *et al* (2011) evaluated several commercially available chemical antifoaming agents for their ability to reduce or eliminate swine manure foams. Six products were selected and of those six, five were tested. The six products were (1) Specialty Silicone Antifoam (2977); (2) Non-Silicone Antifoam, Water-based (220D); (3) Crop Oil; (4) Silicone Antifoam, Oil-based (400); (5) 20% Silicone Antifoam, Water-based (20A); and (6) Specialty Silicone Antifoam,

Water-based (290). The only product not tested was (1), the Specialty Silicone Antifoam (2977) because it did not mix readily with water. Two different methodologies were used to test the foam mitigation chemicals based on each chemical's solubility in water. To test products 2-4 manure was collected from a foaming DPMS and 5 gallons each were placed in two 20 gallon aquariums. Air was then sparged through the aquariums using three sand air stones equally spaced in the bottoms of the aquariums. Once sufficient foam was produced, different dilutions of the products were sprayed on the foam and the amount of solution necessary to eliminate the foam was recorded. To test products (5) and (6) a different methodology was employed which was designed to test their ability to prevent foam formation. In this test, five 20 gallon aquariums were used and five gallons from the same large sample of foaming manure were placed in each aquarium. Three sand air stones were spaced equally in the bottom of each aquarium. Then 14 ml of either agent (5) or (6) were placed in aquariums one and two, 1 ml of either agent (5) or (6) were placed in aquariums three and four, and aquarium five was used as a control. Air was then sparged through each aquarium. It was found that product (4) was the most efficient at eliminating foam when atomized and sprayed directly on the surface of the foam and that products (5) and (6) were capable of preventing foam when used at a rate of 14 ml / 5 gallons of manure but not when used at the reduced rate of 1 ml / 5 gallons of manure. No lower limit of application for products (5) and (6) was determined. In addition to these findings, the cost of treating a typical swine grower finisher deep-pit with dimensions of 240 ft. by 40 ft. by 8 ft. deep was also calculated. It was found that product (4) was the most economical of the products tested with a total estimated cost of $4.04 per barn per treatment (Robert *et al*., 2011).

While the results of Robert *et al* (2011) are promising, validation of the findings on a large scale has not been done. Natural oils have not been scientifically evaluated as anti-foaming

or defoaming agents in swine DPMSs. Furthermore, no research has been done on the fate of antifoaming agents and defoaming agents in swine manure storages or on these agents as potential pollutants when swine slurry is applied to crop land. These questions should be answered before chemical foam mitigation strategies can be employed on a commercial basis.

2.2.3 Mechanical mitigation

Mechanical mitigation involves using physical means to break the foam bubble lamellae through shear stress. Revolving discs, impellers, stirrers, centrifuges, and ultrasound have all been developed to accomplish this in various types of foam generating systems where controlling foam level is important (Vardar-Sukan, 1998; Barber, 2005). In the ensuing discussion, it is convenient to consider foaming systems physically as closed systems, where foam growth is confined by a container and the container wall may play a role in the mitigation process, or as open systems, where foam growth is unconfined and the container wall does not play a role in mitigation. A fermentation bubble column is an example of a closed system, and a swine DPMS is emblematic of an open system. Revolving discs and centrifuges utilize centripetal force to generate cast off droplets which impact and destroy foam on the walls of a closed system. Impellers rely on direct impact of a rotating blade or paddle with foam bubbles to facilitate bubble rupture and can also generate cast off droplets that produce secondary impacts with foam in a closed system. If situated below the liquid surface, impellers may act as stirrers. Stirrers create a vortex that draws foam bubbles back into solution and can be used in conjunction with impellers. Finally, ultrasonic techniques differ from other mechanical mitigation methods. Ultrasonic probes act by accelerating foam drainage resulting in increased rates of bubble rupture rather than directly stressing foam bubble lamellae.

Ultrasonic techniques have been used to mitigate foams since the 1950's; however, these methods are best suited to low viscosity foams such as foams encountered in dairy effluent (Barber, 2005). Ultrasonic techniques rely on cavitation effects caused by the ultrasonic pressure waves to achieve accelerated liquid drainage that results in foam collapse (Morey *et al*., 1999; Patist & Bates, 2008). The crucial factors governing the efficacy of ultrasound as a foam mitigation strategy are power, frequency, and amplitude of the generated pressure waves. The shape of the ultrasonic probe tip and the distance of the probe from the foam surface also play a role in the efficacy of ultrasound as a foam mitigation technique (Sandor & Stein, 1993; Morey *et al*., 1999; Barber, 2005; Patist & Bates, 2008). Increasing the local atmospheric pressure can increase the efficiency of ultrasonic foam destruction, and it was also found that for a given foam there is an optimal temperature at which ultrasonic foam destruction can be achieved (Patist & Bates, 2008).

A different approach to mechanical foam mitigation is a rotating paddle design. This type of foam mitigation device destroys foam primarily through shear stresses induced in the foam lamellae by the spinning motion of the device. In addition to shear stresses, suction and centrifugal forces can also play a significant role in foam destruction. Mechanical foam breakers are often used when other methods of foam control, such as chemical antifoam and defoaming agents, are prohibited by the nature of the process or by regulatory restrictions (Deshpande *et al*., 2000).

Deshpande *et. al.* (2000) compared two novel mechanical foam breakers. The tests were carried out in a glass bubble column which was filled with a foam generating liquid. Humidified air was sparged through the solution to generate foam and the various mechanical mitigation devices were installed 3 cm above the liquid surface. The rotational speed of each device was

varied to determine the lower critical limit at which the rate of foam generation equaled the rate of foam destruction. The two new foam breakers were designed to maximize the shear forces applied to the foams with the hope of designing a more efficient paddle that would operate at lower speeds and reduce power requirements in industrial bubble columns and stirred tank reactors. The first paddle design featured a two bladed paddle with three slits machined into it and the second was a two bladed paddle with 168 needles affixed to it. Results showed that the two unique designs were able to control foam formation at rotational speeds that were 100 to 150 rpm slower than conventional designs (Deshpande *et al*., 2000).

In a different study of mechanical foam breakers, Yamagiwa et. al. (2000) examined the effect of bubble column design on mechanical foam breaker efficiency. They utilized a conventionally designed bubble column and four alternative column designs. The column modifications tested included separating destroyed foam from ascending foam, reducing the velocity of the ascending foam while increasing its residence time to facilitate liquid drainage, and a combination of these two methods. Columns were filled with solution and gas was sparged through them to generate foam. Foam was controlled using a spinning disc foam mitigation device (SDFMD). To control foam, the SDFMD spins rapidly as liquid is pumped over it creating cast off droplets via centrifugal force. Droplets then impact the foam ascending along the column wall rupturing the foam bubbles. It was found that all of their modified designs improved the efficiency of the SPFMD resulting in lower operating rotational speeds. It was also determined that the modification which increased residence time and separated condensed foam from ascending, uncondensed foam was the most efficient modification tested (Yamagiwa *et al*., 2000).

A study by Gutwald and Mersmann (1997) reported a few interesting observations concerning the general effectiveness of mechanical foam breakers. Two mechanical foam breakers were employed, the first being a six bladed paddle-type foam breaker. This device was designed to operate in a closed system with a perforated stator plate separating the area of foam generation from the area of foam destruction. Foam rose through the holes in the stator and was impacted by the rotating blades and was then accelerated and flung centrifugally against the container wall. This type of foam breaker generated two separate impact events on the foam bubbles. The first impact occurred when the foam breaker's blade struck a foam bubble as it rose through the hole in the stator. A second impact occurred when the resulting liquid and condensed foam bubbles were cast off from the foam breaker's blade and struck the vessel wall. The second device tested utilized a spinning rotor, similar to the six-bladed paddle in that it was designed to operate in a closed system and relied on impact as its primary means of foam destruction. It differed in that the stator plate had one hole located in the center of the plate. Foam rose through this opening and entered the rotor where it experienced radial acceleration and was flung outwards impacting the container wall. Three different surfactants were used to generate foam to determine if surfactant type had an impact on a mechanical foam breaker's ability to reduce foam. Results showed that the six bladed foam breaker was superior to the rotor style foam mitigation device in destroying foam created with each surfactant tested. It was also discovered that there is a lower limit to a mechanical foam breaker's ability to reduce foam. In other words, mechanical foam mitigation devices cannot completely separate gas and liquid phases because at some point the required bubble rupture strength exceeds the force a mechanical foam breaker is able to impart to a foam bubble (Gutwald & Mersmann, 1997).

Stirring as foam disruption (SAFD) is a technique that was first articulated by Hoeks *et al* (1997). SAFD is a technique applied to closed bioreactors in which the upper-most stirring impeller's height and blade type are adjusted so as to cause the entrainment of foam into the liquid, as well as rupture bubble lamella via stresses induced by liquid flow (F. Hoeks *et al*., 1997). The authors conducted their experiments in a 20 L bioreactor in which they tested the abilities of a six-bladed 45 degree pitched blade turbine, two Ruston turbines with diameters of 95 and 120 mm, and a Lightnin® A315 hydrofoil to disrupt foam under varying conditions. The experimental conditions varied were speed of rotation, media type, distance from top-most impeller to liquid surface, and superficial gas velocity. It was found that distance from the impeller to the liquid surface was a critical factor, and that stirrers with a smaller ratio of stirrer diameter to reactor diameter was preferred (F. Hoeks *et al*., 1997). The implication of Hoeks *et al* (1997) research is that SAFD is a feasible method of foam control in closed systems. More pertinently, SAFD is best accomplished by positioning a large diameter impeller just above the liquid surface.

In a further inquiry into SAFD, Boon *et al* (2002) assessed a range of impellers in both up-pumping and down-pumping mode in a 0.72 meter diameter vessel with a 1.85 meter height. A synthetic fermentation broth was used to help standardize results and air was sparged through the system using a 0.17 meter diameter ring sparger to generate foam. Four different upper impellers were tested and these were: a Rushton Turbine (Figure 2.2), a Scaba® 6SRGT (Figure 2.3), a Lightnin® A315 (Figure 2.4), and a Scaba® 3SHP1 (Figure 2.5).The Rushton turbine and the Scaba® 6SRGT are only used in one direction as they are radial pumpers, while the Lightnin® A315 and the Scaba® 3SHP1 can be used in upwards and downwards pumping mode by reversing rotation direction. Impeller speed, superficial gas velocity, and height of media

measured from the center of the impeller to the liquid surface were varied in this experiment and the resulting foam height for each configuration was recorded. It was found that in a closed bioreactor, up-pumping hydrofoils gave the best foam control. The author found that this was due to the strong downward currents formed at the container wall which tended to draw foam into the liquid. It was also found that downward pumping hydrofoils could control foam in a closed system, but not as efficiently as the upward pumping hydrofoils (Boon *et al*., 2002).

In summary, ultrasonic methods of foam mitigation are not suitable for use in a swine DPMS due to the large surface area of the pit and the inability to precisely control temperature or barometric pressure within the pit without extensive modifications. Since a DPMS can be considered an open system, SDFMD's are also unlikely to be useful in controlling manure foams. An efficient mechanical foam mitigation device for use in DPMSs should have a design that is both robust and is optimized to impart shear stress to foam bubble lamellae. Such a device should also employ SAFD as described by Hoeks *et al.* (1997). A mechanical foam mitigation device with these design features would destroy foam using both shear stress induced by impact and shear stress induced by fluid flows.

2.3 Implications of the Literature for a Mechanical Foam Destruction Device in a Swine Deep-pit Manure Storage Facility

There were few articles found specifically addressing foam mitigation in swine DPMS and no articles found on the topic of mechanical foam mitigation in swine DPMSs. Chemical antifoam agents have shown promise for controlling manure foams in a laboratory setting, but their efficacy has not been tested on a large scale. Also of concern is the lack of testing on the suitability of chemical antifoams when DPMS are emptied and the waste applied to cropland.

Monensin also may hold promise for controlling swine manure foams, but further research is needed to validate preliminary study findings. Monensin takes time to reduce foam depth, making it unsuitable during emergency situations where manure foam grows rapidly. An effective MFMD would be useful in emergency situations and it would not have the pollution concerns associated with a chemical mitigation strategy. Another advantage a mechanical mitigation system would have over chemical agents or biological pit additives is that chemicals and additives must be purchased repeatedly, whereas a mechanical foam mitigation device would only have to be purchased once. Numerous references were found dealing with foam control in bioreactors, particularly mechanical mitigation of foams in bioreactors. While not direct analogues of a swine DPMS facility, some of the principles articulated in the research concerning mechanical foam control in bioreactors could be instructive in constructing and operating a foam mitigation device for use in swine DPMSs. Particularly of interest are the papers dealing with stirring as foam disruption, which seems to be the most closely related process to that observed for the tested prototype mechanical foam breaker constructed by a private company for researchers at the University of Illinois. Given that a swine DPMS facility is so large as to be considered an open system with respect to fluid flows, it appears that a downward pumping hydrofoil coupled with robust impeller could be effective. Boone *et. al*. (2002) suggests that the vortex created by a downward pumping hydrofoil may be an efficient means to reincorporate foam into the liquid phase of the system (Boon et al., 2002) and a rotating impeller above the liquid phase would impart mechanical shear stress to foam bubbles. Finally, attention should be given to the distance of the hydrofoil below the liquid surface as this was identified as a critical factor in both Boon and Hoek's studies (F. Hoeks *et al*., 1997; Boon *et al*., 2002).

2.4 Figures

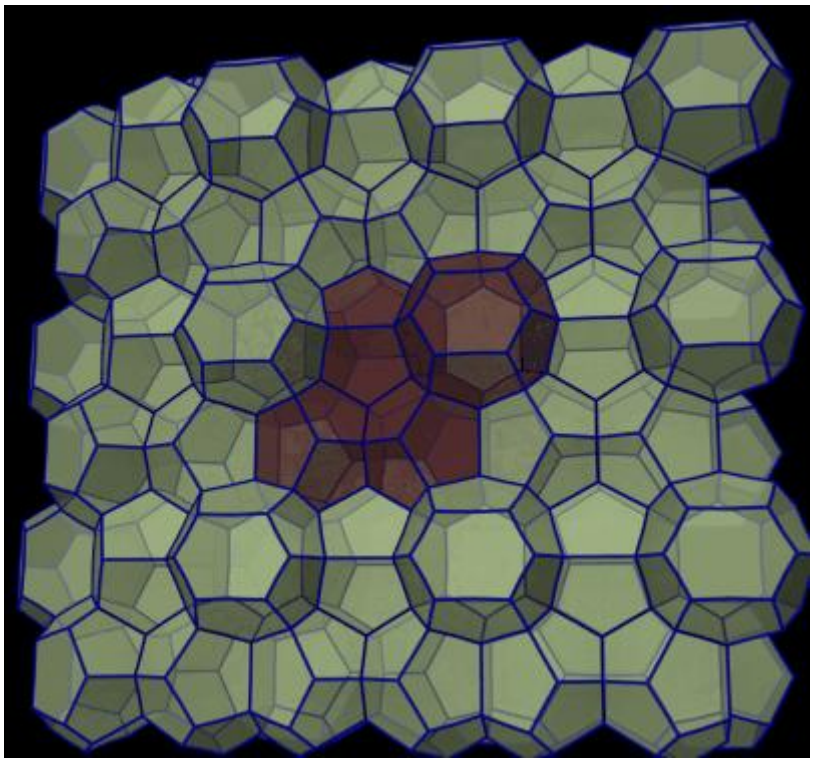

Figure 2.1 – This rendering illustrates the three dimensional geometry of stable foam. Three lamellae meet on an edge, and at a point four edges meet. (The Geometry Junkyard, 2013)

Figure 2.2 - Rushton Turbine (SpringerImages, 2013).

Figure 2.3 - Scaba 6SRGT Turbine (SpringerImages.B, 2013).

Figure 2.4 - Lightnin A315 Impeller (DirectIndustry, 2013).

Figure 2.5 - Scaba 3SHP1 Impeller (SpringerImages.C, 2013).

Chapter 3: Objectives

The following were the objectives of this research:

1. To assess the efficacy of the mechanical foam mitigation device (MFMD) to destroy foam in swine deep pit manure storages.

Is the purpose-built MFMD capable of removing foam from a swine DPMS?

2. To evaluate the difference, if any, of continuous versus episodic device operation and of device installation location.

Is there a difference between continuous and episodic operation?

What is the effect of device installation location?

3. To evaluate the distance over which foam will flow to the device.

Over what distance will a MFMD destroy foam?

Chapter 4: Materials and Methods

4.1 Device Description

The mechanical foam mitigation device consisted of a motor, gear box, stainless steel support stand, and a shaft with six paddles welded to it. The motor was a ½ HP, thermally protected, 1725 rpm electric motor. It was wired to operate off of a 115 V AC electrical supply and drew 8.2 amps of current when operating under a full load. The gear box attached to the motor and reduced the rotational speed from 1,725 rpm to 150 rpm. The motor and gear box were mounted on top of the stainless steel support stand and turned a drive shaft that connected to the paddle shaft. The paddle shaft extended down into the pit where the paddles engaged the foam. The paddle shaft was 2.4 m (95 in) in length and 2.2 cm (.88 in) in diameter. Six paddles were welded to the shaft and each paddle measured 30.9 cm (12.2 in) wide by 18.0 cm (7.1 in) tall. The center of each paddle was hollow so that foam could flow through the paddle. The upper and lower bars of each paddle formed a hydrofoil, angled such that as the shaft and paddle assembly rotated, foam was forced down into the liquid. Paddles were spaced 15.9 cm (6.3 in) apart on the shaft and the bottom paddle was flush with the bottom of the shaft. Each paddle was also offset by 60 degrees from the paddle below it (Figure 4.1).

4.2 Site Description

All testing was conducted at a local swine production facility located in east-central Illinois. In previous years, this producer had experienced foaming problems in various barns at this site. The site consisted of six barns, three of which were used for testing. The barns used for testing were labeled A, B, and C from north to south, with barns A and B being of identical

construction. The majority of testing was conducted in barn A as it had the deepest foam during the testing period. Barns A and B are shown in Figure 4.2 and were 61.3 m (201.1 ft) long by 12.6 m (41.4 ft) wide with four pit ventilation fans installed on the four pump-out port covers. Barn C is also shown in Figure 4.2 and was 58.7 m long (192.5 ft) by 15.6 m (51.2 ft) wide with four pit ventilation fans installed on the four pump-out port covers.

4.3 Foam Volume Measurement Materials

4.3.1 Description

To accurately measure the foam volume in the pit, it was critical to ascertain the foam thickness at any point within the pit. To facilitate this, a floor-to-foam measurement device was constructed using a laser distance meter (model 416D, Fluke Corporation, Everett, WA), with stated accuracy of ±1.5 mm (±0.059 in)[2], mounted on a purpose-built stand. The stand consisted of a 1.203 m (3.95 ft) length of 3.81 cm (1.5 in) diameter schedule 40 PVC pipe (North American Pipe Corp., Houston, TX) fitted with a 3.81 cm (1.5 in) schedule 40 straight coupling (Charlotte Pipe and Foundry Co., Charlotte, NC) on one end and a 3.81 cm (1.5 in) to 7.62 cm (3 in) schedule 40 adapter (Charlotte Pipe and Foundry Co., Charlotte, NC) on the other. A closet flange (product number 43531, Oatey, Cleveland, OH) was fitted to the adapter to act as a foot for the stand and a notch measuring 2.54 cm (1 inch) high by 3.18 cm (1.25 inches) wide was cut in the 1 ½ inch straight coupling to view the display of the laser distance meter (Figure 4.3). Finally a circular spirit level was mounted on the laser distance meter. The purpose of the device was to measure the distance from the floor to the surface of the foam within the pit while insuring that the laser distance meter was perpendicular to a level plane. Prior to testing the

[2] In favorable conditions up to 10 m (33 ft). In unfavorable conditions, the deviation can increase by approximately ±0.15 mm/m (±0.0018 in/ft) for a maximum possible deviation of 7.5 mm (0.30 in) at 60 m (197 ft), (Fluke, 2013)

MFMD, the laser distance meter was validated to insure that it would accurately measure distances when aimed at a foam or liquid surface.

4.3.2 Laser Distance Meter Validation

To validate the laser distance meter's accuracy when using a foam or liquid target, several liters of both foam and liquid manure were collected from the test site. In the lab, eight fixed heights ranging from 0.64 m (2.08 ft) to 2.76 m (8.08 ft) above the floor were measured, marked, and recorded using a tape measure (product number 33-430, Stanley Tools, New Britain, CT) and then with the laser distance meter mounted in its stand. Next, approximately 4 L of foam were placed in a clean bucket and the distance from the surface of the foam to each of the eight fixed heights was measured and recorded first using the tape measure and then the laser distance meter with stand. Once all sixteen measurements were taken, the bucket was emptied, washed, and refilled with approximately 4 L foam and the process repeated. This resulted in three measurements from each of the fixed heights to the foam's surface with the tape measure and three measurements from each of the fixed heights to the foam's surface with the laser distance meter. This process was repeated using liquid manure.

The absolute error of the laser distance meter as compared to the tape measure was calculated and the relative error between the tape measure and laser distance meter was also found. Finally, a paired t-test was used to determine if the laser distance meter was significantly different from the tape measure when measuring to foam, liquid manure, and concrete.

4.4 Trial Setup

4.4.1 Trial Description

This study comprised a series of MFMD runs in the three test barns. A run was defined by the MFMD installation location and the mode of device operation. Devices were either installed in the pump-out port of a barn or inside the barn near the center of the structure. In a run, the MFMD was operated for a predetermined length of time in either continuous or episodic fashion. In all but two runs, device testing was structured such that two devices were installed in a single barn and two runs were conducted simultaneously. The two exceptions to this were Run 1 and Run 15. In both cases only a single device was used. In all other cases, MFMDs were installed in the pump-out ports on opposite sides of the barn and the east and west halves of the barn were treated as independent runs. Prior to the start of a run, baseline foam depth measurements were collected at all points within the barn. Foam depth was also directly measured in a pump-out port and recorded. Devices were then turned on and the time of device startup recorded. All subsequent times were recorded with device startup time defined as t=0. Using the laser distance meter, time series measurements were taken at each of the marked measuring points in blocks of ten. This was done to minimize the time needed to take measurements. The time elapsed since device startup when the first and last measurement of a block was taken was recorded. The average of these two elapsed times was then used as the measurement time for each point within a block of measurements. During episodic runs, the time of device cutoff was noted as was time of device restart. Measurements were taken before each change of operational state for episodic runs and hourly for continuous runs. In Runs 1 through 7 the MFMD was operated continuously while installed in one of the barn's pump-out ports. In Runs 8 through 14 the MFMD was operated episodically while installed in one of the barn's

pump-out ports. Runs 8 and 9 were conducted in Barn A and consisted of one device operating at a duty cycle of 0.5 hours on and 1 hour off and a second device operating on a duty cycle of 1 hour on, 2 hours off. All other episodic duty cycles were 1 hour on, 1 hour off. Run 15 was unique in that the device was installed inside Barn A and operated continuously.

4.4.2 Foam Mitigation Device Location

In Barns A, B, and C, MFMD installation locations were identified. For Runs 1 through 14, the selected device installation locations were the pump-out ports associated with the barns' minimum ventilation fans (Figure 4.2). For Runs 7 and 14 in barn C, new, reinforced pump-out port covers were constructed to support the device and to allow operation of the minimum ventilation fans during testing (Figure 4.4). For Runs 1-6 and 8-13 in Barns A and B, the pump-out covers were removed and a bracket was built from treated lumber to support the device during operation (Figure 4.5). This was done because on the first day of testing in Barn A the side curtains were down and the minimum ventilation fans were not in operation. Thereafter MFMD support bracket was used for the sake of convenience. For Run 15, a single device was installed inside Barn A 6.79 m (22.28 ft) from the north axis of the barn and 29.04 m (95.28 ft) from the west axis of the barn (Figure 4.2). The curtains were lowered to facilitate good air exchange and air quality was monitored using a Dräger Pac 7000 (Draeger Safety Inc., Pittsburgh, PA) equipped to monitor hydrogen sulfide.

4.4.3 Measurement Point Location

Once the installation locations for the MFMD's were determined, foam depth measurement points were defined on the floor of each barn (variable e_i in Figure 4.6) using spray paint to mark the slats. These points were identified so that time series foam depth measurements

could be quickly taken while the devices were in operation. Table 4.1 lists the coordinates of the MFMD's by run and coordinates for each measurement point used in Runs 1-15 can be found in Appendix A.

For Run 1 sixty points were distributed along three lines with twenty points to a line in Barn A (Figure 4.7). The lines radiated out from the device installed in pump-out port C at approximate angles of 45, 90, and 180 degrees, respectively.

Runs 2 and 8 shared the same set of foam depth measurement points (Figure 4.8). Both of these runs were conducted in Barn A. For Runs 2 and 8 the points were primarily arranged along four lines. Three lines radiated out from the device at approximate angles of 30, 90, and 180 degrees. The fourth line of points was located approximately 0.5 m (1.7 ft) from the west wall of the barn and ran parallel to that wall.

Runs 3 and 9 shared the same set of foam depth measurement points (Figure 4.9). Points in Runs 3 and 9 were generally arranged along four lines in Barn A. Three of these lines radiated out from the MFMD at approximate angles of 60, 90, and 180 degrees, respectively, and the fourth line was located approximately 0.5 m (1.7 ft) from the eastern wall of the barn and ran parallel to that wall.

Runs 4 and 11 shared the same set of foam depth measurement points. Points were located along three lines and were also regularly dispersed over the eastern half of Barn A (Figure 4.10). The three lines of points originated at the MFMD and radiated out at angles of approximately 30, 90, and 180 degrees.

Runs 5 and 12 were both done in Barn B and utilized identical foam depth measurement points. The points were arrayed along three lines oriented at angles of approximately 45, 90, and

180 degrees from the MFMD. Points were also distributed at regular intervals in the eastern half of Barn B (Figure 4.11) and the MFMD was installed in pump-out port B.

Runs 6 and 13 shared the same foam depth measurement points and both of these runs took place in Barn B with the device installed in pump-out port D. Points were distributed along three lines radiating out from the MFMD at approximate angles of 45, 90, and 180 degrees. Several points were also located at regular intervals in the western half of Barn B (Figure 4.12).

Foam depth measurement points for Run 7 were arranged along three lines originating at the MFMD and were also distributed regularly over the western half of Barn C (Figure 4.13). The three lines radiated out from the device at angles of approximately 45, 90, and 180 degrees respectively.

The foam depth measurement points of Run 10 were marked out in Barn A along three lines radiating from the MFMD at angles of approximately 30, 90, and 180 degrees. Points were also located at regular intervals in areas the three lines did not pass through (Figure 4.14).

In Run 14 foam depth measurement points were arrayed in three lines radiating out from the device at approximate angles of 45, 90, and 180 degrees respectively. Points were also regularly dispersed over the eastern half of Barn C (Figure 4.15).

For Run 15 foam depth measurement points were along eight lines whose origin was centered on the MFMD. Points were also dispersed at intervals apart from the lines (Figure 4.16). The lines radiated out from the device at angles of 0, 45, 90, 135, 180, 225, 270, and 315 degrees. The coordinates of the MFMD are given in Table 4.1.

4.4.4 Measurement Point Survey

After the foam depth measurement points were marked on the slats, the points were surveyed to determine their position in an X,Y coordinate system as depicted in Figure 4.7 – 4.15 and tabulated in Appendix A. In this coordinate system the north-west corner of the barn was defined as the origin. The X-axis ran from north to south and the Y-Axis ran from west to east. Each foam depth measurement point's position relative to the origin was measured using the laser distance meter (model 416D, Fluke Corporation, Everett, WA) and the measurements were recorded. A laser level (model GL412, Trimble Navigation Limited, Sunnyvale, CA) was used to identify each point's deviation from a datum. This process allowed each point to be accurately located in an X, Y, Z coordinate system and was critical in calculating foam volumes.

4.5 Data Analysis

4.5.1 Foam Depth Calculations

Each run generated an initial, or baseline, foam depth measurement at each point and subsequent time series measurements at each point. Since the raw measurements were taken from the laser distance meter to the surface of the foam, calculations were performed to determine the foam depth at a given point and time. This was accomplished with the following equations using the definitions depicted in Figure 4.6:

$$e_{p,0} = x_{p,0} - B - A_p$$

Where,

$e_{p,0}$= distance from the datum to the surface of the foam at point, p and t=0 (m)

p = the point located within 0.6 m (2 ft) of the pump-out port where the foam depth was directly measured.

t = device operation time (h)

$x_{p,0}$ = the raw baseline measurement at t=0 taken at point, p (m)

B = height of the laser distance meter stand, measured daily and is constant for all measurements taken on that day (m)

A_p = deviation of a foam depth measurement point from the datum and is a constant (m)

$$F = d_p + e_{p,0}$$

Where,

F = the distance from the datum to the liquid surface, a constant (m)

d_p = foam depth measured in the pump-out port and assumed to be the foam depth at p which was located 0.6 m (2 ft) away (m)

Once F was determined, it was possible to calculate the foam depth for all points in the barn using the following equations:

$$e_{i,t} = x_{i,t} - B - A_i$$

Where:

$e_{i,t}$ = distance from the datum to the foam's surface at point "i" at time "t" (m)

$x_{i,t}$ = the raw measurement taken at point "i" at time "t"(m)

A_i = the deviation of point "*i"* from the datum, a constant (m)

$$d_{i,t} = F - e_{i,t}$$

Where:

$d_{i,t}$ = foam depth at point "*i"* at time *"t"* (m)

This series of calculations generated a foam depth for each point in each time series measurement in every run.

4.5.2 Measurement Zones

Measurement points for each of Runs 1-14 were grouped into 2 m (6.6 ft) wide annular zones based on radial distance from the MFMD coordinates (Table 4.1). When installed in the pump-out ports, the MFMD was located outside of the barn. The origin of the radius was moved inside the barn by adding or subtracting 0.6 m (2.0 ft) to the X-value of the device's location coordinates. If X was positive, then 0.6 m (2.0 ft) was subtracted from it and if X was negative 0.6 m (2.0 ft) was added to it. For Run 15 where the device was installed inside Barn A, the origin of the radius was simply the coordinates of the device location. There were thirteen zones for Run 1-14 with radii ranging from 1.0 to 25.0 m (3.3 to 82.0 ft) and Run 15 contained sixteen zones with radii ranging from 1.0 to 31.0 m (3.3 to 101.7 ft). Zone radii and areas are tabulated in Appendix B. Zone areas were calculated using AutoCAD 2011 (Autodesk, Inc., San Rafael, CA). The zone areas, calculated foam depths, and measurement times were entered into a spreadsheet for processing.

4.5.3 Data Processing

For each time series of each run the current foam volume (V), change in foam volume (ΔV), foam destruction rate (FDR), and the foam destruction rate normalized for the initial foam depth (nFDR) were calculated. The steps used to process the initial and final measurements and calculate these values are illustrated below and reported in Table 4.2. The data used in this example come from time series 2 of Run 3. Each numbered step described below corresponds to a numbered column in Table 4.2a (zones 1-7) and 4.2b (zones 8-13).

4.5.3.1 Zone Calculations

1. Each zone's initial foam volume (V_i) was calculated by multiplying the zone area (A) by the initial mean foam depth. For example, zone 1's area was 1.6 m^2 and the initial mean foam depth was 0.172 m for a calculated initial volume of 0.27 m^3.
2. The final volume (V_f) for each zone was determined by multiplying the zone's A by the final mean foam depth. For zone 1, the final mean foam depth (0.162 m) multiplied by the A (1.6 m^2) was 0.25 m^3 (final foam volume).
3. For each zone the mean change in zone depth ($\overline{\Delta d}$) was calculated by subtracting the final mean foam depth ($\bar{d}_f$) from the initial mean foam depth ($\bar{d}_i$). As shown for zone 1: $\overline{\Delta d} = \bar{d}_i - \bar{d}_f$ = 0.172 m - 0.162 m = 0.011 m.
4. The change in mean zone foam depth over time ($\overline{\Delta d}/\Delta t$) was found for each zone by dividing the $\overline{\Delta d}$ (calculated in step 3) by the change in time (Δt = final measurement time – initial measurement time). For zone 1:

   $\overline{\Delta d}/\Delta t$ = 0.011 m/ (2.2 h -1.1 h) = 0.009 m/h

5. Change in zone foam volume (ΔV) was determined by subtracting the zone's final foam volume from the initial foam volume (V_i-V_f). For example, in zone 1:

   $\Delta V = V_i - V_f = 0.27\ m^3 - 0.25\ m^3 = 0.016\ m^3$

6. The percent change in foam volume (ΔV%) was calculated by dividing the zone's ΔV by its V_i and multiplying by 100. For example, in zone 1:

   $\Delta V\% = (\Delta V / V_i)*100 = (0.016\ m^3 / 0.27\ m^3)*100 = 6\%$

7. A foam destruction rate (FDR) of each zone was determined by dividing the zone's ΔV by its Δt. For zone 1:

   $FDR = \Delta V/\Delta t = 0.016\ m^3 / 1.1\ h = 0.01\ m^3/h$

8. The percent FDR (%FDR) was found by dividing the ΔV%, found in step 6, by the Δt. For zone 1:

   $\%FDR = \Delta V/\Delta t = 6\% / 1.1h = 5\%/h$

9. The FDR was then normalized for the initial mean foam depth for that zone (nFDR) at time *t*=0 ($\overline{d_0}$). This was calculated by dividing the FDR (calculated in step 7) by $\overline{d_0}$. For example, in Zone 1:

   $nFDR = FDR / \overline{d_0} = 0.01 m^3/h / 0.275\ m = 0.05\ m^2/h$

10. The normalized FDR expressed as a percent (% nFDR) was calculated by dividing the %FDR by $\overline{d_0}$ (0.275 m). For zone 1:

    $\%\ nFDR = \%FDR / \overline{d_0} = 5\%/h / 0.275\ m = 20\ \%/h\text{-}m$

4.5.3.2 Series Summary Calculations

Upon completion of steps 1 through 10 for each zone within a time series measurement, calculations were performed to summarize each series. Each step used to summarize the previous calculations are outlined below and shown in the 'Series 2 Summary' row of Table 4.2b.

The series area (A_s) is the sum of the areas of all thirteen zones in the series (A_i, i=1 to 13). For series 2 of Run 3, A_s = 371.1 m^2. Series initial mean foam depth ($\overline{d_{i,s}}$) is a weighted average of each zone's mean depth ($\overline{d_i}$, i=1 to 13) and A_i. For example, $\overline{d_{i,s}}$ for series 2 is found as follows:

$$\overline{d_{i,s}} = \sum_{i=1}^{13} d_i * A_i/A_s$$

$$\overline{d_{i,2}} = \frac{(0.172\ m * 1.6\ m^2) + (0.226\ m * 12.6\ m^2) \ldots + (0.282\ m * 6.5\ m^2)}{371.1 m^2} = 0.273\ m$$

The series initial mean time ($\overline{t_{i,s}}$) is the average time for the initial foam depth measurements taken for each zone. In series 2, $\overline{t_{i,s}}$ = 1.3 h. Series initial volume ($V_{i,s}$) is a sum of the initial zone foam volumes for each zone. For example, in series 2 $V_{i,s}$ = 101.5 m^3.

The series final mean foam depth ($\overline{d_{f,s}}$) is a weighted average of the final mean foam depth ($\overline{d_f}$) and A for each zone. For example, series 2's final mean foam depth is found as follows:

$$\overline{d_{f,s}} = \sum_{i=1}^{13} d_i * A_i/A_s$$

$$\overline{d_{f,2}} = \frac{(0.172\ m * 1.6\ m^2) + (0.226\ m * 12.6\ m^2) \ldots + (0.282\ m * 6.5\ m^2)}{371.1 m^2} = 0.265\ m$$

Final mean time, ($\overline{t_{f,s}}$), for the series is an average of the final foam measurement times for all the zones. For example in series 2, $\overline{t_{f,s}}$ = 2.4 h. The series final foam volume ($V_{f,s}$) is a sum the final zone foam volumes of the series. In series 2, $V_{f,s}$ = 98.2 m^3.

Series mean change in foam depth ($\overline{\Delta d_s}$) is the difference of $\overline{d_{i,s}}$ and $\overline{d_{f,s}}$. For example, in series 2 $\overline{\Delta d_s}$ = 0.009 m. Series change in foam depth over time ($\overline{\Delta d_s}$ / $\overline{\Delta t_s}$) is obtained by dividing $\overline{\Delta d_s}$ by the series mean change in time ($\overline{\Delta t_s}$ = $\overline{t_{f,s}}$ - $\overline{t_{i,s}}$). Using series 2 as an example, $\overline{\Delta d_s}$ / $\overline{\Delta t_s}$= 0.009 m / (2.4 h – 1.3 h) = 0.008 m/h. Series change in foam volume (ΔV_s) is the sum of zone changes in foam volume (ΔV). In series 2, the sum of the ΔV's resulted in ΔV_s = 3.3 m^3. The series percent change in foam volume ($\%\Delta V_s$) is obtained by dividing ΔV_s by $V_{i,s}$ and multiplying the result by 100. For example, in series 2:
$\%\Delta V_s = \Delta V_s / V_{i,s}$ = (3.3 m^3 / 101.5 m^3)*100 = 3%. Series foam destruction rate (sFDR) is calculated by dividing ΔV_s by Δt_s. For example, in series 2

sFDR = $\Delta V_s / \Delta t_s$ = (3.3 m^3 / (2.4 h – 1.3 h) = 3.0 m^3 / h. The percent sFDR results from dividing the $\%\Delta V_s$ by $\overline{\Delta t_s}$. For example, the series 2 percent sFDR = $\%\Delta V_s / \Delta t_s$ = 3%/ 1.1 h = 3%. The sFDR was normalized for initial mean foam depth ($\overline{d_{s,0}}$) by dividing the sFDR by $\overline{d_{s,0}}$. For series 2, the normalized sFDR = sFDR/ $\overline{d_{s,0}}$= 3.0 m^3 / 0.289 m = 10.3 m^2 / h. The normalized sFDR was also expressed as a percent and was determined by dividing the %sFDR by $\overline{d_{s,0}}$. In series 2, normalized percent sFDR = %sFDR / $\overline{d_{s,0}}$ = 3% / 0.289 m = 10 % / h-m.

4.5.3.3 Run Summary Calculations

Once summary values for each time series were calculated, the run was summarized in terms of change in foam volume, percent change in foam volume, foam destruction rate, percent foam destruction rate, foam destruction rate normalized for initial foam depth, and foam destruction rate normalized for initial foam depth expressed as a percent. The series summary values calculated in section 4.5.3.2 were used determine the overall values for a run. The steps

taken to summarize a run are outlined below and are also presented in Table 4.3. Each numbered step described below corresponds to a numbered column in Table 4.3.

1. The change in foam volume for a run is the sum of the series changes in foam volume (ΔV_s). For example, in Run 3 the overall change in foam volume was 18.36 m^3.
2. The run percent change in foam volume for a run is the sum of the series percent changes in zone volume. Using Run 3 as an example, the run percent change in foam volume was 18%.
3. The run foam destruction rate (rFDR) is the average of the series foam destruction rates. Its standard deviation was also computed and the minimum and maximum values reported. For run 3, the rFDR was 3.40 m^3/h, the standard deviation was 0.85 m^3/h, and minimum and maximum values of 2.38 and 4.70 m^3/h, respectively.
4. The percent rFDR is the average of the series percent foam destruction rates. The standard deviation, minimum, and maximum values for the rFDR were also reported. For example, in Run 3 the rFDR was 3% with a standard deviation of 1% and minimum and maximum values of 3 and 4%, respectively.
5. The rFDR normalized for initial foam depth is the average of the series normalized foam destruction rates. As in steps 3 and 4, the standard deviation, minimum, and maximum values were found. In Run 3, the normalized rFDR was 11.76 m^2/h with a standard deviation of 2.95 m^2/h. The minimum and maximum normalized rFDR for run 3 were 8.22 and 16.25 m^2/h, respectively.
6. The normalized rFDR expressed as a percent is the average of the series normalized foam destruction rates expressed as percents. The standard deviation was calculated and the minimum and maximum values were found. For example, Run 3 had a

normalized rFDR expressed as a percent of 12 %/h-m, with a standard deviation of 3 %/h-m and a minimum and maximum of 9 and 15 %/h-m, respectively.

4.5.3.4 Summary of Data

The preceding sections describe how data were summarized by time series and by run. MFMD performance was evaluated by tabulating and graphing the summary data resulting from these calculations.

4.6 Figures

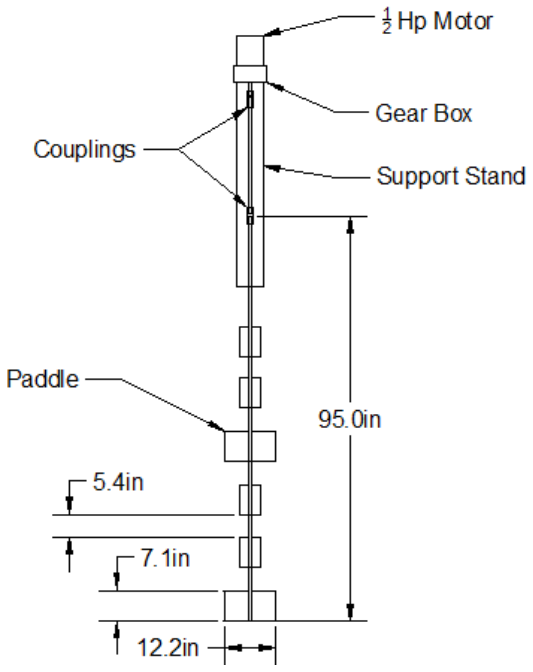

Figure 4.1 – Basic schematic of the foam mitigation device. The paddles of the device are offset sixty degrees from each other and the top and bottom of each paddle is angled so that as the paddle shaft assembly rotates, foam is forced down into the liquid layer.

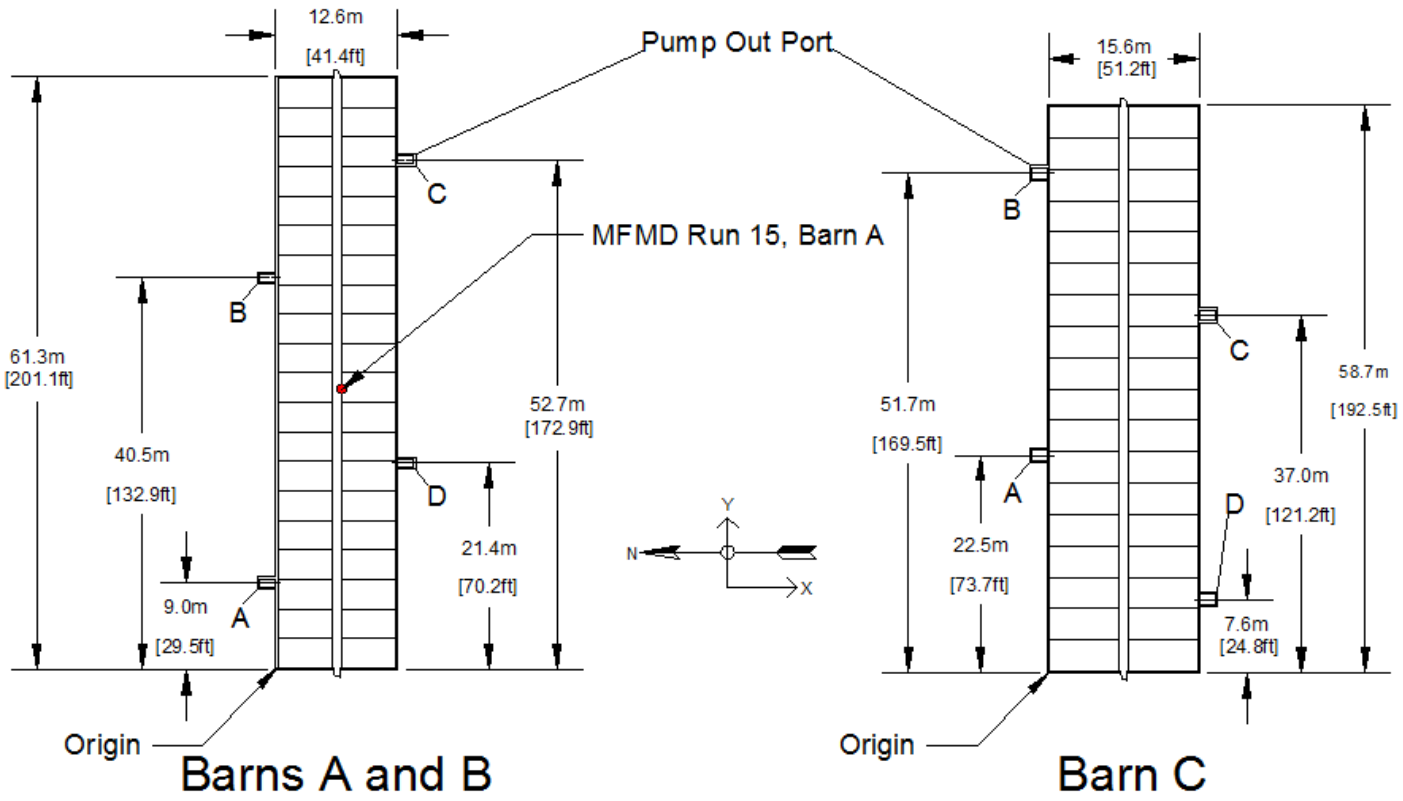

Figure 4.2 - Schematic of Barns A, B, and C showing dimensions, pens, pump-out ports, origin of the coordinate system, and the device installation location for Run 15.

Figure 4.3 - Fluke® 416D laser distance meter mounted on purpose-built measurement stand.

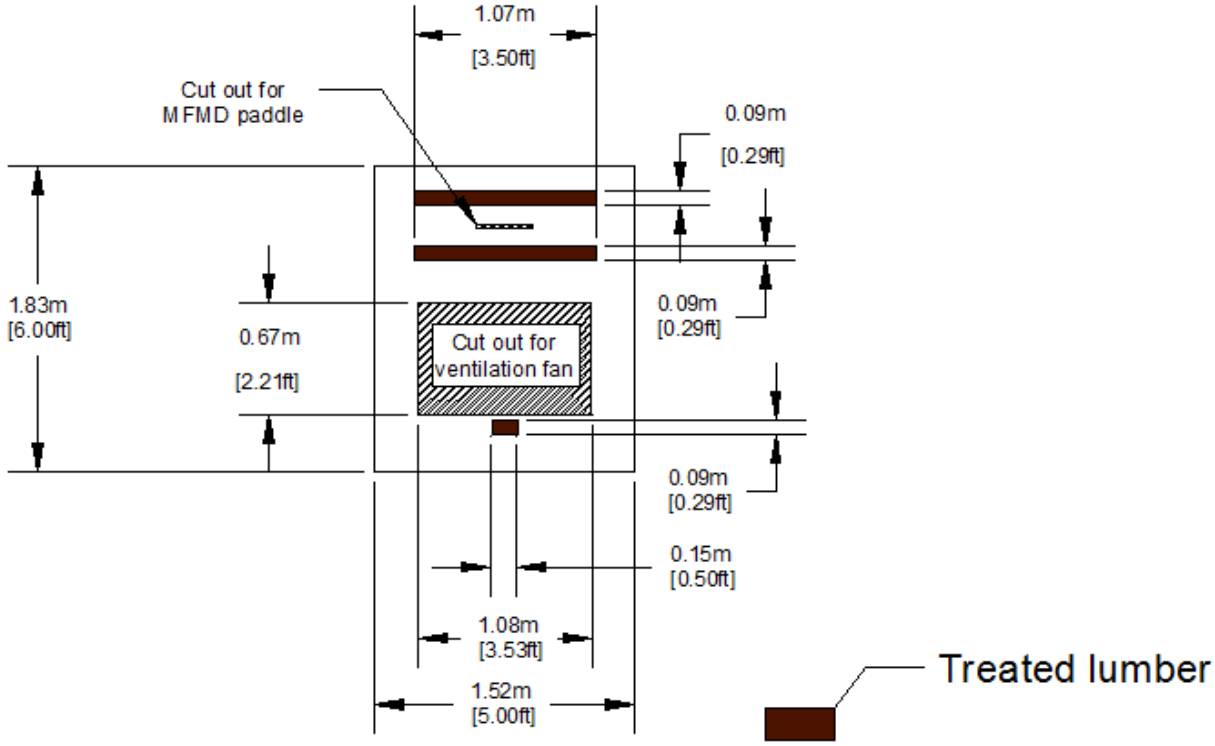

Figure 4.4 - Schematic of reinforced pump-out port covers constructed for Barn C.

Figure 4.5 - Bracket built to support the mechanical foam mitigation device when installed in the pump-out ports of Barns A and B.

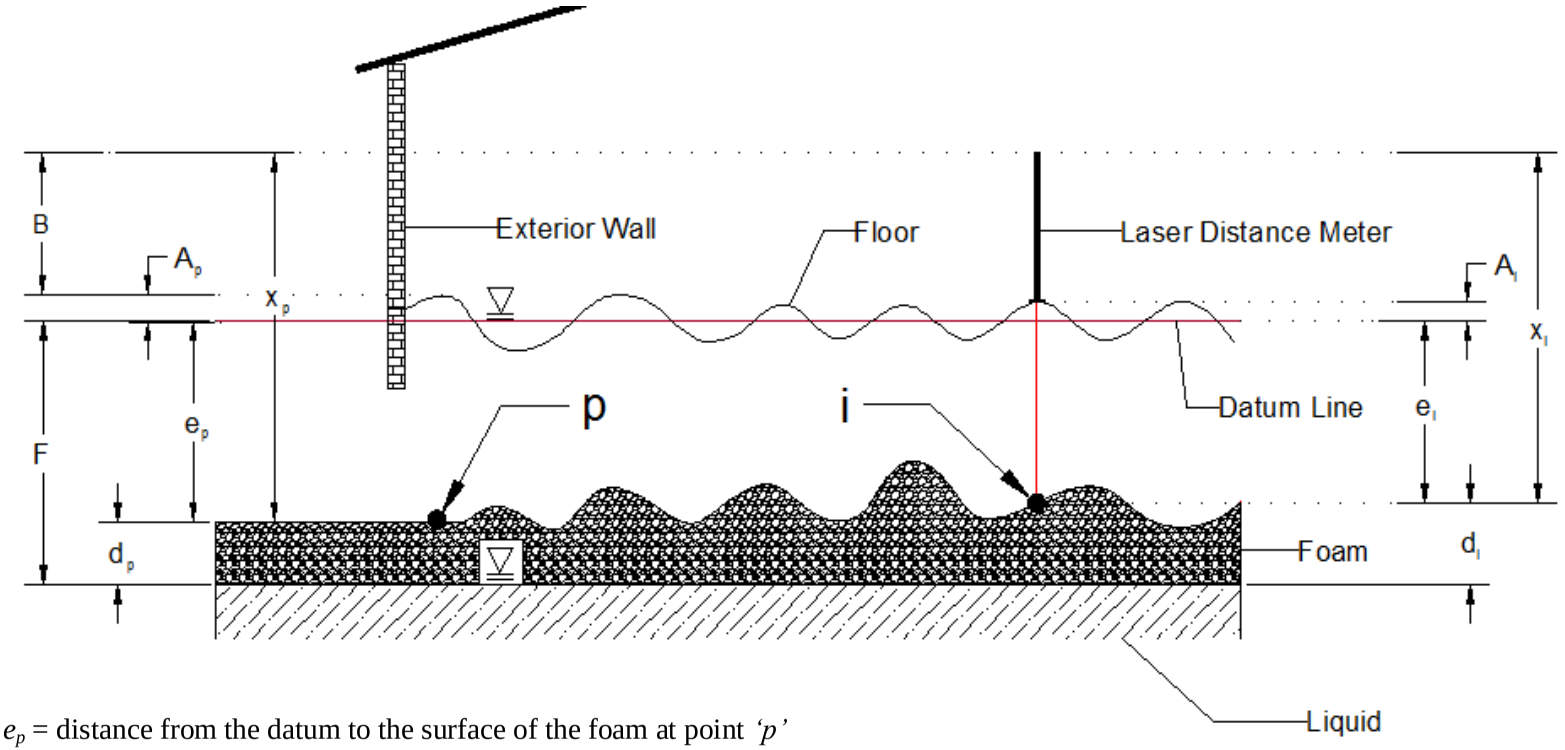

e_p = distance from the datum to the surface of the foam at point *'p'*

p = the foam depth measurement point located within 0.6 m (2 ft) of the pump-out port where the foam depth was directly measured

B = height of the laser distance meter stand, a constant for a run

A_p = deviation of '*p*' from the datum line, a constant

x_p = raw baseline measurement at *p*

d_p = foam depth in the pump-out port within 0.6 m (2 ft) of *p*, directly measured

F = distance from the datum to the liquid surface, a constant

e_i = distance from the datum to the foam's surface at point 'i'

i = a foam depth measurement point other than 'p'

x_i = raw measurement taken at 'i'

A_i = the deviation of 'i' from the datum, a constant

d_i = calculated foam depth at 'i'

Figure 4.6 - Variables used in foam depth calculations at unique measurement points defined.

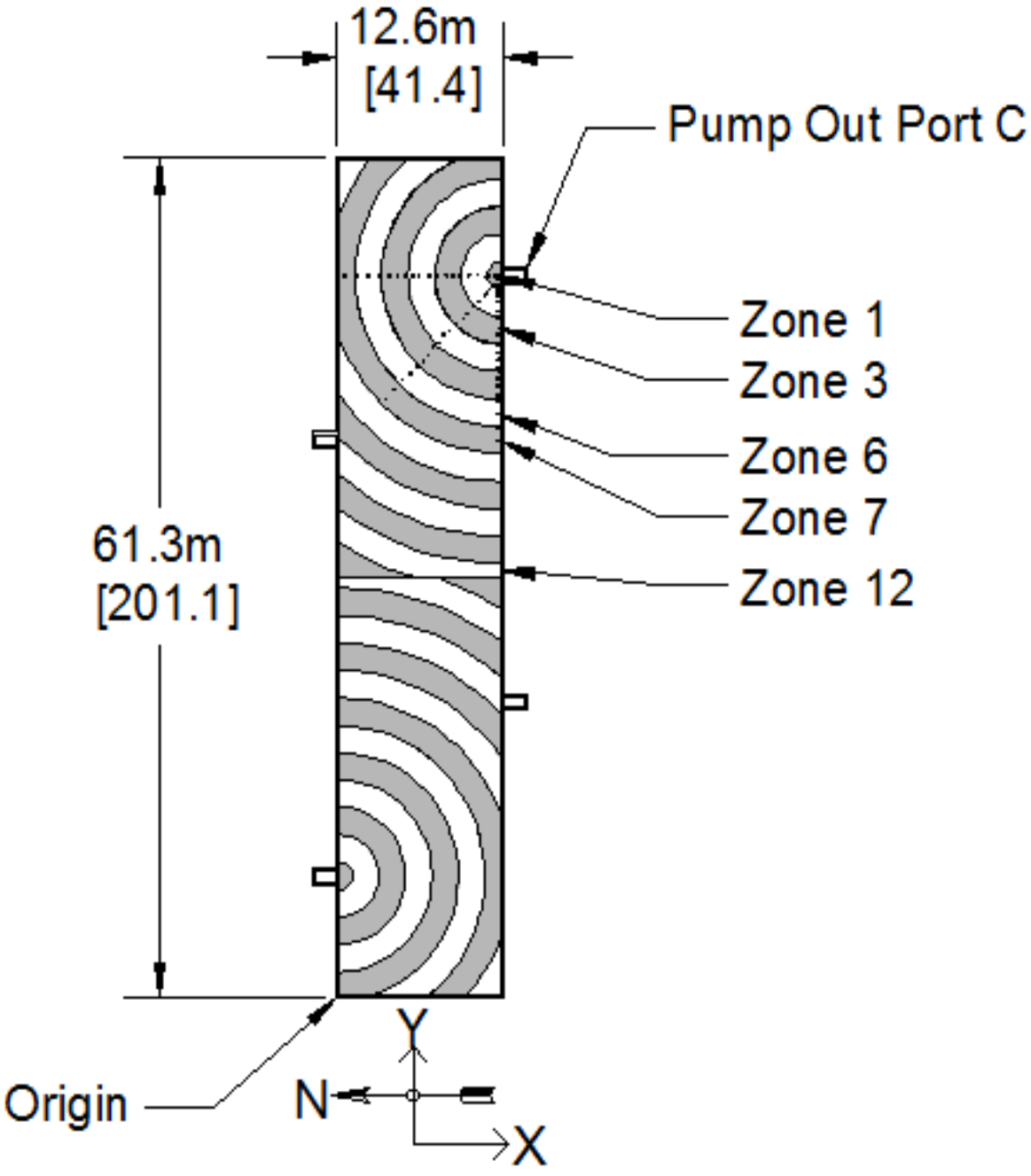

Figure 4.7 – Locations of Run 1 foam depth measurement points with device installed in Barn A, pump-out port C. See Table A.1 for measurement point coordinates.

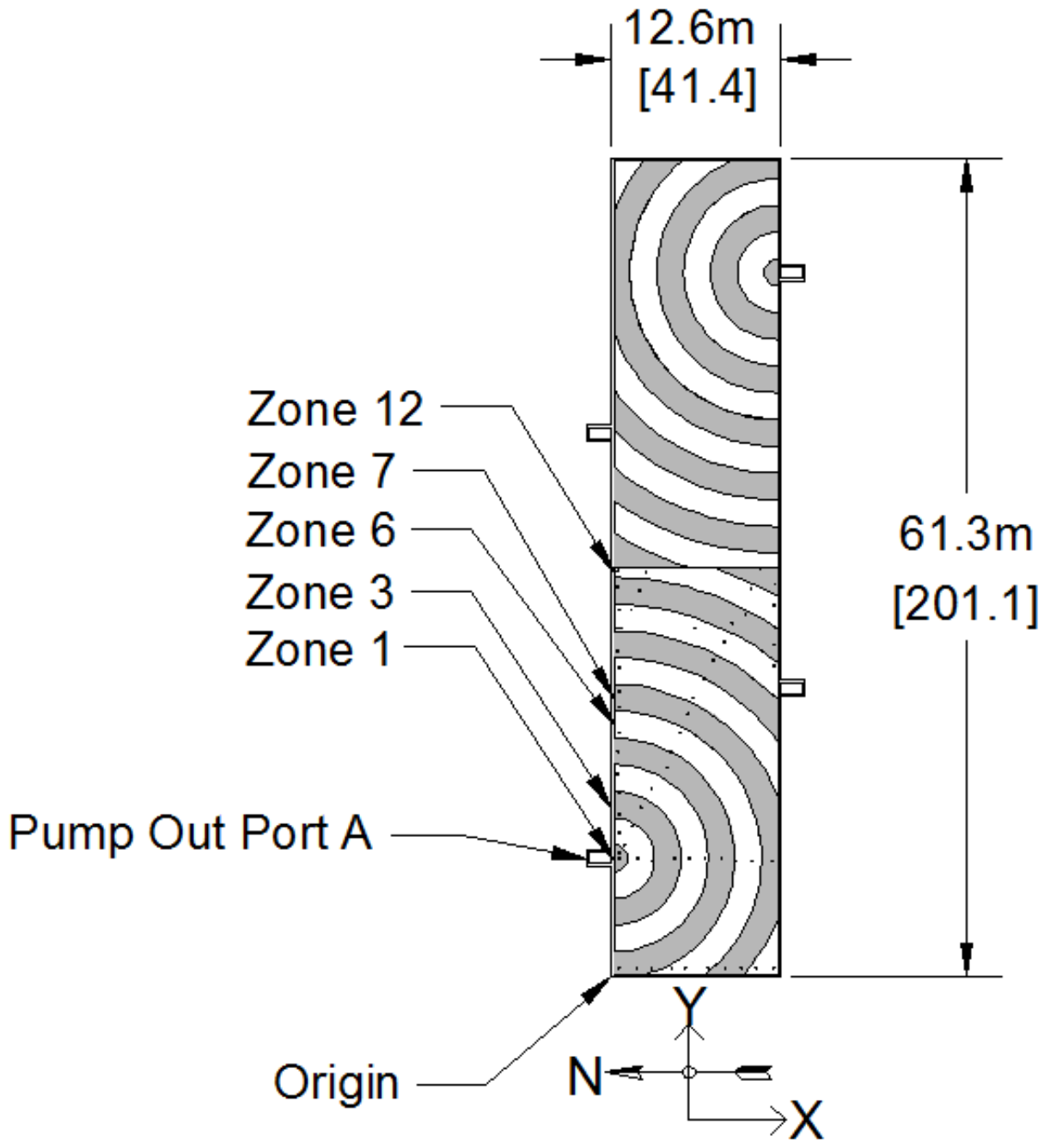

Figure 4.8 - Locations of foam depth measurement points for Runs 2 and 8 in which the device installed in Barn A, pump-out port A. See Table A.2 for measurement point coordinates.

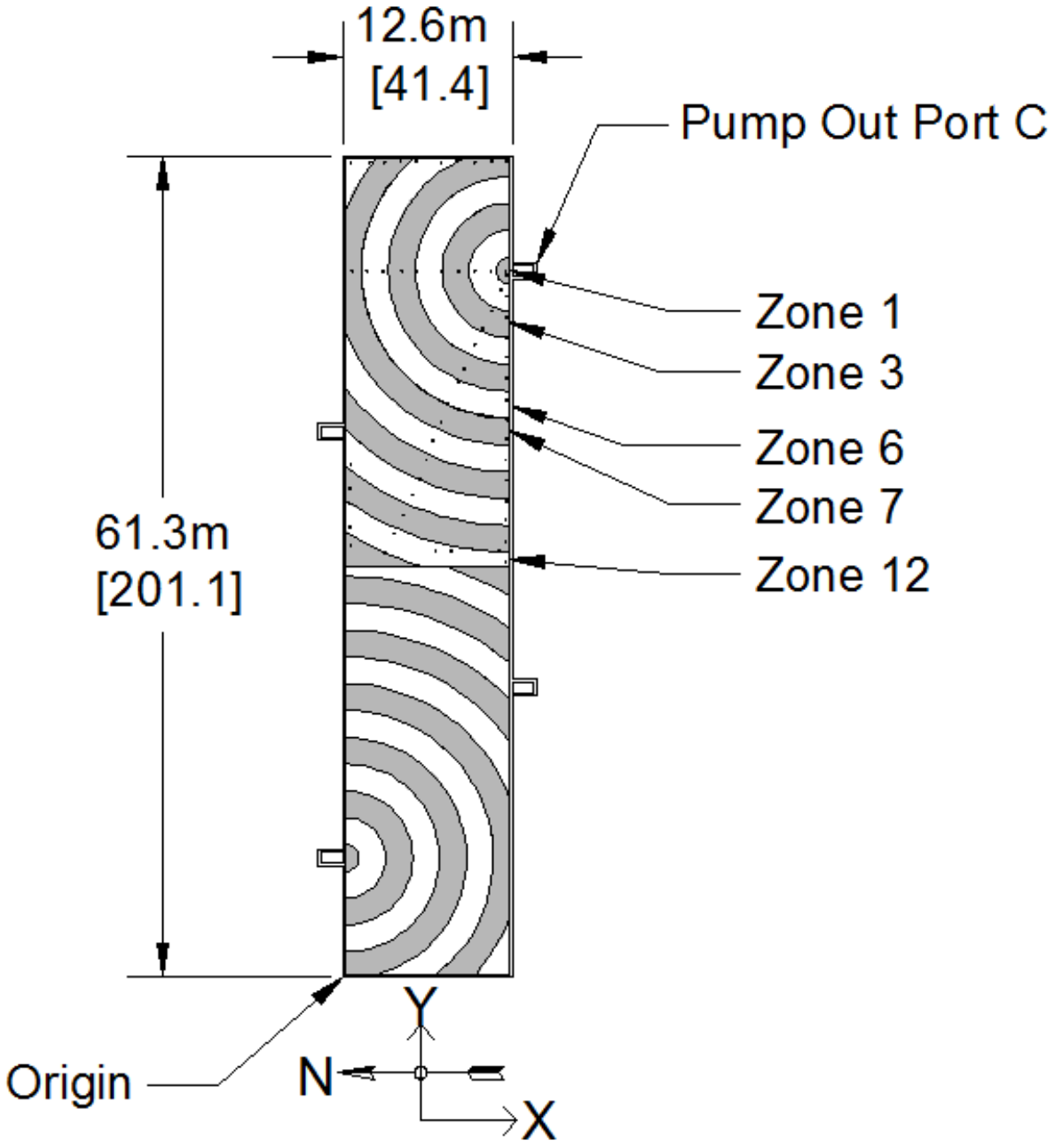

Figure 4.9 - Locations of foam depth measurement points for Runs 3 and 9 in which the device installed in Barn A, pump-out port C. See Table A.3 for measurement point coordinates.

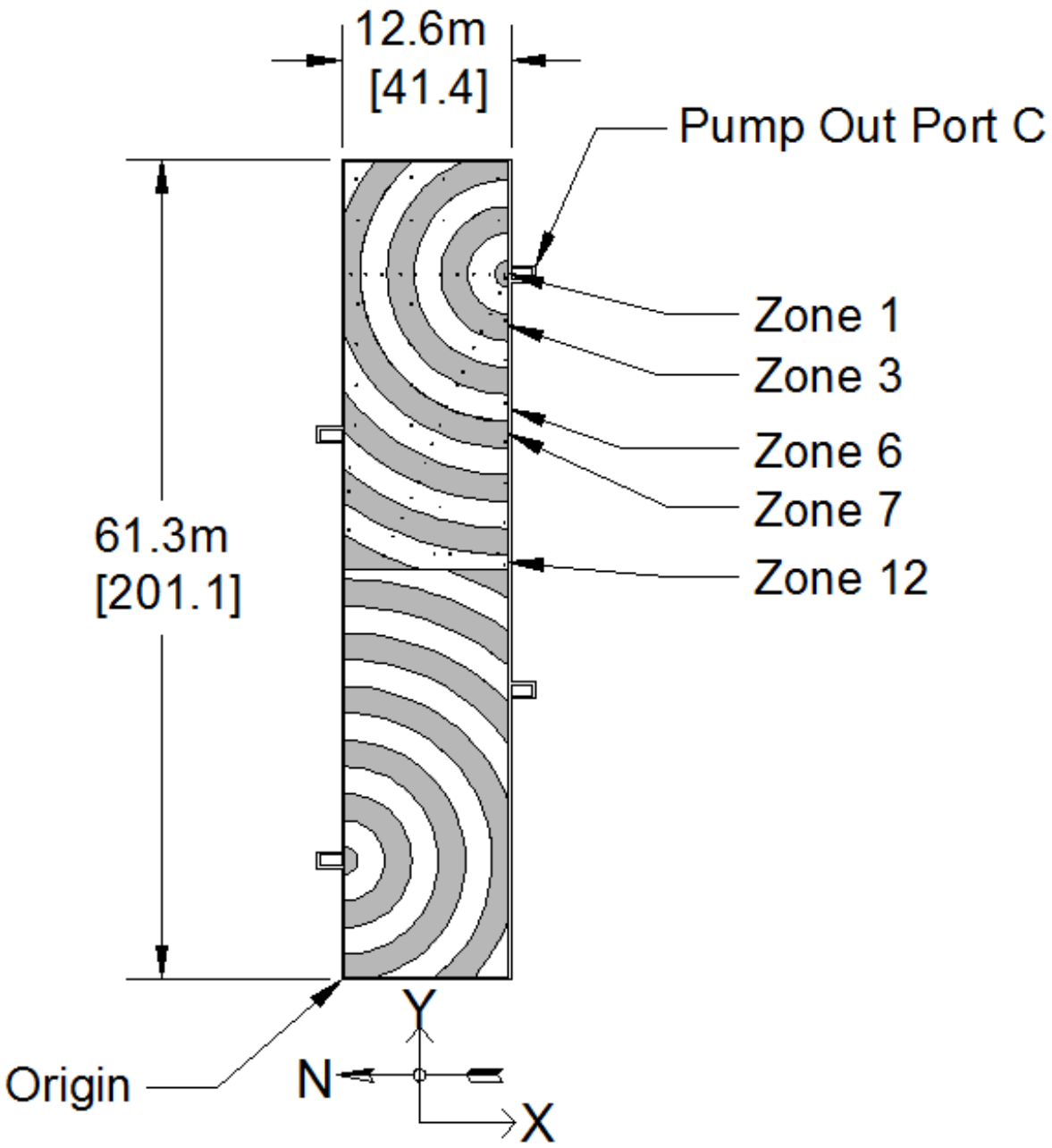

Figure 4.10 - Locations of foam depth measurement points for Runs 4 and 11 in which the device installed in Barn A, pump-out port C. See Table A.4 for measurement point coordinates.

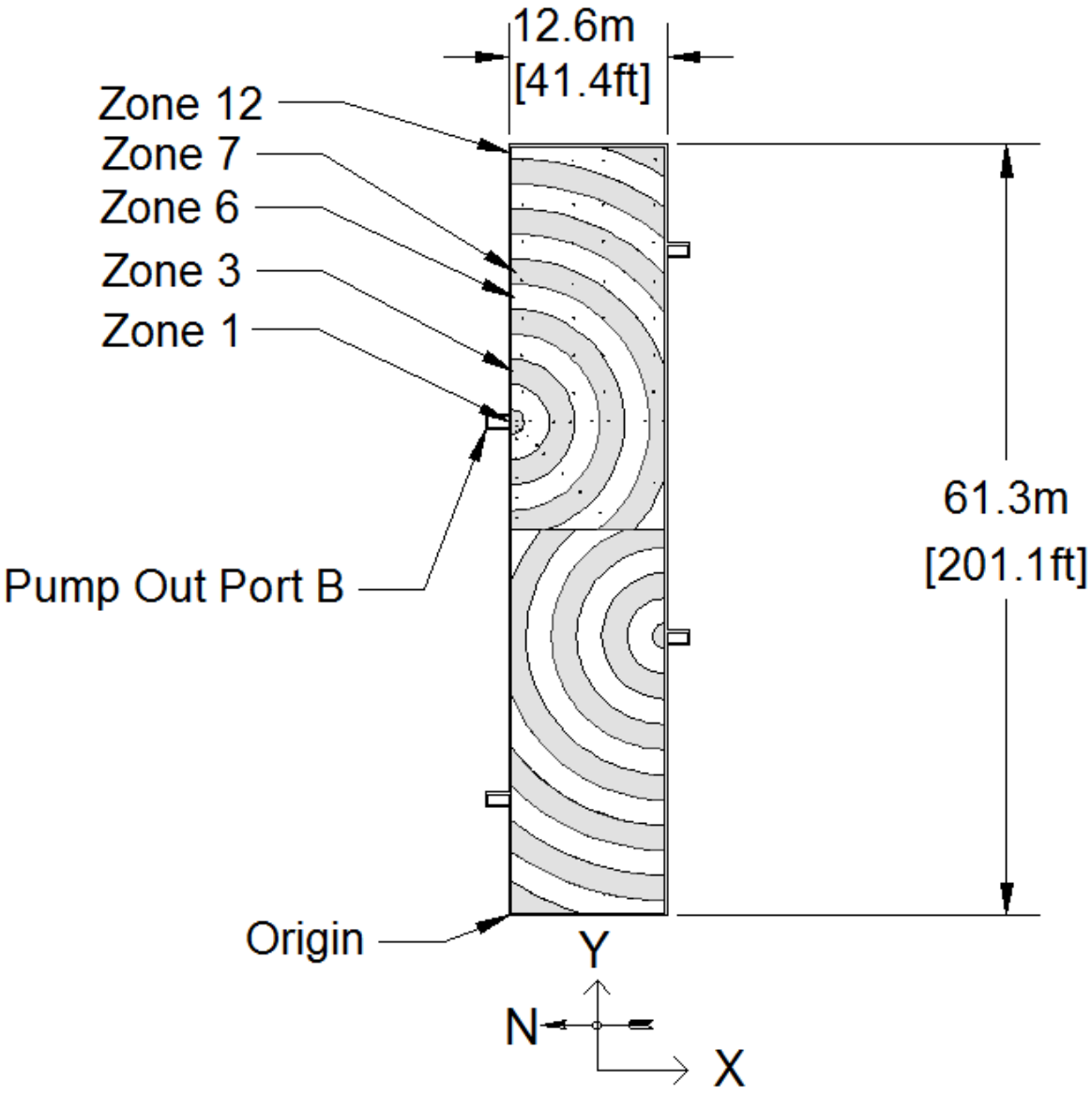

Figure 4.11 - Locations of foam depth measurement points for Runs 5 and 12 in which the device installed in Barn B, pump-out port B. See Table A.5 for measurement point coordinates.

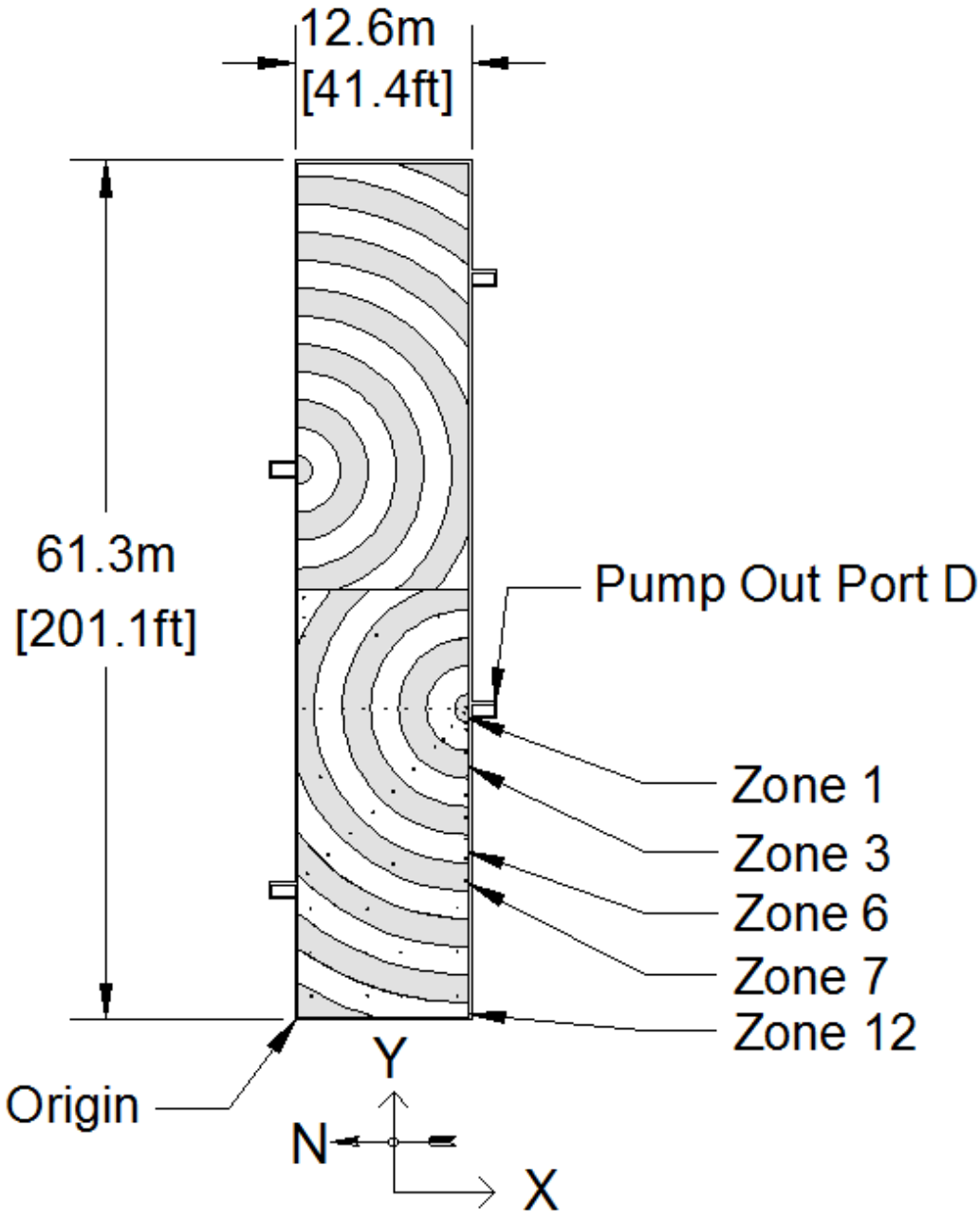

Figure 4.12 - Locations of foam depth measurement points for Runs 6 and 13 in which the device installed in Barn B, pump-out port D. See Table A.6 for measurement point coordinates.

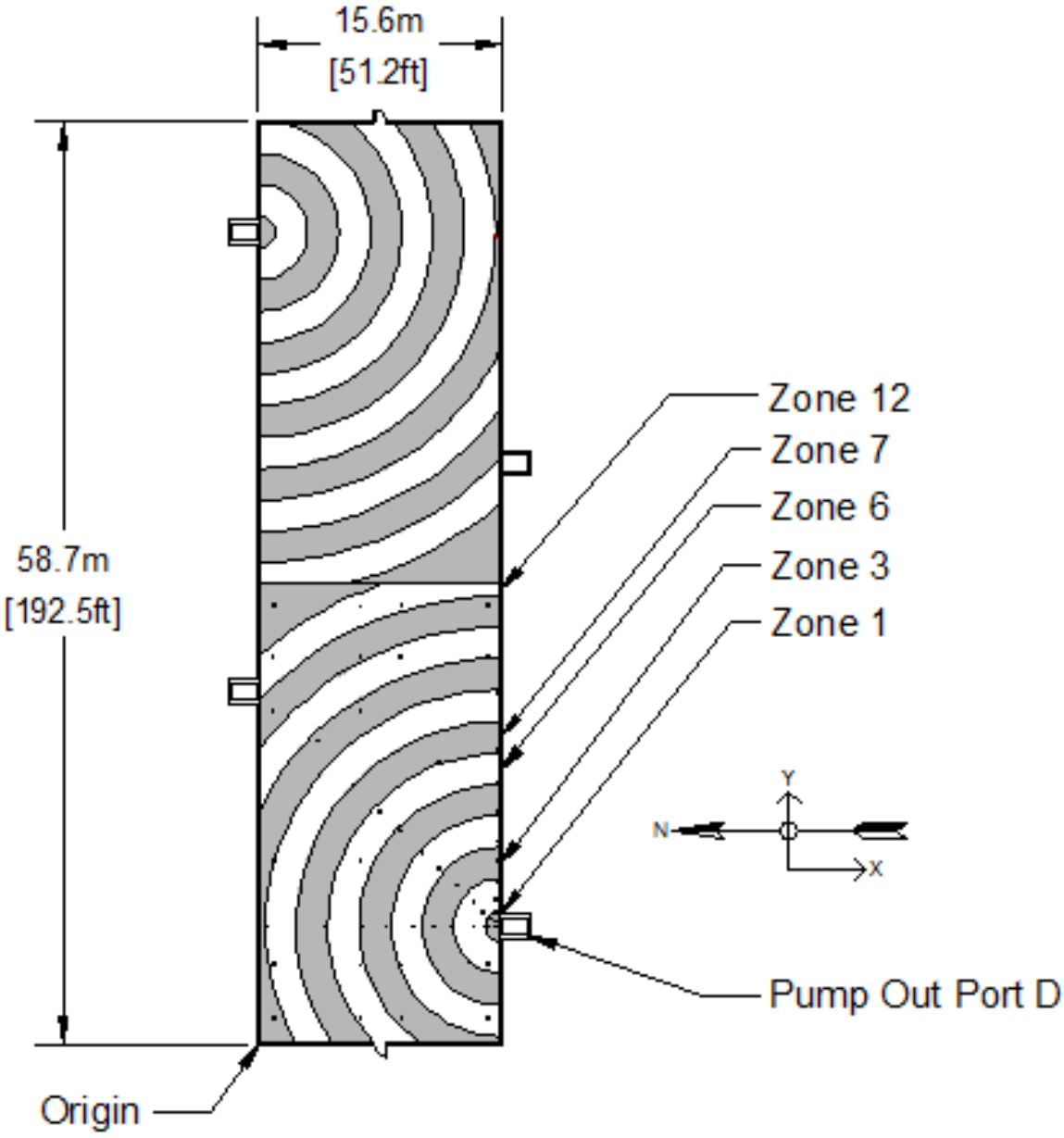

Figure 4.13 - Locations of foam depth measurement points for Run 7 in which the device installed in Barn C, pump-out port D. See Table A.7 for measurement point coordinates.

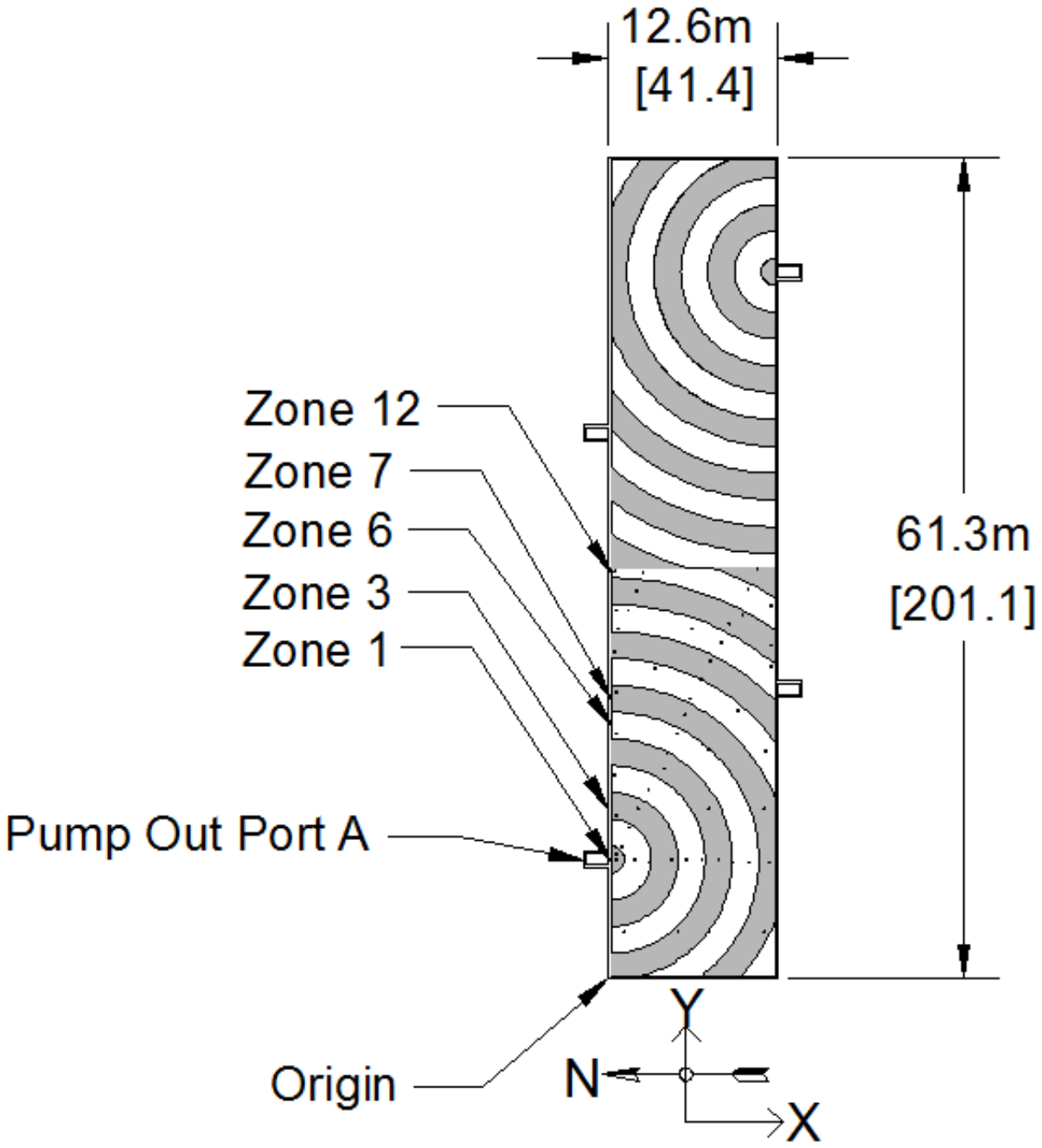

Figure 4.14 - Locations of foam depth measurement points for Run 10 in which the device installed in Barn A, pump-out port A. See Table A.8 for measurement point coordinates.

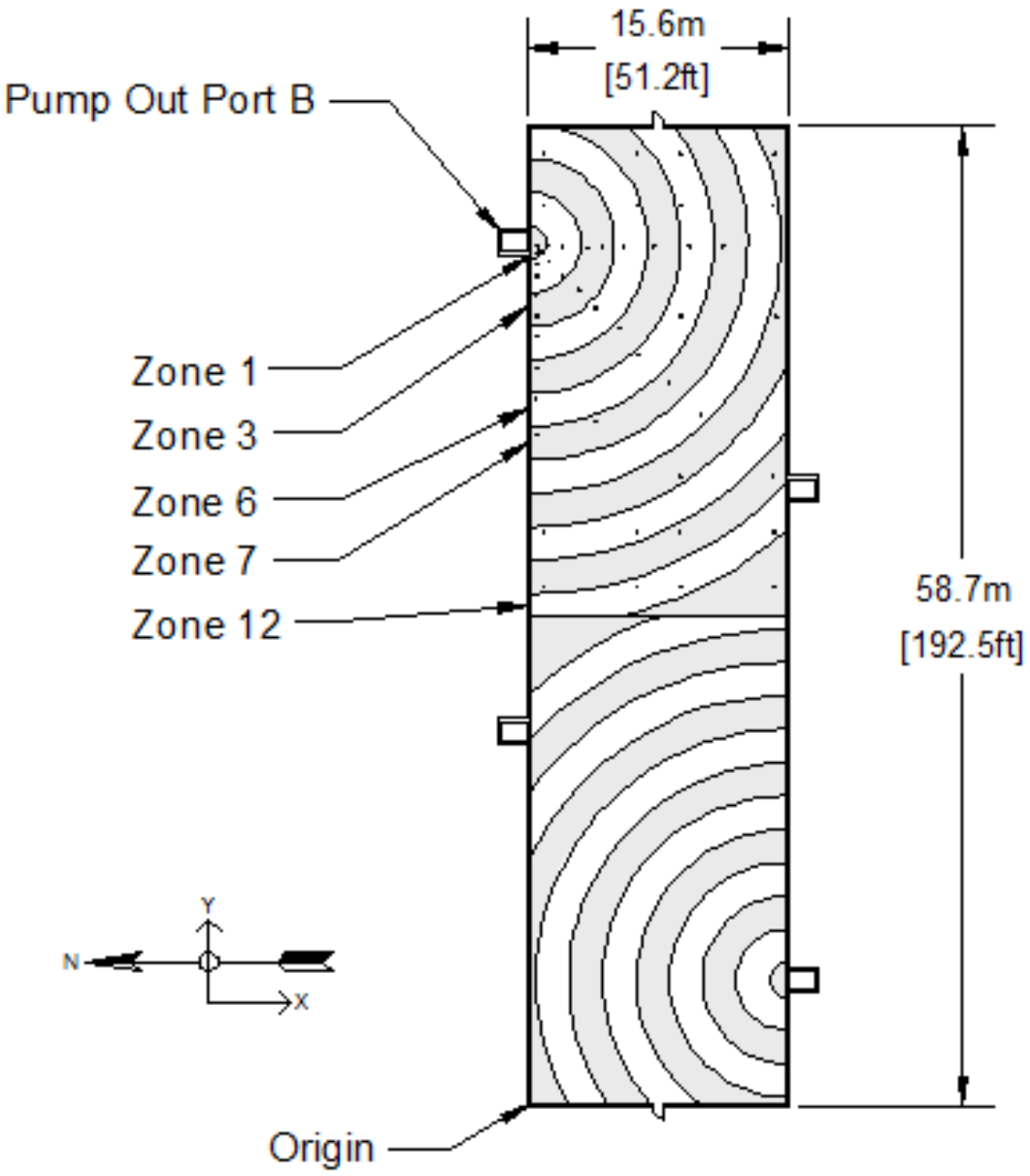

Figure 4.15 - Locations of foam depth measurement points for Run 14 in which the device installed in Barn C, pump-out port B. See Table A.9 for measurement point coordinates.

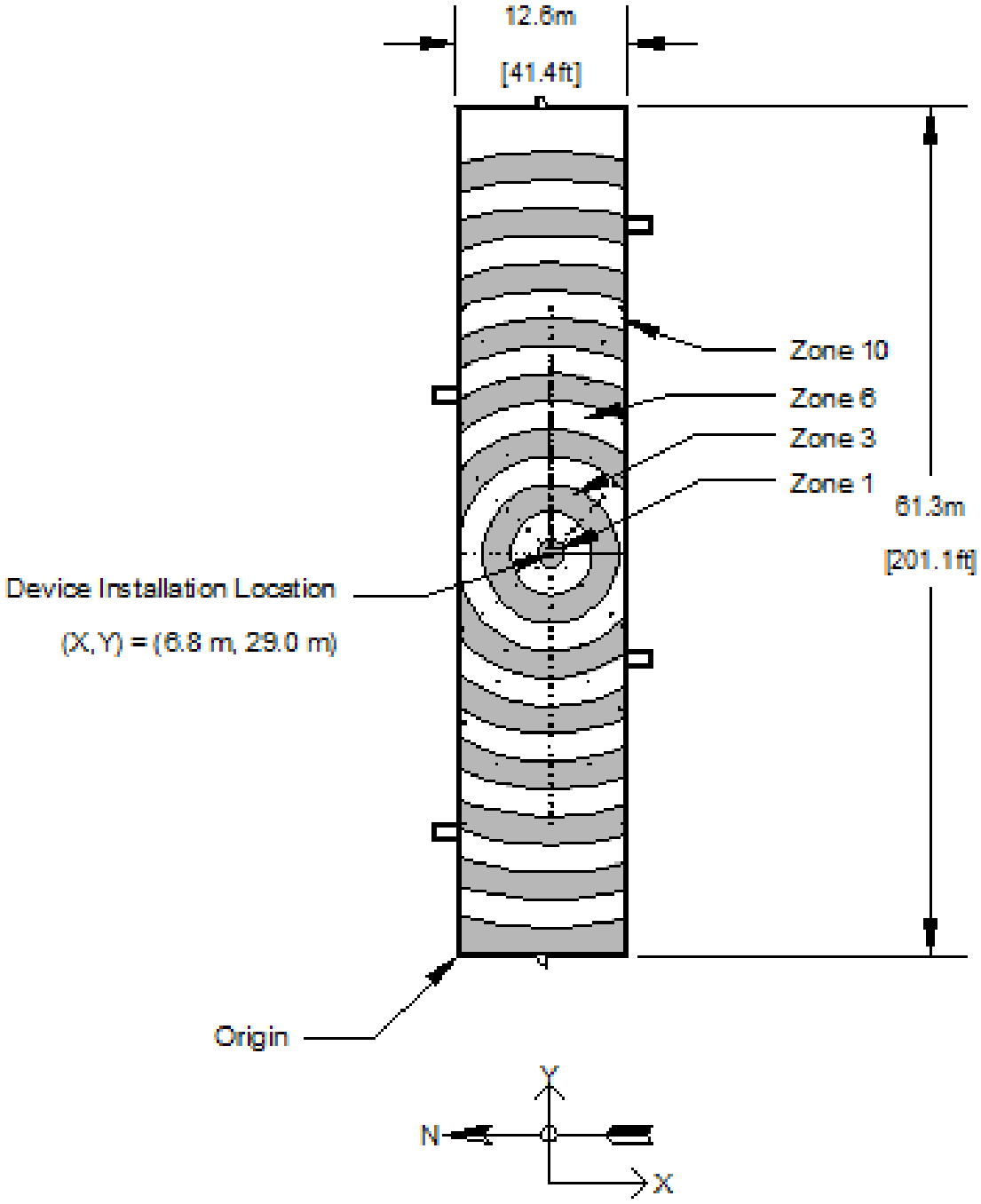

Figure 4.16 - Locations of foam depth measurement points for Run 15 in which the device installed inside Barn A at the (X,Y) = (6.8 m, 29.0 m). See Table A.10 for measurement point coordinates.

4.7 Tables

Table 4.1 – Mechanical foam mitigation device installation location coordinates. Please refer to Figure 4.2 for coordinate system origin and pump-out port locations.

Run	Barn	Pump Out Port	Operation C=Continuous E=Episodic	X		Y	
				(m)	*(ft)*	*(m)*	*(ft)*
1	A	C	C	12.8	42.0	52.7	172.9
2	A	A	C	-0.6	-2.0	9.0	29.5
3	A	C	C	12.8	42.0	52.7	172.9
4	A	C	C	12.8	42.0	52.7	172.9
5	B	B	C	-0.6	-2.0	40.5	132.9
6	B	D	C	12.8	42.0	21.4	70.2
7	C	D	C	15.9	52.2	7.6	24.9
8	A	A	E	-0.6	-2.0	9.0	29.5
9	A	C	E	12.8	42.0	52.7	172.9
10	A	A	E	-0.6	-2.0	9.0	29.5
11	A	C	E	12.8	42.0	52.7	172.9
12	B	B	E	-0.6	-2.0	40.5	132.9
13	B	D	E	12.8	42.0	21.4	70.2
14	C	B	E	-0.6	-2.0	51.7	169.6
15	A	-----	C	6.8	22.3	29.0	95.1

Table 4.2a – An example of the steps used to process one set of time series data collected from one run of device testing.

Numbers above columns refer to steps outlined in Section 4.4.3								1							2	3	4	5	6	7	8	9	10
Zone	# of Points	A (m^2)		*Initial Foam Measurements*						*Final Foam Measurements*							Δ d (mm)	Δ d / Δ t (mm/h)	Δ V		Δ V / Δ t (FDR)		nFDR (FDR / d_i)	
								Mean	V_i (m^3)						V_f (m^3)			(m^3)	%	(m^3)/h	%	m^2/h	%/h-m
1	2	1.6	d_i (m)	0.183	0.161			0.172	0.27	0.164	0.159			0.162	0.004	0.159	0.164	0.25	11	9	0.016	6%	0.01	5%	0.05	20%
			t_i (h)	1.1	1.2			1.1		2.2	2.3			2.2	0.0	2.2	2.3									
2	4	12.6	d_i (m)	0.222	0.248	0.243	0.190	0.226	2.84	0.209	0.231	0.215	0.195	0.213	0.015	0.195	0.231	2.67	13	12	0.166	6%	0.15	5%	0.52	18%
			t_i (h)	1.1	1.1	1.2	1.3	1.2		2.2	2.2	2.3	2.4	2.3	0.1	2.2	2.4									
3	4	25.1	d_i (m)	0.276	0.258	0.247	0.255	0.259	6.51	0.255	0.236	0.238	0.245	0.244	0.009	0.236	0.255	6.12	16	14	0.390	6%	0.35	5%	1.24	19%
			t_i (h)	1.1	1.2	1.3	1.3	1.2		2.2	2.3	2.4	2.4	2.3	0.1	2.2	2.4									
4	5	37.7	d_i (m)	0.267 0.250	0.230	0.248	0.250	0.249	9.39	0.271 0.246	0.249	0.233	0.246	0.249	0.014	0.233	0.271	9.39	0	0	0.000	0%	0.00	0%	0.00	0%
			t_i (h)	1.1 1.3	1.1	1.2	1.2	1.2		2.2 2.4	2.2	2.3	2.3	2.3	0.1	2.2	2.4									
5	6	48.8	d_i (m)	0.308 0.276	0.337 0.257	0.242	0.248	0.278	13.57	0.301 0.279	0.320 0.261	0.236	0.241	0.273	0.033	0.236	0.320	13.32	5	4	0.244	2%	0.22	2%	0.74	5%
			t_i (h)	1.0 1.2	1.0 1.3	1.0	1.1	1.1		2.2 2.3	2.2 2.4	2.2	2.2	2.2	0.1	2.2	2.4									
6	8	51.4	d_i (m)	0.273 0.249	0.284 0.217	0.280 0.276	0.279 0.270	0.266	13.67	0.259 0.243	0.270 0.212	0.257 0.251	0.240 0.256	0.249	0.017	0.212	0.270	12.77	18	16	0.899	7%	0.81	6%	2.88	21%
			t_i (h)	1.0 1.1	1.0 1.2	1.0 1.3	1.1 1.3	1.1		2.2 2.2	2.2 2.3	2.2 2.4	2.2 2.4	2.2	0.1	2.2	2.4									
7	6	51.4	d_i (m)	0.270 0.349	0.273 0.273	0.261	0.326	0.292	15.02	0.263 0.323	0.264 0.268	0.245	0.326	0.282	0.034	0.245	0.326	14.48	11	9	0.540	4%	0.49	3%	1.64	11%
			t_i (h)	1.0 1.2	1.0 1.3	1.1	1.2	1.1		2.2 2.3	2.2 2.4	2.2	2.3	2.2	0.1	2.2	2.4									

Table 4.2b – An example of the steps used to process one set of time series data collected from one run of device testing continued.

Numbers above columns refer to steps outlined in Section 4.4.3									1								2	3	4	5	6	7	8	9	10
Zone	# of Points	A (m^2)		*Initial Foam Measurements*						*Final Foam Measurements*								Δ d (mm)	Δ d / Δ t (mm/h)	Δ V		Δ V / Δ t (FDR)		nFDR (FDR / d_i)	
								Mean	V_i (m^3)					Mean	SD	Min	Max	V_f (m^3)			(m^3)	%	(m^3)/h	%	m^2/h	%/h-m
8	4	33.6	d_i (m)	0.300	0.286	0.267	0.285	0.285	9.55	0.289	0.279	0.270	0.279	0.279	0.008	0.270	0.289	9.37	5	5	0.176	2%	0.16	2%	0.53	6%
			t_i (h)	1.0	1.0	1.2	1.3	1.1		2.2	2.2	2.3	2.4	2.2	0.1	2.2	2.4									
9	3	27.8	d_i (m)	0.284	0.279	0.319		0.294	8.17	0.253	0.274	0.284		0.270	0.016	0.253	0.284	7.51	24	22	0.658	8%	0.60	7%	2.05	25%
			t_i (h)	1.2	1.3	1.4		1.3		2.3	2.4	2.5		2.4	0.1	2.3	2.5									
10	4	26.8	d_i (m)	0.268	0.279	0.278	0.299	0.281	7.54	0.279	0.273	0.271	0.295	0.280	0.011	0.271	0.295	7.50	2	1	0.040	1%	0.04	0%	0.13	2%
			t_i (h)	1.2	1.2	1.4	1.6	1.4		2.3	2.3	2.5	2.7	2.5	0.2	2.3	2.7									
11	4	26.2	d_i (m)	0.276	0.286	0.263	0.257	0.271	7.09	0.274	0.288	0.259	0.254	0.269	0.015	0.254	0.288	7.04	2	2	0.046	1%	0.04	1%	0.15	2%
			t_i (h)	1.2	1.4	1.6	1.8	1.5		2.3	2.5	2.7	2.9	2.6	0.2	2.3	2.9									
12	7	21.6	d_i (m)	0.271 0.266	0.258 0.269	0.337 0.282	0.275	0.280	6.05	0.273 0.258	0.270 0.265	0.326 0.268	0.277	0.277	0.023	0.258	0.326	5.99	3	3	0.065	1%	0.06	1%	0.20	3%
			t_i (h)	1.2 1.8	1.4 1.8	1.6 1.8	1.6	1.6		2.3 2.9	2.5 2.9	2.7 2.9	2.7	2.7	0.2	2.3	2.9									
13	2	6.5	d_i (m)	0.272	0.292			0.282	1.83	0.250	0.296			0.273	0.033	0.250	0.296	1.77	9	8	0.058	3%	0.05	3%	0.19	10%
			t_i (h)	1.4	1.6			1.5		2.5	2.7			2.6	0.2	2.5	2.7									
Series 2 Summary		A_s (m^2)							$V_{i,s}$ (m^3)								$V_{f,s}$ (m^3)	Δd_s (mm)	$\Delta d_s / \Delta t_s$ (mm/h)	ΔV_s (m^3)	%	$\Delta V_s / \Delta t_s$ (sFDR) (m^3)/h	%	sFDR / $d_{i,s}$ m^2/h	%/h-m
		371.1						Mean $d_{i,s}$ (m)	0.273[1]								98.2[2]	9[1]	8[1]	3.3[2]	3%	3.0[2]	3%	10.3[2]	10%
								Mean $t_{i,s}$ (h)	1.3																

[1] Weighted average (by zone area)

[2] Sum of zones

Table 4.3 – An example of the steps used to process time series summary values from one run of device testing to summarize that run.

Numbers above columns refer to steps outlined in Section 4.4.3.3					1	2	3	4	5	6
	Δt_s[1] (h)	$V_{f,s}$ (m^3)	Δd_s (m)	$\Delta d_s / \Delta t_s$ (m/h)	ΔV_s (m^3)	%	$\Delta V_s / \Delta t_s$ (sFDR) (m^3)/h	%	sFDR / $d_{i,s}$ m^2/h	%/h-m
Time Series 1	1.3	101.49	0.016	0.013	5.92	6%	4.70	4%	16.25	15%
Time Series 2	1.1	98.19	0.009	0.008	3.30	3%	2.99	3%	10.35	10%
Time Series 3	1.0	94.58	0.010	0.009	3.62	4%	3.48	4%	12.04	12%
Time Series 4	0.9	92.44	0.006	0.006	2.13	2%	2.38	3%	8.22	9%
Time Series 5	1.0	89.05	0.009	0.009	3.39	4%	3.46	4%	11.95	13%
Run 3 Summary				Mean	-	-	3.40	3%	11.76	12%
				Sum	18.36	18%	-	-	-	-
				SD	-	-	0.85	1%	2.95	3%
				Min	-	-	2.38	3%	8.22	9%
				Max	-	-	4.70	4%	16.25	15%

[1] Series final mean time minus series initial mean time

Chapter 5: Results

5.1 Laser Distance Meter Validation

The laser distance meter was validated using a thirty foot tape measure accurate to 1/16 in. Measurements were made to manure foam, liquid manure, and concrete surfaces using both devices. A paired t-test was then used to compare measurements made with the laser distance meter to those made with the tape measure for each surface.

When taking measurements with the tape measure, difficulty was encountered measuring to both foam and liquid surfaces. It was nearly impossible to avoid pushing the end of the tape measure through the foam or liquid's surface and this difficulty biased measurements made with the tape measure to these surfaces. The mean absolute difference between the tape measure and the laser distance meter was -5 mm (-0.2 in) with a standard deviation of 2 mm (0.1 in) when measuring to a manure foam surface (Table 5.1). When measuring to a liquid surface, the mean absolute difference was -3mm (-0.1 in) with a standard deviation of 2 mm (0.1 in) (Table 5.2). Measurements with both devices to foam and liquid surfaces were significantly different when compared using paired t-tests ($P<0.001$). Due to the bias in these measurements, they were excluded and only the set of measurements made to a concrete surface were used to validate the laser distance meter.

The mean absolute difference between the tape measure and the laser distance meter was 0.0 mm (0.0 in) with a standard deviation of 1 mm (0.0 in) when measuring to a concrete surface (Table 5.3). The maximum absolute difference observed was 3 mm (0.1 in). The measurements obtained using the tape measure and the laser distance meter when measuring to a concrete surface were not significantly different when analyzed using a paired t-test (p-value = 0.347).

Based on these results, it was concluded that the laser distance meter could be used in this experiment.

5.2 Results from MFMD Runs

5.2.1 Introduction

Fifteen MFMD runs were conducted as summarized previously in Table 4.1. In Runs 1 through 7 MFMD's were installed in the barns' pump-out ports and were operated continuously. Runs 8 through 14 also had the MFMD's installed in the barns' pump-out ports, but in these runs the devices were operated episodically. Run 15 was a special case of continuous operation in which the MFMD was installed inside near the center of Barn A. For each run, the total change in foam volume (ΔV), the average foam destruction rate (FDR), and the normalized foam destruction rate (nFDR) were calculated. Foam depths did not differ greatly between runs and because of this, the MFMD was evaluated on the basis of the change foam volume and FDR (Table 5.4 and 5.5).

5.2.2 Continuous Runs

Runs 1 through 4 took place in Barn A. Initial mean foam depths ranged from 0.222 m (8.8 in) to 0.320 m (12.6 in) (Table 5.4). In these four runs, the MFMDs were installed in the manure pump-out ports and were operated continuously for up to 5.5 h. Percent ΔV ranged from a minimum of 10% in Run 4 to a maximum 18% in Run 3. This equated to 6.2 m^3 (218.6 ft^3) and 18.4 m^3 (648.4 ft^3) in Runs 4 and 3, respectively. Each FDR for Runs 1-4 was calculated and was found to be approximately 3%/h (Table 5.6 – 5.9). Run 2 was notable because after about 4.5 h of device operation, the observation was made that foam no longer appeared to be flowing to the

MFMD. The data validated this observation and in time series 5, taken during the final hour of operation, the ΔV was 0% with an FDR of 0%/h (Table 5.7), indicating that runout had been reached.

Run 15 was a special case of continuous operation, since the MFMD was installed inside Barn A rather than in one of the barn's pump-out ports. The initial foam depth for this run was 0.232 m (9.1 in) and the device operated for 3.7 h (Table 5.4). In that time it destroyed 19% of the initial foam volume present (Table 5.10) which equates to 10.7 m^3 (378.6 ft^3) of foam. The average FDR for this run was 6%/h (±2%/h).

Runs 5, 6, and 7 all had initial foam depths of less than 0.1 m (4.0 in) and ΔV's that ranged from 2% in Run 5 to 6% in Run 6. Run 6 destroyed 1.9 m^3 (65.2 ft^3) of foam and Runs 5 and 7 destroyed 0.7 m^3 (25.4 ft^3) and 0.7 m^3 (24.3 ft^3) of foam, respectively. Each run had a FDR of 2%/h or less (Table 5.4). Runs 5 and 6 were both conducted in Barn B using pump-out ports B and D, respectively and Run 7 was conducted in Barn C with the device installed in pump-out port D. These three runs demonstrated that the MFMD was not particularly effective at eliminating foam for depths less than about 0.1 m (4.0 in), thus these three continuous runs were excluded from further analysis.

5.2.3 Episodic Runs

Runs 8 through 11 were all conducted in Barn A. Run 8 utilized a duty cycle of 1 h on: 2 h off. Run 9 was assigned a duty cycle of 0.5 h on: 1 h off. Runs 10 and 11 both had duty cycles of 1 h on: 1 h off. Foam depths ranged from 0.254 m (10.0 in) to 0.348 m (13.7 in) (Table 5.5) and the longest run duration occurred in Run 8 at 6.7 h with a total of 2.6 h of device run time. Percent ΔV ranged from 8% in Run 10 to 11% in Run 8 and this equated to a 7.4 m^3 (263.1 ft^3)

to 13.5 m^3 (476.7 ft^3) reduction in foam volume, respectively. The FDR in Runs 8 and 9 was 5%/h. Runs 10 and 11had FDRs of 4%/h and 5%/h, respectively (Table 5.11-5.14).

Runs 12, 13, and 14 all had initial foam depths less than 0.1 m (4.0 in) (Table 5.5). The minimum percent ΔV was 0% and occurred in Run 13. The maximum percent ΔV was 11% and came in Run 14. Run 14 destroyed 3.2 m^3 (111.4 ft^3) of foam and its FDR was 5%/h. Runs 12 and 13 had FDRs of 2%/h and 0%/h respectively. These three runs were excluded from further analysis for reasons previously given in section 5.2.2.

5.3 MFMD Performance Assessment

5.3.1 Introduction

To assess the MFMD performance, answers were sought to three specific questions. The first question was: "Is the purpose-built mechanical foam mitigation device capable of removing foam from swine deep-pit manure storage?" The second question was: "Is there a difference between episodic and continuous operation?" The final question was: "Over what distance will a MFMD destroy foam?" To answer these questions, data from runs conducted in Barn A (Runs 1-4, 8-11, and 15) were utilized and continuous and episodic runs were analyzed separately. Although the MFMD was operated continuously in Run 15, it was analyzed separately due to its unique installation location. Data from Runs 5-7 and 12-14 were excluded based upon reasons given in section 5.2.2.

5.3.2 General Efficacy of MFMD

To determine the general efficacy of the MFMD, the cumulative percent ΔV for each time series measurement within a run was plotted against elapsed time for that run. Runs 1-4 and Run 15 were plotted together and Runs 8-11 were plotted together (Figure 5.1 and Figure 5.2).

Next, time series measurements from Runs 1-4taken between 0.5 to 1.5 h of elapsed time were grouped together, as were time series measurements taken between 1.5 to 2.5 h, 2.5 to 3.5 h, 3.5 to 4.5 h, and >4.5 h of elapsed time. Once grouped, the average cumulative percent ΔV and the average elapsed time were calculated for each grouping. Runs 8-11were similarly grouped and averaged (Table 5.15 and Table 5.16). Since Run 15 differed from Runs 1-4 and 8-11in installation location, time series measurements from Run 15 were simply reported.

On average in Runs 1-4 (continuous operation, MFMD installed in the pump-out port), the device caused a $\overline{\Delta V}$ = 3% of the initial foam volume destroyed in 1.0 h of elapsed time, $\overline{\Delta V}$ = 6% in 2.0 h, $\overline{\Delta V}$ = 9% in 3.1 h, $\overline{\Delta V}$ = 12% in 3.9 h, and $\overline{\Delta V}$ = 16% of the initial foam volume destroyed in 5.1 h of elapsed time (far right column in Table 5.15). On average in Runs 8-11 (episodic operation, MFMD installed in the pump-out port), the device caused a $\overline{\Delta V}$ = 3% of the initial foam volume destroyed in 0.8 h of elapsed time, $\overline{\Delta V}$ = 5% in 2.1 h, $\overline{\Delta V}$ = 8% in 2.8 h, $\overline{\Delta V}$ = 8% in 3.7 h, and $\overline{\Delta V}$ = 11% of the initial foam volume destroyed in 5.9 h of elapsed time (far right column in Table 5.16). In Run 15 ΔV = 10% of the initial foam volume destroyed in 1.2 h of elapsed time, ΔV = 15% in 2.3 h, and ΔV = 19% of the initial foam volume destroyed in 3.3 h of elapsed time. It should be noted that elapsed time is distinct from device operation time. Elapsed time is the time elapsed since the start of a run and began when the MFMD was initially turned on. Device operation time is defined as the actual number of hours the device was

operating during a run. In continuous runs elapsed time = device operation time, however in episodic runs these values differed. Runs 8-11 had device operation times of 2.6, 2.0, 2.0, and 2.0 h respectively (Table 5.5). A more thorough comparison of operating strategies and the effect device operation time on performance will be made in section 5.3.3.

The results obtained from analyzing the mean percent $\overline{\Delta V}$ of Runs 1-4 and 8-11 and the percent ΔV of Run 15 show that the device is able to destroy foam. These results indicate that in foam depths ranging from 0.222 m (8.8 in) to 0.348 m (13.7 in) the MFMD is capable of destroying up to 11% of the foam volume present in 5.9 h of elapsed time when operated episodically and installed in a pump-out port;16% of the initial foam volume present in 5.1 h of elapsed time when operated continuously and installed in a pump-out port; and 19% of the initial foam volume present in 3.3 h of elapsed time when operated continuously and installed inside, near the center of the barn. Thus, in all tested operating strategies, the MFMD measurably destroyed foam.

5.3.3 Comparison of Operation Strategies

As noted in section 5.3.2, when comparing continuous versus episodic operation in terms of cumulative percent foam volume destroyed over elapsed time, continuous operation appears superior; however, this approach fails to account for the fact that in an episodic run the MFMD is only active for a portion of the total run elapsed time. To accurately assess differences in episodic and continuous operation, comparisons must be made on the basis of foam destruction rate (FDR). The FDR was calculated in terms of device operation time rather than elapsed time (section 4.5.3) making it a suitable metric to compare episodic and continuous operation schemes.

For Runs 1-4 (continuous operation), the mean FDR for each run was very consistent with a value of 3%/h for each Run and a range of 0 to 4%/h. The minimum FDR occurred at the end of Run 2. During the last hour of Run 2 it was observed that foam stopped flowing to the device and this was interpreted as the device reaching runout. The FDR calculated for time series 5 in Run 2 confirms this observation. The maximum FDR observed in Runs 1-4 was 4%/h and occurred in Runs 1, 2, and 3. Run 15 was different from the other continuous runs and had a mean FDR of 6%/h (standard deviation = 2%/h) (Table 5.17). Run 15 featured the MFMD installed inside the barn while in Runs 1 through 4 the device was installed in a pump port. In light of this difference, Run 15 was not considered when comparing episodic operation to continuous operation in Barn A and will be discussed in the next section.

The mean FDR values for episodic Runs 8-11 ranged from 4%/h to 5%/h and a minimum of 3%/h and a maximum of 6%/h. The minimum FDR occurred in both Runs 8 and 10. The maximum FDR occurred in Runs 9 and 10 (Table 5.18). Run 8 featured a duty cycle of 1 h on: 2 h off; Run 9 had a duty cycle of 0.5 h on: 1 h off; and Runs 10 and 11 had duty cycles of 1 h on: 1 h off.

Based on these results, episodic operation has an advantage over continuous operation in terms of FDR in foam depths greater than 0.200 m (8.8 in) when the MFMD is installed in a pump-out port. Figure 5.3, which depicts time series FDRs for Runs 1-4, 8-11, and 15 conducted in Barn A plotted against elapsed time, highlights this trend in that data points from episodic runs (hollow shapes) are generally located higher on the graph than data points from continuous runs (solid shapes). However, the mean difference between the average FDR for episodic and continuous operation is 2%/h which is smaller than the mean FDR for continuous operation (3%/h) (Table 5.17 and 5.18). This indicates that while a MFMD operated episodically destroys

more foam while it is running, the improved performance is not significant enough to overcome the loss of foam destruction when the device is idle when compared to a continuously operated device. The implication is that over the same period of elapsed time, continuous operation will destroy a greater volume of foam than episodic operation, at least in the cases tested by these runs.

5.3.4 Installation Location

Only runs that featured continuous operation of the MFMD in Barn A were used to assess differences in pump-out port versus inside the barn installation. In Run 15 the MFMD was installed inside, near the center of Barn A while Runs 1 through 4 had the device installed in one of the barn's pump-out ports. During Run 15, the total $\Delta V = 19\%$ of the initial foam volume destroyed in 3.3 h of elapsed time compared to $\Delta V = 12\%$ in 3.8 h for Run 1, $\Delta V = 14\%$ in 5.5 h for Run 2, $\Delta V = 18\%$ in 5.3 h for Run 3, and $\Delta V = 9\%$ in 3.3 h for Run 4. When time series measurements taken at similar elapsed times are compared, Run 15 appears to have an even greater advantage over Runs 1-4. At 3.3 h of elapsed time, $\Delta V = 19\%$ of initial volume of foam destroyed for Run 15; at 3.2 h, $\Delta V = 9\%$ for Run 1; at 3.7 h, $\Delta V = 10\%$ for Run 2; at 3.4 h, $\Delta V = 12\%$ for Run 3; and at 3.3 h, $\Delta V = 9\%$ for Run 4(Table 5.19).

The mean percent FDR for Run 15 was 6%/h (±2%/h). Runs 1-4 had mean percent FDRs of 3%/h (±1%/h), 3%/h (±2%/h), 3%/h (±1%/h), and 3%/h (±1%/h), respectively. The maximum FDR observed in Run 15 was recorded with the first time series measurement at 1.2 h elapsed time and was 8%/h. The two subsequent times series measurements for Run 15 had FDRs of 4%/h and occurred at 2.3 h and 3.3 h of elapsed time. The maximum FDR observed in time series measurements from Runs 1-4 was 4%/h and occurred in times series 2 and 5 of Run 1 at

1.2 h and 3.8 h of elapsed time, respectively; time series 4 of Run 2 at 4.5 h of elapsed time; and times series 1, 3, and 5 of Run 3 at 1.3 h, 3.4 h, and 5.3 h of elapsed time, respectively (Table 5.17).

The results detailed in section 5.3.4 seem to indicate that installing the device inside the barn may offer an advantage to pump-out port installation. Caution should be taken when interpreting these results as only one run was conducted with the device installed within the barn. Further testing should be conducted to validate this conclusion and to better quantify the difference in device performance by installation location.

5.3.5 MFMD Performance over Distance

The cumulative change in foam volume over time in zones 3, 6, 7, and 12 was examined to ascertain the foam's response to the MFMD as distance increased. Zones 3, 6, 7, and 12 were annular in shape, 2 m (6.56 ft) wide, and had radii measuring 3.0 m (9.8 ft), 9.0 m (29.5 ft), 11.0 m (36.1 ft), and 21.0 m (68.9 ft) along the arc closest to the device. Runs 1 through 4 were analyzed together and Runs 8 through 11 were also grouped together for analysis. Run 15 was not examined in this analysis due to its unique installation location and because time series measurements were only collected out to zone 6, 9.0 m (29.5 ft) from the device. Time series measurements for zones 3, 6, 7, and 12 were extracted from each run and the cumulative percent foam volume destroyed was plotted against elapsed time for each run by zone. Time series measurements within each zone were then grouped by elapsed time and the groups averaged to get a mean cumulative percent foam volume destroyed for each hour. The working hypothesis behind this analysis was that zones closer to the device would see a reduction in volume sooner

than zones further away from the device and at some distance from the device gravity driven foam flow would cease.

This methodology was useful in examining the data from the continuous runs but was unhelpful in the analysis of the episodic runs. Episodic runs had fewer times series measurements collected while the device was in operation per unit of time elapsed relative to continuous runs. During continuous, runs time series measurements were taken hourly, but during episodic runs time series measurements were collected before each change in operational state, thus only half the measurements were collected when the MFMD was in operation. For example, if Run 8 had been a continuous run, over the 6.7 hour duration six time series measurements would have been collected. Since Run 8 had a duty cycle of 1 h on: 2 h off, only three time series measurements were collected that were useful for analysis. The result was that some groupings of episodic time series measurements contained a single time series measurement from a single run. Because of this, continuous Runs 1-4 were used to evaluate the foam's response to the MFMD as distance from the device increased.

At approximately1 h of elapsed time, zones 3, 6, 7 and 12 of Runs 1-4 had mean cumulative percent ΔVs of 4% (±4%), 3% (±3%), 1% (±1%), and 2% (±1%) initial foam volume destroyed, respectively. At approximately3 h of elapsed time, zones 3, 6, 7 and 12 of Runs 1-4 had mean cumulative percent ΔVs of 15% (±5%), 13% (±4%), 7% (±4%), and 5% (±2%) initial foam volume destroyed, respectively. At approximately5.1 h of elapsed time, zones 3, 6, 7 and 12 of Runs 1-4 had mean cumulative percent ΔVs of 23% (±7%), 18% (±3%), 18% (±1%), and 11% (±3%) initial foam volume destroyed, respectively(Table 5.20).

Figure 5.4 clearly shows that as distance from the device increases, the mean percentage of foam volume destroyed decreases, but foam is eliminated throughout the area of interest. This data indicates that when an MFMD is installed in a pump out port and operated continuously, a small gradient is established in the foam. Foam destruction is greatest in zones closest to the device, creating a void in the foam. Foam located more distantly from the MFMD flows into this void, but since the device destroys foam at a point, the foam flow effectively encounters a bottle neck and slows. Thus, as distance from the device increases, the change in volume in response to device operation decreases. These results demonstrate that when installed in a pump-out port and operated continuously, the device is able to draw foam over a radial distance of at least 21.0 m (68.9 ft). Further research is needed to establish the maximum distance over which the device will remove foam, to determine if that distance varies with significant changes in foam depth, and to determine the optimum location of an MFMD in a Barn.

5.4 Figures

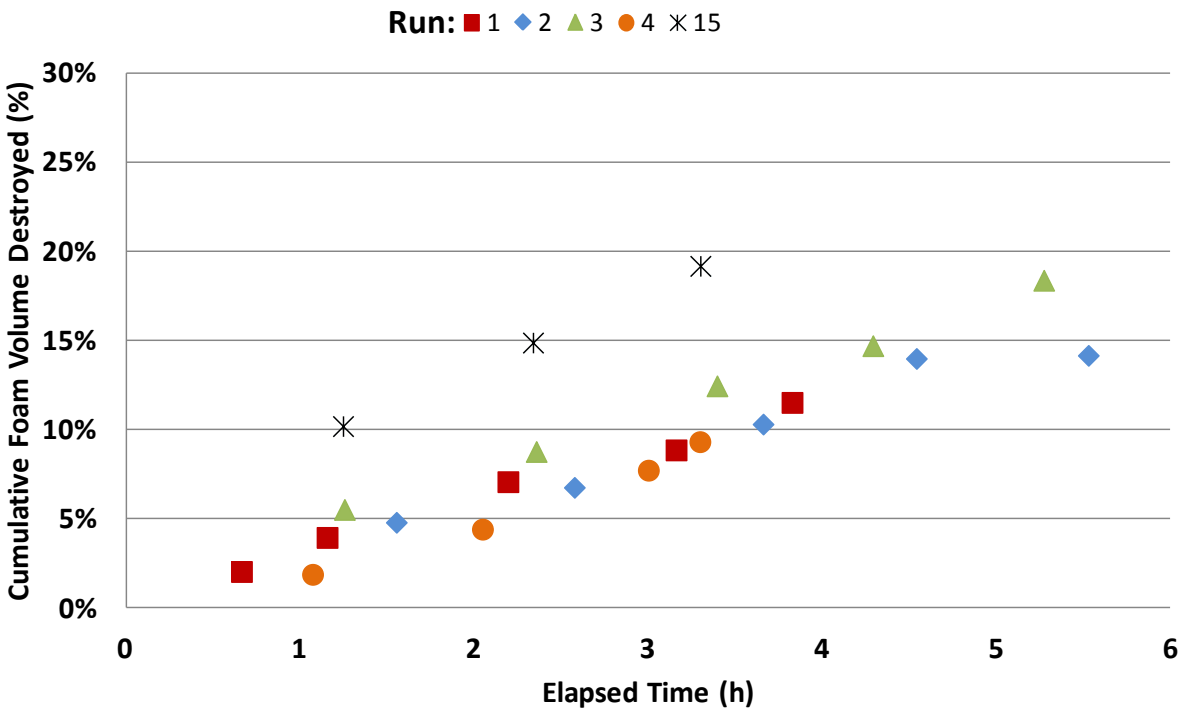

Figure 5.1- Cumulative percent of initial foam volume destroyed plotted against time elapsed since device start up for Runs 1-4 and 15. In these runs the device was installed in a pump-out port of Barn A and operated continuously (Table 4.1 and Figure 4.2).

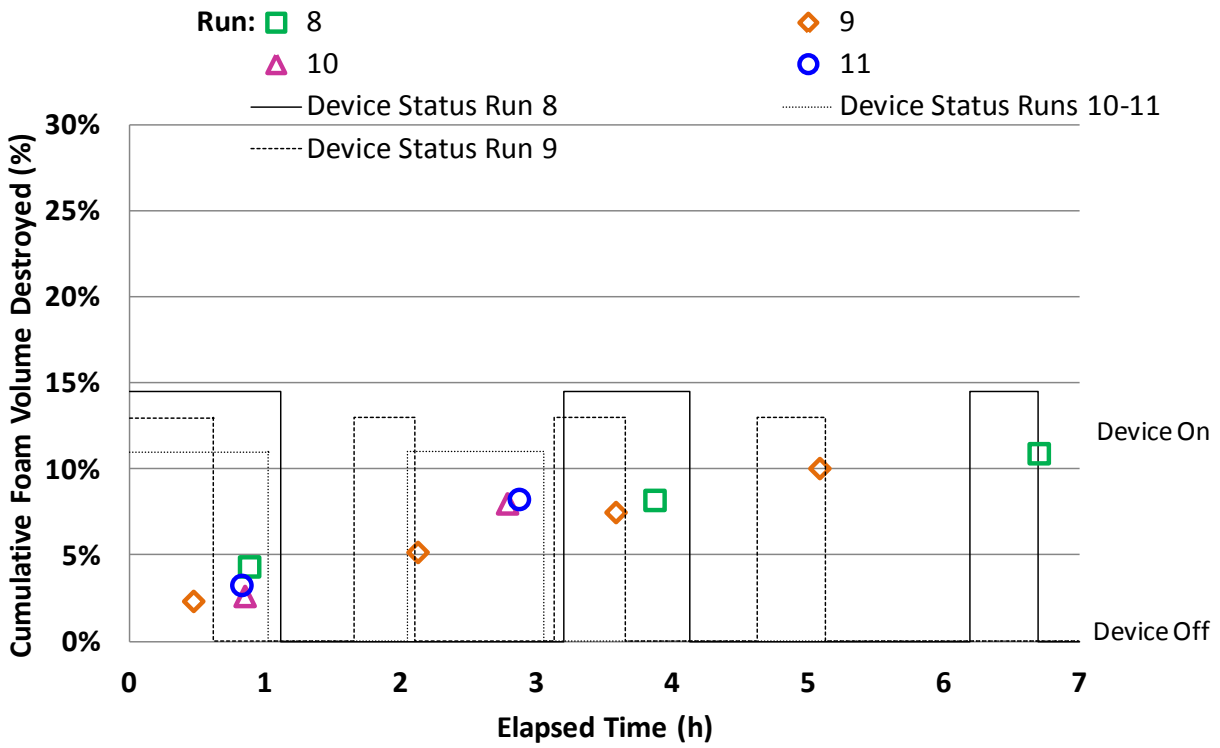

Figure 5.2 - Cumulative percent initial foam volume destroyed plotted against time elapsed since device start up for Runs 8-11.

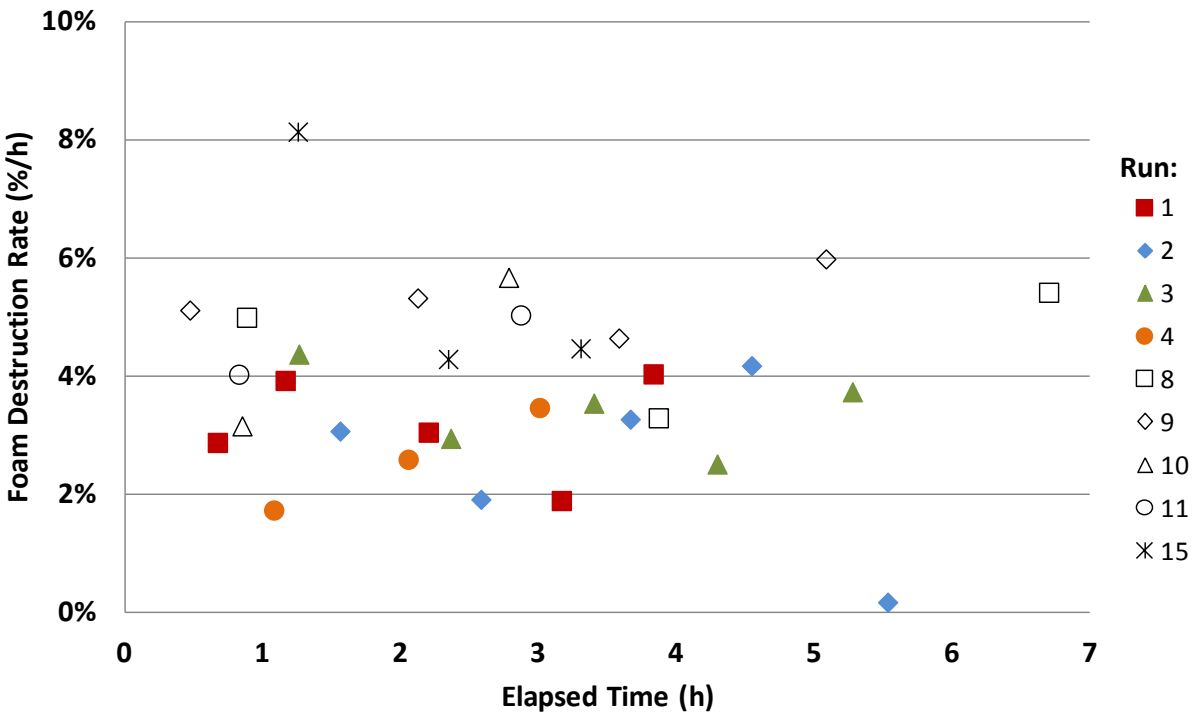

Figure 5.3 - Foam destruction rate calculated for each time series measurement in Runs 1-4, 8-11, and 15. The foam destruction rate was calculated based upon the change in foam volume and the change in device operation time between measurement intervals.

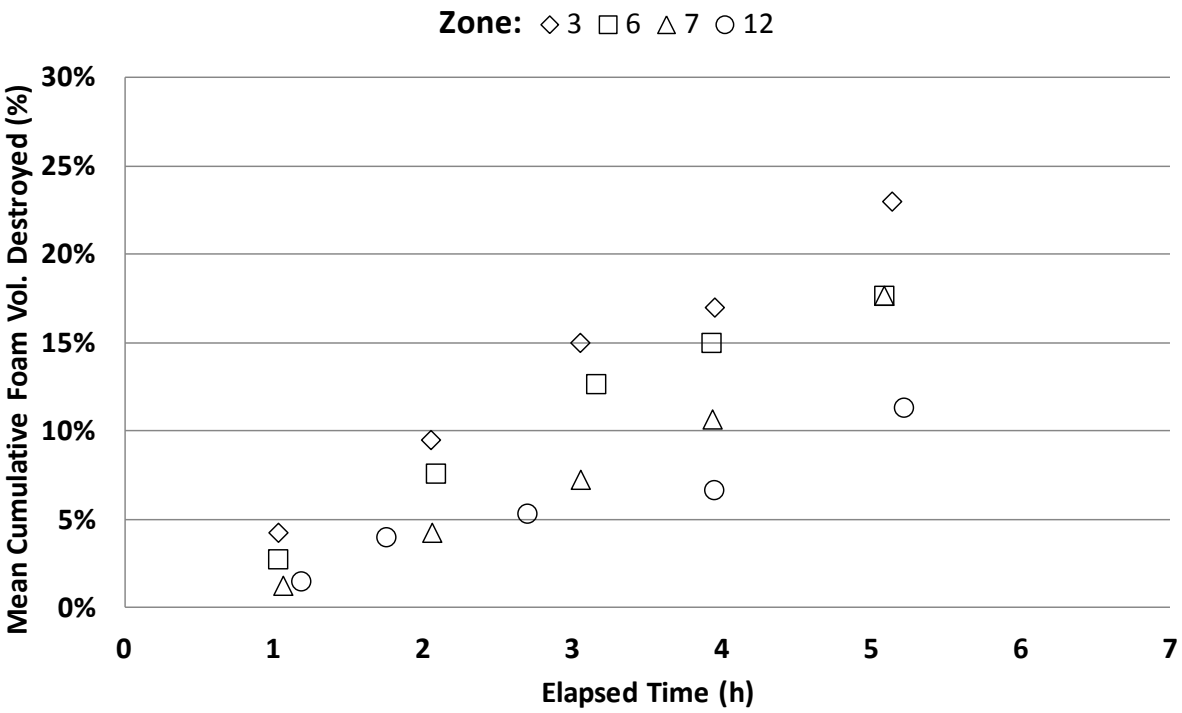

Figure 5.4 – Mean cumulative percent of initial foam volume destroyed from continuous Runs 1-4 plotted over elapsed time at different distances from the device. See Table B.1 for zone definitions.

5.5 Tables

Table 5.1 - Laser distance meter validation measurements made to a manure foam surface.

	Tape Measure		Laser Distance Meter		Absolute Difference		Relative Difference
	(m)	(in)	(m)	(in)	(m)	(in)	%
	0.566	22.3	0.574	22.6	-0.008	-0.3	-1.3%
	0.871	34.3	0.876	34.5	-0.005	-0.2	-0.6%
	1.176	46.3	1.181	46.5	-0.005	-0.2	-0.4%
	1.481	58.3	1.488	58.6	-0.008	-0.3	-0.5%
	1.786	70.3	1.791	70.5	-0.005	-0.2	-0.3%
	2.093	82.4	2.098	82.6	-0.005	-0.2	-0.2%
	2.395	94.3	2.403	94.6	-0.008	-0.3	-0.3%
	2.700	106.3	2.703	106.4	-0.003	-0.1	-0.1%
	0.561	22.1	0.566	22.3	-0.005	-0.2	-0.9%
	0.866	34.1	0.869	34.2	-0.003	-0.1	-0.3%
	1.171	46.1	1.176	46.3	-0.005	-0.2	-0.4%
	1.476	58.1	1.481	58.3	-0.005	-0.2	-0.3%
	1.781	70.1	1.783	70.2	-0.003	-0.1	-0.1%
	2.085	82.1	2.090	82.3	-0.005	-0.2	-0.2%
	2.390	94.1	2.395	94.3	-0.005	-0.2	-0.2%
	2.695	106.1	2.695	106.1	0.000	0.0	0.0%
	0.556	21.9	0.559	22.0	-0.003	-0.1	-0.5%
	0.859	33.8	0.861	33.9	-0.003	-0.1	-0.3%
	1.163	45.8	1.168	46.0	-0.005	-0.2	-0.4%
	1.468	57.8	1.473	58.0	-0.005	-0.2	-0.3%
	1.773	69.8	1.778	70.0	-0.005	-0.2	-0.3%
	2.080	81.9	2.083	82.0	-0.003	-0.1	-0.1%
	2.383	93.8	2.390	94.1	-0.008	-0.3	-0.3%
	2.687	105.8	2.690	105.9	-0.003	-0.1	-0.1%
Mean	1.6	64.1	1.632	64.3	-0.005	-0.2	-0.4%
S.D.	0.7	28.1	0.713	28.1	0.002	0.1	0.3%
Min	0.6	21.9	0.559	22.0	-0.008	-0.3	-1.3%
Max	2.7	106.3	2.703	106.4	0.000	0.0	0.0%

Table 5.2 - Laser distance meter validation measurements made to a liquid manure surface.

	Tape Measure		Laser Distance Meter		Absolute Difference		Relative Difference
	(m)	(in)	(m)	(in)	(m)	(in)	%
	0.566	22.3	0.569	22.4	-0.003	-0.1	-0.4%
	0.869	34.2	0.874	34.4	-0.005	-0.2	-0.6%
	1.173	46.2	1.179	46.4	-0.005	-0.2	-0.4%
	1.478	58.2	1.483	58.4	-0.005	-0.2	-0.3%
	1.786	70.3	1.786	70.3	0.000	0.0	0.0%
	2.088	82.2	2.093	82.4	-0.005	-0.2	-0.2%
	2.393	94.2	2.395	94.3	-0.003	-0.1	-0.1%
	2.697	106.2	2.700	106.3	-0.003	-0.1	-0.1%
	0.541	21.3	0.544	21.4	-0.003	-0.1	-0.5%
	0.846	33.3	0.848	33.4	-0.003	-0.1	-0.3%
	1.151	45.3	1.153	45.4	-0.003	-0.1	-0.2%
	1.455	57.3	1.458	57.4	-0.003	-0.1	-0.2%
	1.760	69.3	1.763	69.4	-0.003	-0.1	-0.1%
	2.065	81.3	2.070	81.5	-0.005	-0.2	-0.2%
	2.370	93.3	2.372	93.4	-0.003	-0.1	-0.1%
	2.675	105.3	2.675	105.3	0.000	0.0	0.0%
	0.556	21.9	0.561	22.1	-0.005	-0.2	-0.9%
	0.859	33.8	0.866	34.1	-0.008	-0.3	-0.9%
	1.166	45.9	1.168	46.0	-0.003	-0.1	-0.2%
	1.468	57.8	1.473	58.0	-0.005	-0.2	-0.3%
	1.773	69.8	1.778	70.0	-0.005	-0.2	-0.3%
	2.080	81.9	2.085	82.1	-0.005	-0.2	-0.2%
	2.385	93.9	2.388	94.0	-0.003	-0.1	-0.1%
	2.687	105.8	2.690	105.9	-0.003	-0.1	-0.1%
Mean	1.620	63.8	1.624	63.9	-0.003	-0.1	-0.3%
S.D.	0.713	28.1	0.713	28.1	0.002	0.1	0.2%
Min	0.541	21.3	0.544	21.4	-0.008	-0.3	-0.9%
Max	2.697	106.2	2.700	106.3	0.000	0.0	0.0%

Table 5.3 - Laser distance meter validation measurements made to a concrete surface.

	Tape Measure		Laser Distance Meter		Absolute Difference		Relative Difference
	(m)	(in)	(m)	(in)	(m)	(in)	%
	0.330	13.0	0.328	12.9	0.003	0.1	0.8%
	0.635	25.0	0.635	25.0	0.000	0.0	0.0%
	0.937	36.9	0.937	36.9	0.000	0.0	0.0%
	1.242	48.9	1.242	48.9	0.000	0.0	0.0%
	1.547	60.9	1.547	60.9	0.000	0.0	0.0%
	1.852	72.9	1.852	72.9	0.000	0.0	0.0%
	2.156	84.9	2.156	84.9	0.000	0.0	0.0%
	2.461	96.9	2.461	96.9	0.000	0.0	0.0%
	2.764	108.8	2.764	108.8	0.000	0.0	0.0%
Mean	1.547	60.9	1.547	60.9	0.000	0.0	0.1%
S.D.	0.833	32.8	0.834	32.8	0.001	0.0	0.3%
Min	0.330	13.0	0.328	12.9	0.000	0.0	0.0%
Max	2.764	108.8	2.764	108.8	0.003	0.1	0.8%

Table 5.4 - Summary table listing the initial foam depth, total elapsed time, change in volume, and the percent foam volume destroyed per hour for mechanical foam mitigation devices installed in the pump-out ports and continuously operated. Summary calculations by series are provided in Tables 5.6-5.10 for Runs 1-4 and 15 and in Tables C.1-C.3 for Runs 5-7.

Run	d_i		Total Elapsed t	Δ V			Δ V / Δ t (FDR)[1]
	(m)	(ft)	(h)	(m^3)	(ft^3)	%	%/h
1	0.320	1.05	3.8	8.1	286.0	12%	3%
2	0.290	0.95	5.5	14.5	511.7	15%	3%
3	0.289	0.95	5.3	18.4	648.4	18%	3%
4	0.222	0.73	3.0	6.2	218.6	10%	3%
5	0.092	0.30	3.0	0.7	25.4	2%	1%
6	0.075	0.24	3.6	1.9	65.2	6%	2%
7	0.052	0.17	2.9	0.7	24.3	3%	1%
15	0.232	0.76	3.7	10.7	378.6	19%	6%

[1] Foam Destruction Rate - average of time series FDR's

Table 5.5 - Summary table listing the initial foam depth, total elapsed time, device operation time, change in volume, and the percent foam volume destroyed per hour for mechanical foam mitigation devices installed in the pump-out ports and episodically operated. Summary calculations by series are provided in Tables 5.11-5.14 for Runs 8-11 and in Tables C.4-C.6 for Runs 12-14.

Run	d_i		Total Elapsed t	Device Operation t	Δ V			Δ V / Δ t (FDR)[1]
	(m)	(ft)	(h)	(h)	(m^3)	(ft^3)	%	%/h
8	0.348	1.14	6.7	2.6	13.5	476.7	11%	5%
9	0.335	1.10	5.1	2.0	11.9	419.8	10%	5%
10	0.254	0.83	2.8	2.0	7.4	263.1	8%	4%
11	0.270	0.88	2.9	2.0	8.2	287.9	8%	5%
12	0.097	0.32	0.8	2.2	2.0	70.6	5%	2%
13	0.070	0.23	1.0	2.0	0.0	0.0	0%	0%
14	0.064	0.21	3.5	2.3	3.2	111.4	11%	5%

[1] Foam Destruction Rate - average of time series FDR's

Table 5.6 - Run 1 summary calculations. In this run the device was installed in pump-out port C of Barn A (Figure 4.2) and operated continuously.

	t_e[1]	Δt_s[2]	$V_{f,s}$		Δd_s		$\Delta d_s / \Delta t_s$		ΔV_s			$\Delta V_s / \Delta t_s$ (sFDR)			sFDR / $d_{i,s}$		
	(h)	(h)	(m^3)	(f^3)	(m)	(f)	(m/h)	(f/h)	(m^3)	(f^3)	%	m^3/h	f^3/h	%/h	m^2/h	f^2/h	%/h-m
Time Series 1	0.7	0.7	72.53	2561.5	0.006	0.02	0.010	0.03	1.50	52.9	2%	2.25	79.4	3%	7.04	75.8	10%
Time Series 2	1.2	0.5	71.15	2512.5	0.006	0.02	0.012	0.04	1.39	49.0	2%	2.82	99.5	4%	8.83	95.0	12%
Time Series 3	2.2	1.0	68.92	2433.9	0.010	0.03	0.009	0.03	2.23	78.6	3%	2.14	75.7	3%	6.71	72.2	9%
Time Series 4	3.2	1.0	67.69	2390.5	0.005	0.02	0.005	0.02	1.23	43.4	2%	1.27	44.9	2%	3.99	42.9	6%
Time Series 5	3.8	0.7	65.89	2326.8	0.008	0.03	0.012	0.04	1.80	63.7	3%	2.71	95.6	4%	8.48	91.3	13%
Run 1 Summary								Mean	-	-	-	2.2	79.0	3%	7.0	75.5	10%
								Sum	8.1	287.6	12%	-	-	-	-	-	-
								SD	-	-	-	0.6	21.6	1%	1.9	20.6	3%
								Min	-	-	-	1.3	44.9	2%	4.0	42.9	6%
								Max	-	-	-	2.8	99.5	4%	8.8	95.0	13%

[1] Time elapsed since device start up

[2] Series final mean device operation time minus series initial mean device operation time

Table 5.7 - Run 2 summary calculations. In this run the device was installed in pump-out A port of Barn A (Figure 4.2) and operated continuously.

	t_e[1]	Δt_s[2]	$V_{f,s}$		Δd_s		$\Delta d_s / \Delta t_s$		ΔV_s			$\Delta V_s / \Delta t_s$ (sFDR)			sFDR / $d_{i,s}$		
	(h)	(h)	(m^3)	(f^3)	(m)	(f)	(m/h)	(f/h)	(m^3)	(f^3)	%	m^3/h	f^3/h	%/h	m^2/h	f^2/h	%/h-m
Time Series 1	1.6	1.6	102.70	3626.8	0.014	0.05	0.009	0.03	5.16	182.3	5%	3.32	117.1	3%	11.42	122.9	11%
Time Series 2	2.6	1.0	100.69	3555.7	0.005	0.02	0.005	0.02	2.01	71.1	2%	1.97	69.5	2%	6.78	73.0	7%
Time Series 3	3.7	1.1	97.11	3429.5	0.010	0.03	0.009	0.03	3.58	126.3	4%	3.30	116.5	3%	11.36	122.2	11%
Time Series 4	4.5	0.9	93.53	3303.1	0.010	0.03	0.011	0.04	3.58	126.3	4%	4.06	143.4	4%	13.99	150.5	14%
Time Series 5	5.5	1.0	93.37	3297.4	0.000	0.00	0.000	0.00	0.16	5.7	0%	0.16	5.8	0%	0.56	6.1	1%
Run 2 Summary								Mean	-	-	-	2.6	90.5	3%	8.8	94.9	9%
								Sum	14.5	511.7	15%	-	-	-	-	-	-
								SD	-	-	-	1.5	54.3	2%	5.3	57.0	5%
								Min	-	-	-	0.2	5.8	0%	0.6	6.1	1%
								Max	-	-	-	4.1	143.4	4%	14.0	150.5	14%

[1] Time elapsed since device start up

[2] Series final mean device operation time minus series initial mean device operation time

Table 5.8 - Run 3 summary calculations. In this run the device was installed in pump-out port C of Barn A (Figure 4.2) and was operated continuously.

	t_e[1]	Δt_s[2]	$V_{f,s}$		Δd_s		$\Delta d_s / \Delta t_s$		ΔV_s			$\Delta V_s / \Delta t_s$ (sFDR)			sFDR / $d_{i,s}$		
	(h)	(h)	(m^3)	(f^3)	(m)	(f)	(m/h)	(f/h)	(m^3)	(f^3)	%	m^3/h	f^3/h	%/h	m^2/h	f^2/h	%/h-m
Time Series 1	1.3	1.3	101.49	3584.2	0.016	0.05	0.013	0.04	5.92	209.0	6%	4.70	166.1	4%	16.25	174.9	15%
Time Series 2	2.4	1.1	98.19	3467.6	0.009	0.03	0.008	0.03	3.30	116.5	3%	2.99	105.8	3%	10.35	111.4	10%
Time Series 3	3.4	1.0	94.58	3339.9	0.010	0.03	0.009	0.03	3.62	127.7	4%	3.48	123.0	4%	12.04	129.5	12%
Time Series 4	4.3	0.9	92.44	3264.6	0.006	0.02	0.006	0.02	2.13	75.3	2%	2.38	84.1	3%	8.22	88.5	9%
Time Series 5	5.3	1.0	89.05	3144.8	0.009	0.03	0.009	0.03	3.39	119.9	4%	3.46	122.1	4%	11.95	128.6	13%
Run 3 Summary								Mean	-	-	-	3.40	120.2	3%	11.76	126.6	12%
								Sum	18.4	648.4	18%	-	-	-	-	-	-
								SD	-	-	-	0.85	30.1	1%	2.95	31.7	2%
								Min	-	-	-	2.38	84.1	3%	8.22	88.5	9%
								Max	-	-	-	4.70	166.1	4%	16.25	174.9	15%

[1] Time elapsed since device start up

[2] Series final mean device operation time minus series initial mean device operation time

Table 5.9 - Run 4 summary calculations. In this run the device was installed in pump-out port C of Barn A (Figure 4.2) and was operated continuously.

	t_e[1]	Δt_s[2]	$V_{f,s}$		Δd_s		$\Delta d_s / \Delta t_s$		ΔV_s			$\Delta V_s / \Delta t_s$ (sFDR)			sFDR / $d_{i,s}$		
	(h)	(h)	(m^3)	(f^3)	(m)	(f)	(m/h)	(f/h)	(m^3)	(f^3)	%	m^3/h	f^3/h	%/h	m^2/h	f^2/h	%/h-m
Time Series 1	1.1	1.1	80.80	2853.5	0.004	0.01	0.004	0.01	1.54	54.2	2%	1.43	50.5	2%	6.44	69.4	8%
Time Series 2	2.1	1.0	78.75	2781.2	0.006	0.02	0.006	0.02	2.05	72.4	3%	2.10	74.1	3%	9.46	101.8	12%
Time Series 3	3.0	1.0	76.15	2689.2	0.007	0.02	0.007	0.02	2.61	92.0	3%	2.74	96.6	3%	12.33	132.7	16%
Time Series 4[3]	4.4	0.3	74.92	2645.9	0.003	0.01			1.23	43.3	2%						
Run 4 Summary								Mean	-	-	-	2.09	73.7	3%	9.41	101.3	12%
								Sum	7.4	261.9	10%	-	-	-	-	-	-
								SD	-	-	-	0.65	23.1	1%	2.94	31.7	4%
								Min	-	-	-	1.43	50.5	2%	6.44	69.4	8%
								Max	-	-	-	2.74	96.6	3%	12.33	132.7	16%

[1] Time elapsed since device start up

[2] Series final mean device operation time minus series initial mean device operation time

[3] Time series 4 not used in run summary rate calculations

Table 5.10 - Run 15 summary calculations. In this run the device was installed inside Barn A (Figure 4.2) and operated continuously.

	t_e[1] (h)	Δt_s[2] (h)	$V_{f,s}$ (m^3)	(f^3)	Δd_s (m)	(f)	$\Delta d_s / \Delta t_s$ (m/h)	(f/h)	ΔV_s (m^3)	(f^3)	%	$\Delta V_s / \Delta t_s$ (sFDR) m^3/h	f^3/h	%/h	sFDR / $d_{i,s}$ m^2/h	f^2/h	%/h-m
Time Series 1	1.2	1.2	52.80	1864.5	0.024	0.08	0.019	0.06	5.99	211.4	10%	4.79	169.1	8%	20.63	222.1	35%
Time Series 2	2.3	1.1	50.32	1777.1	0.010	0.03	0.009	0.03	2.48	87.4	5%	2.27	80.1	4%	9.77	105.2	19%
Time Series 3	3.3	1.0	48.16	1700.6	0.009	0.03	0.009	0.03	2.17	76.5	4%	2.25	79.5	4%	9.70	104.4	19%
Time Series 4[3]	5.4	0.4	48.06	1697.3	0.000	0.00			0.09	3.3	0%						
Run 15 Summary								Mean	-	-	-	3.10	109.6	6%	13.37	143.9	24%
								Sum	10.7	378.6	19%	-	-	-	-	-	-
								SD	-	-	-	1.46	51.6	2%	6.29	67.7	9%
								Min	-	-	-	2.25	79.5	4%	9.70	104.4	19%
								Max	-	-	-	4.79	169.1	8%	20.63	222.1	35%

[1] Time elapsed since device start up

[2] Series final mean device operation time minus series initial mean device operation time

[3] Time series 4 not used in run summary calculations

Table 5.11 - Run 8 summary calculations. In this run the device was installed in pump-out port A of Barn A (Figure 4.2) and operated on a duty cycle of 1 h on: 2 h off.

	t_e[1] (h)	Δt_s[2] (h)	$V_{f,s}$ (m^3)	(f^3)	Δd_s (m)	(f)	$\Delta d_s / \Delta t_s$ (m/h)	(f/h)	ΔV_s (m^3)	(f^3)	%	$\Delta V_s / \Delta t_s$ (sFDR) m^3/h	f^3/h	%/h	sFDR / $d_{i,s}$ m^2/h	f^2/h	%/h-m
Time Series 1	0.9	0.9	122.09	4311.7	0.015	0.05	0.017	0.06	5.61	198.1	4%	6.39	225.6	5%	18.34	197.4	14%
Time Series 2	3.9	1.2	117.37	4145.0	0.013	0.04	0.011	0.04	4.72	166.7	4%	4.03	142.3	3%	11.57	124.5	9%
Time Series 3	6.7	0.5	114.19	4032.5	0.009	0.03	0.017	0.06	3.19	112.5	3%	6.37	224.9	5%	18.28	196.8	16%
Run 8 Summary								Mean	-	-	-	5.60	197.6	5%	16.06	172.9	13%
								Sum	13.5	477.3	11%	-	-	-	-	-	-
								SD	-	-	-	1.36	47.9	1%	3.90	41.9	3%
								Min	-	-	-	4.03	142.3	3%	11.57	124.5	9%
								Max	-	-	-	6.39	225.6	5%	18.34	197.4	16%

[1] Time elapsed since device start up

[2] Series final mean device operation time minus series initial mean device operation time

Table 5.12 - Run 9 summary calculations. In this run the device was installed in pump-out port C of Barn A (Figure 4.2) and operated on a duty cycle of 0.5 h on: 1 h off.

	t_e[1] (h)	Δt_s[2] (h)	$V_{f,s}$ (m^3)	(f^3)	Δd_s (m)	(f)	$\Delta d_s / \Delta t_s$ (m/h)	(f/h)	ΔV_s (m^3)	(f^3)	%	$\Delta V_s / \Delta t_s$ (sFDR) m^3/h	f^3/h	%/h	sFDR / $d_{i,s}$ m^2/h	f^2/h	%/h-m
Time Series 1	0.5	0.5	119.22	4210.1	0.008	0.03	0.017	0.06	2.91	102.9	2%	6.26	221.0	5%	18.69	201.1	15%
Time Series 2	2.1	0.5	115.82	4090.3	0.009	0.03	0.017	0.06	3.39	119.8	3%	6.35	224.4	5%	18.97	204.2	16%
Time Series 3	3.6	0.5	113.14	3995.4	0.007	0.02	0.015	0.05	2.69	94.9	2%	5.39	190.2	5%	16.08	173.1	14%
Time Series 4	5.1	0.4	110.24	3893.2	0.008	0.03	0.019	0.06	2.89	102.2	3%	6.78	239.4	6%	20.24	217.8	18%
Run 9 Summary								Mean	-	-	-	6.194	218.8	5%	18.49	199.1	16%
								Sum	11.9	419.8	10%	-	-	-	-	-	-
								SD	-	-	-	0.584	20.6	1%	1.74	18.8	2%
								Min	-	-	-	5.387	190.2	5%	16.08	173.1	14%
								Max	-	-	-	6.779	239.4	6%	20.24	217.8	18%

[1] Time elapsed since device start up

[2] Series final mean device operation time minus series initial mean device operation time

Table 5.13 - Run 10 summary calculations. In this run the device was installed in pump-out port of A Barn A (Figure 4.2) and operated on a duty cycle of 1 h on: 1 h off.

	t_e[1] (h)	Δt_s[2] (h)	$V_{f,s}$ (m^3)	(f^3)	Δd_s (m)	(f)	$\Delta d_s / \Delta t_s$ (m/h)	(f/h)	ΔV_s (m^3)	(f^3)	%	$\Delta V_s / \Delta t_s$ (sFDR) m^3/h	f^3/h	%/h	sFDR / $d_{i,s}$ m^2/h	f^2/h	%/h-m
Time Series 1	0.8	0.8	91.64	3236.3	0.007	0.02	0.008	0.03	2.52	88.9	3%	2.98	105.2	3%	11.75	126.4	12%
Time Series 2	2.8	0.9	86.71	3062.1	0.013	0.04	0.014	0.05	4.93	174.2	5%	5.20	183.8	6%	20.53	220.9	22%
Run 10 Summary								Mean	-	-	-	4.091	144.5	4%	16.14	173.7	17%
								Sum	7.4	263.1	8%	-	-	-	-	-	-
								SD	-	-	-	1.574	55.6	2%	6.21	66.8	7%
								Min	-	-	-	2.978	105.2	3%	11.75	126.4	12%
								Max	-	-	-	5.204	183.8	6%	20.53	220.9	22%

[1] Time elapsed since device start up

[2] Series final mean device operation time minus series initial mean device operation time

Table 5.14 - Run 11 summary calculations. In this run the device was installed in pump-out port C of Barn A (Figure 4.2) and operated on a duty cycle of 1 h on: 1 h off.

	t_e[1] (h)	Δt_s[2] (h)	$V_{f,s}$ (m^3)	(f^3)	Δd_s (m)	(f)	$\Delta d_s / \Delta t_s$ (m/h)	(f/h)	ΔV_s (m^3)	(f^3)	%	$\Delta V_s / \Delta t_s$ (sFDR) m^3/h	f^3/h	%/h	sFDR / $d_{i,s}$ m^2/h	f^2/h	%/h-m
Time Series 1	0.8	0.8	96.75	3416.7	0.009	0.03	0.011	0.04	3.32	117.2	3%	4.04	142.7	4%	14.98	161.3	15%
Time Series 2	2.9	1.0	91.92	3246.0	0.013	0.04	0.013	0.04	4.83	170.7	5%	4.88	172.3	5%	18.09	194.7	19%
Run 11 Summary								Mean	-	-	-	4.46	157.5	5%	16.54	178.0	17%
								Sum	8.2	287.9	8%	-	-	-	-	-	-
								SD	-	-	-	0.59	20.9	1%	2.20	23.6	3%
								Min	-	-	-	4.04	142.7	4%	14.98	161.3	15%
								Max	-	-	-	4.88	172.3	5%	18.09	194.7	19%

[1] Time elapsed since device start up

[2] Series final mean device operation time minus series initial mean device operation time

Table 5.15 - Time series cumulative percent of initial foam volume destroyed for Run 1-4 grouped by elapsed time and averaged. The resulting mean is the average cumulative percent of initial foam volume destroyed during each hour of elapsed time for continuous runs conducted in Barn A.

0.5 to 1.5 h	Run	R1	R1	R3	R4	Mean
	t_e (h)[1]	0.7	1.2	1.3	1.1	1.0
	ΔV %[2]	2%	4%	6%	2%	3%
1.5 to 2.5 h	Run	R1	R2	R3	R4	Mean
	t_e (h)[1]	2.2	1.6	2.4	2.1	2.0
	ΔV %[2]	7%	5%	9%	4%	6%
2.5 to 3.5 h	Run	R1	R2	R3	R4	Mean
	t_e (h)[1]	3.2	2.6	3.4	3.3	3.1
	ΔV %[2]	9%	7%	12%	9%	9%
3.5 to 4.5 h	Run	R1	R2	R3		Mean
	t_e (h)[1]	3.8	3.7	4.3		3.9
	ΔV %[2]	12%	10%	15%		12%
>4.5 h	Run	R2	R2	R3		Mean
	t_e (h)[1]	4.5	5.5	5.3		5.1
	ΔV %[2]	14%	14%	18%		16%

[1] Time elapsed since start of run

[2] Cumulative percent initial volume destroyed

Table 5.16 - Time series cumulative percent of initial foam volume destroyed for Runs 8-11 grouped by elapsed time and averaged. The resulting mean is the average cumulative percent of initial foam volume destroyed during each hour of elapsed time for episodic runs conducted in Barn A.

0.5 to 1.5 h	Run	R8	R9	R10	R11	Mean
	t_e (h)[1]	0.9	0.5	0.8	0.8	0.8
	ΔV %[2]	4%	2%	3%	3%	3%
1.5 to 2.5 h	Run	R9				Mean
	t_e (h)	2.1				2.1
	ΔV %	5%				5%
2.5 to 3.5 h	Run	R10	R11			Mean
	t_e (h)	2.8	2.9			2.8
	ΔV %	8%	8%			8%
3.5 to 4.5 h	Run	R8	R9			Mean
	t_e (h)	3.9	3.6			3.7
	ΔV %	8%	8%			8%
>4.5 h	Run	R8	R9			Mean
	t_e (h)	6.7	5.1			5.9
	ΔV %	11%	10%			11%

[1] Time elapsed since start of run

[2] Cumulative percent initial volume destroyed

Table 5.17 - Foam destruction rate by time series for runs conducted in Barn A in which the device was operated continuously. Runs 1 through 4 featured the device installed in a pump-out port, while in Run 15 the device was installed inside the Barn.

			Time Series					Mean	SD	Min	Max
			1	2	3	4	5				
Run 1	Elapsed t	(h)	0.7	1.2	2.2	3.2	3.8				
	Δt	(h)	0.7	0.5	1.0	1.0	0.7	0.8	0.2	0.5	1.0
	$\Delta V / \Delta t$ (FDR)	$(m^3)/h$	1.13	1.51	1.15	0.69	1.45	1.19	0.33	0.69	1.51
		%	3%	4%	3%	2%	4%	3%	1%	2%	4%
Run 2	Elapsed t	(h)	1.6	2.6	3.7	4.5	5.5				
	Δt	(h)	1.6	1.0	1.1	0.9	1.0	1.1	0.3	0.9	1.6
	$\Delta V / \Delta t$ (FDR)	$(m^3)/h$	3.32	1.97	3.30	4.06	0.16	2.56	1.54	0.16	4.06
		%	3%	2%	3%	4%	0%	3%	2%	0%	4%
Run 3	Elapsed t	(h)	1.3	2.4	3.4	4.3	5.3				
	Δt	(h)	1.3	1.1	1.0	0.9	1.0	1.1	0.1	0.9	1.3
	$\Delta V / \Delta t$ (FDR)	$(m^3)/h$	4.70	2.99	3.48	2.38	3.46	3.40	0.85	2.38	4.70
		%	4%	3%	4%	3%	4%	3%	1%	3%	4%
Run 4	Elapsed t	(h)	1.1	2.1	3.0						
	Δt	(h)	1.1	1.0	1.0			1.0	0.1	1.0	1.1
	$\Delta V / \Delta t$ (FDR)	$(m^3)/h$	1.43	2.10	2.74			2.09	0.65	1.43	2.74
		%	2%	3%	3%			3%	1%	2%	3%
Run 15	Elapsed t	(h)	1.2	2.3	3.3						
	Δt	(h)	1.2	1.1	1.0			1.1	0.1	1.0	1.2
	$\Delta V / \Delta t$ (FDR)	$(m^3)/h$	4.79	2.27	2.25			3.10	1.46	2.25	4.79
		%	8%	4%	4%			6%	2%	4%	8%

Table 5.18 - Foam destruction rate by time series for runs conducted in Barn A in which the device was installed in a pump-out port and operated episodically.

			Time Series				Mean	SD	Min	Max
			1	2	3	4				
Run 8	Elapsed t	(h)	0.9	3.9	6.7					
	Δ t	(h)	0.9	1.2	0.5		0.9	0.3	0.5	1.2
	Δ V / Δ t (FDR)	$(m^3)/h$	6.39	4.03	6.37		5.60	1.36	4.03	6.39
		%	5%	3%	5%		5%	1%	3%	5%
Run 9	Elapsed t	(h)	0.5	2.1	3.6	5.1				
	Δ t	(h)	0.5	0.5	0.5	0.4	0.5	0.0	0.4	0.5
	Δ V / Δ t (FDR)	$(m^3)/h$	6.26	6.35	5.39	6.78	6.19	0.58	5.39	6.78
		%	5%	5%	5%	6%	5%	1%	5%	6%
Run 10	Elapsed t	(h)	0.8	2.8						
	Δ t	(h)	0.8	0.9			0.9	0.1	0.8	0.9
	Δ V / Δ t (FDR)	$(m^3)/h$	2.98	5.20			4.09	1.57	2.98	5.20
		%	3%	6%			4%	2%	3%	6%
Run 11	Elapsed t	(h)	0.8	2.9						
	Δ t	(h)	0.8	1.0			0.9	0.1	0.8	1.0
	Δ V / Δ t (FDR)	$(m^3)/h$	4.04	4.88			4.46	0.59	4.04	4.88
		%	4%	5%			5%	1%	4%	5%

Table 5.19 - Cumulative percent foam volume destroyed for Runs 1 through 4 and Run 15. In these runs the device was operated continuously. Runs 1 through 4 featured the device installed in a pump-out port in Barn A while Run 15 had the device installed inside Barn A.

		Time Series				
		1	2	3	4	5
Run 1	t_e (h)[1]	0.7	1.2	2.2	3.2	3.8
	ΔV %[2]	2%	4%	7%	9%	12%
Run 2	t_e (h)[1]	1.6	2.6	3.7	4.5	5.5
	ΔV %[2]	5%	7%	10%	14%	14%
Run 3	t_e (h)[1]	1.3	2.4	3.4	4.3	5.3
	ΔV %[2]	6%	9%	12%	15%	18%
Run 4	t_e (h)[1]	1.1	2.1	3.0	3.3	
	ΔV %[2]	2%	4%	8%	9%	
Run 15	t_e (h)[1]	1.2	2.3	3.3		
	ΔV %[2]	10%	15%	19%		

[1] Time elapsed since start of run

[2] Cumulative percent initial volume destroyed

Table 5.20 - Average cumulative percent foam volume of time series measurements from Zones 3, 6, 7, and 12 of Runs 1, 2, 3, 4, and 15 grouped by elapsed time. These data are plotted in Figure 5.4.

	Zone 3					Zone 6				
Elapsed t (h)	Series t (h)	Mean $\Delta V\%_{cum}$ [1]	SD	Min	Max	Series t (h)	Mean $\Delta V\%_{cum}$ [1]	SD	Min	Max
0.5 to 1.5	1.1	6%	4%	0%	11%	1.1	4%	3%	0%	8%
1.5 to 2.5	2.1	11%	5%	4%	16%	2.1	8%	4%	4%	13%
2.5 to 3.5	3.1	16%	5%	11%	22%	3.2	14%	4%	10%	18%
3.5 to 4.5	3.9	17%	5%	13%	22%	3.9	15%	3%	13%	18%
4.5>	5.1	23%	7%	17%	30%	5.1	18%	3%	16%	21%
	Zone 7					Zone 12				
Elapsed t (h)	Series t (h)	Mean $\Delta V\%_{cum}$ [1]	SD	Min	Max	Series t (h)	Mean $\Delta V\%_{cum}$ [1]	SD	Min	Max
0.5 to 1.5	1.1	1%	1%	0%	2%	1.2	2%	1%	1%	2%
1.5 to 2.5	2.1	4%	2%	2%	6%	1.7	4%	1%	3%	5%
2.5 to 3.5	3.0	7%	4%	4%	11%	2.7	5%	2%	4%	7%
3.5 to 4.5	3.9	11%	5%	6%	15%	3.9	7%	4%	4%	11%
4.5>	5.1	18%	1%	17%	18%	5.2	11%	3%	9%	14%

[1] Average of the cumulative percent foam volume destroyed for time series measurements in that group from runs 1, 2, 3, 4, and 15

Chapter 6: Summary and Conclusions

6.1 Summary of Results

The goal of this study was to evaluate the ability of a mechanical foam mitigation device to eliminate foam in foaming swine deep manure storages. Results showed that the MFMD was capable of destroying foam at rates ranging from 3% of initial foam volume destroyed per hour to 6% of initial foam volume destroyed per hour based on installation location and operation strategy.

Results showed that while episodic operation improved the foam destruction rate, the increase in rate did not make up for the time the device spent idle. Based on this finding, it is recommended that this specific design of MFMD be operated continuously. Run 2 established 5 h to be the maximum time for continuous operation in foam depths ranging from 0.222 m (8.8 in) to 0.348 m (13.7 in) with the device installed in a pump-out port. Testing also showed that MFMDs were able to establish a gradient in the foam over a distance of at least 21 m (68.9 ft) that resulted in foam flow towards the device in foam depths ranging from 0.222 m (8.8 in) to 0.348 m (13.7 in) with the device installed in a pump-out port.

While testing, it was observed that debris floating in the pit occasionally became entangled in the paddles of the device, reducing its effectiveness by disrupting foam flow. In one instance, a pig sorting paddle became lodged in the paddles. This caused the motor to over-heat and tripped the internal breaker. When using this device, the paddles should be inspected regularly to prevent device down time and to insure peak performance. Other implementation challenges are access to swine barns, access to manure pits, and power supply for the device. Many swine producers have established biosecurity protocols and access to barns is restricted.

This complicates future device testing as well as installation and service should the devices be offered commercially. Variation in pump-out port and pump-out port cover construction can make device installation problematic. At the site used for this study, pump-out port dimensions differed between Barn C and Barns A and B. During this study, supplying power to the MFMD was challenging as there were no outlets located near the pump-out ports. To remedy this, extension cords were purchased and run from inside the barn to the device. If this method is used to supply power to the device, care must be taken to secure extension cords well out reach of pigs.

Installing the device inside the barn appeared to offer improved performance over pump-out port installation, but it must be stressed that only one run consisting of three time series measurements was conducted with the device installed inside the barn. Air quality was not assessed during this test and it is unknown what hazards operating the device within a barn poses. Further research should be conducted to evaluate air quality when operating the device inside a swine confinement barn. Testing should also be done to validate this study's findings of the MFMD's performance when installed inside a barn.

Foam depths during the trial ranged from 0.052 m (0.17 ft) to 0.348 m (1.14 ft). Future testing should evaluate the device's performance in foam depths significantly greater than 0.348 m (1.14 ft) both when installed in the pump-out ports and when installed inside the barn. Research should be conducted to determine optimal device placement both when installed inside a barn and when installed in a barn's pump-out port. Results from this study seem to indicate that two devices are needed to eliminate foam within swine barns measuring 61.3 m (201.1 ft) long and up to 15.6 m (51.2 ft) wide; however these findings should be validated and further investigated.

No assessment was made concerning the cost associated with purchasing and operating a MFMD. Future studies should include economic analysis of device purchase and operation and draw comparisons to other foam control strategies on this basis.

6.2 Recommendations for Future Research

- Research should be conducted to evaluate the effect of MFMD operation on indoor air quality when the device is installed inside a barn
- The finding that inside-the-barn installation offers improved performance over pump-out port installation should be validated
- Device performance in foam depths greater than 0.348 m (1.14 ft) should be evaluated
- Future research should be conducted to optimize MFMD placement when installed inside a barn and when installed within a barn's pump-out ports
- Economic analysis should be performed of device purchase and operation and compare the costs of operating a MFMD with other foam control strategies
- Future studies should examine modifications of the prototype MFMD to minimize power consumption while the device is in operation. One possibility is modifying the device so that the paddle shaft only engages the foam and the first few inches of liquid manure.

References

Barber, W. 2005. Anaerobic digester foaming; causes and solutions. *Water21* 9(1); 45–49.

Boon, L. A., F. W. J. M. M. Hoeks , R. G. J. M. Van Der Lans , W. Bujalski, M. O. Wolff, and A. W. Nienow. 2002. Comparing a range of impellers for " stirring as foam disruption ". *Biochem. Eng. J.* 10; 183–195.

Choiniere, Y. (2004). Explosion of a deep pit finishing pig barn, investigation report on biogas production. ASAE/CSAE Meeting Paper No. 044092 (Vol. 0300). St. Joseph, Mich.:ASABE.

Clanton, C., L. Jacobson, and D. Schmidt. 2012. Monensin addition to swine manure deep-pits for foaming control. Minneapolis, Minn.; University of Minnesota Cooperative Extension. Available at: http://www.mnpork.com/FileLibrary/States/MN/MPB Research/2012/Adding_monensin_to_swine_deep_pit_ foaming.pdf. Accessed 21 December 2012.

Deshpande, N. S., M. Barigou, and A. Marlon. 2000. Mechanical suppression of the dynamic foam head in bubble column reactors. *Chem. Eng. Process.* 39(3): 207–217.

DirectIndustry. 2013. Products. Direct Industry. Marseille, France. Available at: http://www.directindustry.com/prod/lightnin/3-blades-agitator-impellers-axial-flow-24564-59975.html. Accessed on: 12 March, 2013

Donham, K. J., L. W. Knapp, R. Monson, and K. Gustafoson. 1982. Acute toxic exposure to gases from liquid manure. *J.Occup. Med.* 24(2): 142–145.

Elanco. 2013. Elanco. Greenfield, Ind. Available at: https://www.elancocentral.com/rumensin_90_label.pdf. Accessed on: 18 March, 2013

Etoc, A., F. Delvigne, J. Lecomte, and P. Thonart. 2006. Foam control in fermentation bioprocess. *Appl. Biochem. Biotechnol.* 129: 392–404.

Fluke. 2013. Laser distance meters. Fluke Corporation. Evertt, Wash. Available at: http://www.fluke.com/fluke/usen/laser-distance-meters/fluke-416d-laser-distance-meter.htm?PID=69324. Accessed on: 15 March, 2013

Ganidi, N., S. Tyrrel, and E. Cartmell. 2009. Anaerobic digestion foaming causes--a review. *Bioresour. Technol.* 100(23): 5546–54.

Gutwald, S., and A. Mersmann. 1997. Mechanical foam breaking - a physical model for impact effects with high speed rotors. *Chem. Eng. Technol.* 20(2): 76–84.

Hoeks, F., C. Wees-Tangerman, K. Gasser, H. Mommers, S. Schmid, and K. Luyben. 1997. Stirring as foam disruption (SAFD) technique in fermentation processes. *Can. J. Chem. Eng.* 75(6): 1018–1029.

Junker, B. 2007. Foam and its mitigation in fermentation systems. *Biotechnol. Progr.* 23(4): 767–84.

Kinsey, R. E. 2009. Safety alert - explosions in swine confinement barns while pumping pits. Eagam, Minn.: Minnesota Grain and Feed Association. Available at: http://www.mgfa.org/userfiles/file/Safety Alert-Explosions in Swin Confinement Barns.pdf. Accessed 13 July 2012.

Klatte, S., F. A. Rainey, and R. M. Kroppenstedt. 1994. Transfer of rhodococcus aichiensis tsukamura 1982 and nocardia amarae lechevalier and lechevalier 1974 to the genus gordona as gordona aichiensis comb. nov. and gordona amarae comb. nov. *Int. J. Syst. Bacter.* 44(4): 769–773.

Masse, D., R. Droste, K. Kennedy, N. Patni, and J. Munroe. 1997. Potential for the psychrophilic anaerobic treatment of swine manure using a sequencing batch reactor. *Can. Agric. Eng.* 39(1): 25–33.

Moody, L., R. Burns, and R. Muhlbauer. (2009). Deep-pit swine facility flash fires and explosions : sources , occurrences , factors , and management . Des Moines, Iowa.: National Pork Board. Available at: http://www.pork.org/ResearchDetail/1349/DeepPitSwineFacility.aspx. Accessed 22 June 2012.

Morey, M., N. Deshpande, and M. Barigou. 1999. Foam destabilization by mechanical and ultrasonic vibrations. *J. Colloid Iinterface Sci.* 219(1),: 90–98.

Muehling, A. J. 1970. Gases and odors from stored swine wastes. *J. of Anim. Sci.* 30: 526–531.

National Pork Board. 2012. National Pork Board 2012 strategic plan and budget. Des Moines, Iowa: National Pork Board. Available at: http://www.pork.org/filelibrary/AboutUs/2012NPBStrategicPlanAndBudgetBook.pdf. Accessed 19 December 2012.

Niekerk, A. Van, J. Kawahigashi, D. Reichlin, and A. Malea. 1987. Foaming in anaerobic digester: a survey and laboratory investigation. *J. Water Pollut. Contr. Fed.* 59(5): 249–253.

Patist, A., and D. Bates. 2008. Ultrasonic innovations in the food industry: from the laboratory to commercial production. *Innov. Food Sci. Emerg. Technol.* 9(2): 147–154.

Pelton, R. 2002. A review of antifoam mechanisms in fermentation. *J. Ind. Microbiol. Biotechnol.* 29:149–154.

Pepple, L. M., R. S. Gates, T. L. Funk, and A. D. Kent. 2012. Microbial community analysis on liquid swine manure for foaming.CIGR-AgEng2012. Paper No. C-1353. Valencia, Spain.:CIGR-AgEng2012

Pugh, R. 1996. Foaming, foam films, antifoaming and defoaming. *Adv. Colloid Interface Sci.* 64(95): 67–142.

Rahman, S., R. DeSutter, and Q. Zhang. 2011. Efficacy of a microbial additive in reducing odor, ammonia, and hydrogen sulfide emissions from farrowing-gestation swine operation. *Eng. Int.: CIGR* 13(3): 1–9.

Rehberger, J., E. Davis, A. Baker, T. Parrott, A.Veldkamp,and T. Rehberger. 2009. A preliminary comparison of the bacterial communities of foaming and non-foaming swine manure pits. *J. Anim. Sci.*, 87(E-Suppl. 2).

Rehberger, J., E. Davis, A. Veldkamp, T. Parrott, and T. Rehberger. 2010. Comparison of nutrient and microbial profiles in foaming and non-foaming swine manure pits. *J. Anim. Sci.* 88:(E-Suppl. 2).

Robert, M., A. Kasimati, A. C. Clarindo, T. C. Bragatto, T. Funk, and R. S. Gates. 2011. Evaluation of commercial products to mitigate swine manure foam. ASABE Paper No. 1100021. St. Joseph, Mich.: ASABE

Sandor, N., and H. N. Stein. 1993. Foam destruction by ultrasonic vibrations. *J. Colloid Interface Sci.* 161: 265–267.

SpringerImages.a. 2013. Springer Science and Business Media. New York, N.Y.. Available at: http://www.springerimages.com/Images/LifeSciences/1-10.1007_s10295-003-0023-7-1. Accessed: 12 March, 2013

SpringerImages.b. 2013. Springer Science and Business Media. New York, N.Y.. Available at: http://www.springerimages.com/Images/LifeSciences/1-10.1007_s10295-003-0023-7-3. Accessed: 12 March, 2013

SpringerImages.c. 2013. Springer Science and Business Media. New York, N.Y.. Available at: http://www.springerimages.com/Images/LifeSciences/1-10.1007_s10295-003-0023-7-2. Accessed: 12 March, 2013

The Geometry Junkyard. 2013. University of California. Irvine, Cal. Available at: http://www.ics.uci.edu/~eppstein/junkyard/kelvin-large.gif. Accessed 17 March, 2013

Tsang, Y. F., S. N. Sin, and H. Chua. 2008. Nocardia foaming control in activated sludge process treating domestic wastewater. *Bioresource technology* 99(9): 3381–8.

USDA-NASS. 2012a. Farms, land in farms, and livestock operations 2011 summary. ISSN:1930-7128. Washinton, D.C.:USDA National Agricultural Statistics Service

USDA-NASS.2012b. Quarterly hogs and pigs.ISSN: 1949-1921. Washington, D.C.: USDA National Agricultural Statistics Service

Vardar-Sukan, F. 1988. Efficiency of natural oils as antifoaming agents in biopr ocesses . *J. Chem. Technol. Biotechnol.* 43: 39–47.

Vardar-Sukan, F. 1991. Effects of natural oils on foam collapse in bioprocesses. *Biotechnol. Lett.* 13(2): 107–112.

Vardar-Sukan, F. 1998. Foaming : consequences , prevention and destruction. *Biotechnol. Adv.* 16: 913–948.

Varley, J., A. K. Brown, J. W. R. Boyd, P. W. Dodd, and S. Gallagher. 2004. Dynamic multi-point measurement of foam behaviour for a continuous fermentation over a range of key process variables. *Biochem. Eng. J.* 20(1): 61–72.

Yamagiwa, K., M. Yoshida, and A. Ohkawa. 2000. Biological treatment of highly foaming pharmaceutical wastewater by modified bubble-column under mechanical foam control. *Water Sci. Technol.* 42:331–337.

Appendix A: Foam Depth Measurement Coordinates

Table A.1 – Foam depth measurement point coordinates for Run 1 in Barn A, pump-out port C. See Figure 4.7 for a schematic of these points and for the origin defined.

Point	X		Y		Point	X		Y	
	(m)	*(ft)*	*(m)*	*(ft)*		*(m)*	*(ft)*	*(m)*	*(ft)*
1001	12.0	39.0	52.5	172.3	1031	12.0	39.0	46.9	154.0
1002	11.7	38.0	52.5	172.1	1032	12.0	39.0	46.4	152.3
1003	11.4	37.0	52.5	172.2	1033	12.0	39.0	45.7	149.9
1004	11.1	36.0	52.4	172.1	1034	12.0	39.0	45.0	147.7
1005	10.5	34.0	52.6	172.5	1035	12.0	39.0	44.5	146.0
1006	9.8	32.0	52.5	172.3	1036	12.0	39.0	43.8	143.7
1007	9.1	30.0	52.5	172.2	1037	12.0	39.0	43.3	142.0
1008	8.6	28.0	52.5	172.2	1038	12.0	39.0	42.4	139.1
1009	8.1	26.0	52.5	172.3	1039	12.0	39.0	41.4	135.7
1010	7.4	24.0	52.5	172.4	1040	12.0	39.0	40.5	132.9
1011	6.8	22.0	52.5	172.4	1041	11.6	38.3	51.8	170.0
1012	6.0	20.0	52.5	172.3	1042	11.4	37.6	51.5	168.8
1013	5.6	18.0	52.5	172.3	1043	11.2	36.9	51.3	168.2
1014	5.0	16.0	52.5	172.3	1044	11.0	36.2	51.1	167.7
1015	4.4	14.0	52.5	172.2	1045	10.6	34.8	50.6	166.0
1016	3.8	12.0	52.5	172.3	1046	10.2	33.3	50.3	164.9
1017	3.0	10.0	52.5	172.3	1047	9.7	31.9	49.7	163.1
1018	2.2	7.0	52.5	172.3	1048	9.4	30.5	49.4	162.0
1019	1.3	4.0	52.5	172.3	1049	8.8	29.1	49.0	160.8
1020	0.4	1.0	52.5	172.3	1050	8.3	27.7	48.5	159.1
1021	12.0	39.0	52.2	171.1	1051	7.9	26.3	48.2	158.0
1022	12.0	39.0	51.8	169.9	1052	7.5	24.9	47.6	156.2
1023	12.0	39.0	51.4	168.8	1053	7.1	23.5	47.3	155.1
1024	12.0	39.0	51.1	167.7	1054	6.7	22.1	46.7	153.4
1025	12.0	39.0	50.6	165.9	1055	6.4	20.7	46.3	151.7
1026	12.0	39.0	49.9	163.6	1056	5.9	19.2	45.9	150.6
1027	12.0	39.0	49.4	161.9	1057	5.4	17.8	45.4	148.9
1028	12.1	39.0	48.7	159.7	1058	4.8	15.7	44.9	147.2
1029	12.0	39.0	48.2	158.0	1059	4.1	13.6	44.2	144.9
1030	12.0	39.0	47.4	155.7	1060	3.5	11.5	43.5	142.6

Table A.2 - Foam depth measurement point coordinates for Runs 2 and 8 in Barn A, pump-out port A. See Figure 4.8 for a schematic of these points and the origin defined.

Point	X		Y		Point	X		Y	
	(m)	*(ft)*	*(m)*	*(ft)*		*(m)*	*(ft)*	*(m)*	*(ft)*
1121	0.4	1.4	0.5	1.7	1151	0.3	1.1	24.2	79.2
1122	1.7	5.5	0.5	1.7	1152	0.3	1.1	25.9	85.0
1123	2.8	9.2	0.5	1.7	1153	0.4	1.1	27.3	89.5
1124	4.3	14.2	0.5	1.7	1154	0.3	1.1	29.0	95.2
1125	5.3	17.3	0.5	1.7	1161	0.8	2.6	9.7	31.9
1126	7.0	22.9	0.5	1.7	1162	1.4	4.7	11.1	36.5
1127	8.3	27.3	0.5	1.7	1163	2.0	6.7	12.5	41.0
1128	9.5	31.1	0.5	1.7	1164	2.8	9.2	13.9	45.7
1129	10.6	34.8	0.5	1.6	1165	4.0	13.1	15.5	50.8
1130	11.9	39.1	0.5	1.7	1166	4.2	13.7	16.7	54.7
1131	0.4	1.3	8.7	28.5	1167	4.9	16.1	18.1	59.3
1132	1.8	5.8	8.7	28.6	1168	5.5	18.0	19.5	63.8
1133	2.9	9.5	8.5	28.0	1169	5.9	19.3	20.7	67.9
1134	4.5	14.6	8.7	28.4	1170	6.7	22.1	22.1	72.5
1135	5.6	18.3	8.7	28.6	1171	7.4	24.3	23.5	77.0
1136	6.8	22.4	8.7	28.5	1172	8.2	26.8	24.9	81.7
1137	8.0	26.3	8.7	28.5	1173	8.8	29.0	26.3	86.1
1138	9.1	29.7	8.5	28.0	1174	9.8	32.3	26.9	88.2
1139	10.3	33.9	8.5	27.9	1175	10.2	33.4	28.9	94.7
1140	11.8	38.8	8.5	27.9	1116	2.4	7.7	30.1	98.7
1141	0.4	1.4	9.1	29.7	1117	1.9	6.1	28.7	94.2
1142	0.4	1.1	10.6	34.7	1118	1.3	4.2	27.3	89.5
1143	0.4	1.2	12.0	39.2	1119	0.5	1.7	25.9	85.1
1144	0.4	1.2	13.6	44.5	1120	6.0	19.5	25.9	85.1
1145	0.3	1.0	15.0	49.0	1096	12.0	39.3	29.2	95.9
1146	0.3	1.1	16.7	54.7	1097	11.9	39.1	27.6	90.6
1147	0.4	1.1	18.1	59.2	1098	12.0	39.2	26.0	85.4
1148	0.4	1.1	20.0	65.6	1099	11.9	39.2	24.7	80.9
1149	0.4	1.2	21.2	69.6	1100	11.9	39.1	23.1	75.9
1150	0.4	1.2	23.0	75.3					

Table A.3 - Foam depth measurement point coordinates for Runs 3 and 9 in Barn A, pump-out port C. See Figure 4.9 for a schematic of these points and the origin defined.

Point	X		Y		Point	X		Y	
	(m)	*(ft)*	*(m)*	*(ft)*		*(m)*	*(ft)*	*(m)*	*(ft)*
1061	12	39.2	60.7	199.2	1091	12	39.3	36.9	120.9
1062	10.9	35.8	60.7	199.1	1092	12	39.2	35.3	115.7
1063	9.6	31.3	60.6	199	1093	11.9	39.1	33.9	111.2
1064	8.3	27.1	60.7	199	1094	11.9	39.2	32.3	106
1065	7.1	23.2	60.6	198.9	1095	11.9	39.1	30.8	101
1066	5.3	17.4	60.7	199.1	1101	11.6	38	51.1	167.7
1067	4.1	13.4	60.7	199	1102	10.9	35.8	49.5	162.3
1068	2.9	9.4	60.6	199	1103	10.2	33.5	48.2	158
1069	1.8	5.8	60.6	198.9	1104	9.6	31.6	47	154
1070	0.4	1.3	60.6	198.9	1105	8.8	28.9	45.2	148.4
1071	11.9	38.9	52.5	172.3	1106	8.4	27.7	44.2	144.9
1072	10.8	35.4	52.5	172.4	1107	7.6	24.9	42.6	139.7
1073	9.6	31.6	52.5	172.3	1108	7.1	23.4	41.2	135.2
1074	8.4	27.4	52.5	172.3	1109	6.5	21.3	39.8	130.6
1075	7.2	23.5	52.5	172.4	1110	6	19.7	38.4	126.1
1076	5.3	17.3	52.5	172.2	1111	5.5	18.2	37	121.5
1077	4.2	13.6	52.5	172.2	1112	5	16.2	35.8	117.6
1078	2.8	9.3	52.5	172.3	1113	4.3	14	34.3	112.5
1079	1.6	5.4	52.5	172.3	1114	3.6	11.9	32.9	107.8
1080	0.5	1.5	52.5	172.3	1115	2.9	9.6	31.5	103.3
1081	12	39.3	52.2	171.1	1156	0.4	1.1	32	104.9
1082	12	39.4	50.6	165.9	1157	0.3	1.1	33.4	109.5
1083	12	39.4	49	160.8	1158	0.3	1	35.1	115.2
1084	12	39.3	47.5	155.7	1159	0.3	1.1	36.3	119.2
1085	12	39.3	46.1	151.1	1160	0.4	1.2	38.1	124.9
1086	12	39.4	44.5	146	1177	11.4	37.5	31.6	103.7
1087	12	39.3	42.9	140.8	1178	9.5	31.2	31.7	103.9
1088	12	39.3	41.4	135.7	1179	7.9	25.8	31.6	103.8
1089	12	39.3	40	131.1	1180	6.7	21.9	31.6	103.8
1090	11.9	39.2	38.4	126					

Table A.4 - Foam depth measurement point coordinates for Runs 4 and 11 in Barn A, pump-out port C. See Figure 4.10for a schematic of these points and the origin defined.

Point	X		Y		Point	X		Y	
	(m)	*(ft)*	*(m)*	*(ft)*		*(m)*	*(ft)*	*(m)*	*(ft)*
1071	11.9	38.9	52.5	172.3	1112	5.0	16.2	35.8	117.6
1072	10.8	35.4	52.5	172.4	1113	4.3	14.0	34.3	112.5
1073	9.6	31.6	52.5	172.3	1114	3.6	11.9	32.9	107.8
1074	8.4	27.4	52.5	172.3	1115	2.9	9.6	31.5	103.3
1075	7.2	23.5	52.5	172.4	1181	11.4	37.3	59.6	195.6
1076	5.3	17.3	52.5	172.2	1182	7.4	24.2	59.6	195.6
1077	4.2	13.6	52.5	172.2	1183	5.0	16.4	59.7	195.7
1078	2.8	9.3	52.5	172.3	1184	0.9	2.9	59.6	195.5
1079	1.6	5.4	52.5	172.3	1185	1.0	3.2	56.5	185.3
1080	0.5	1.5	52.5	172.3	1186	5.0	16.3	56.5	185.3
1081	12.0	39.3	52.2	171.1	1187	7.4	24.2	56.5	185.4
1083	12.0	39.4	49.0	160.8	1188	11.5	37.6	56.5	185.3
1085	12.0	39.3	46.1	151.1	1189	5.0	16.3	50.3	164.9
1087	12.0	39.3	42.9	140.8	1190	1.0	3.3	50.3	164.9
1089	12.0	39.3	40.0	131.1	1191	0.9	3.0	47.3	155.2
1091	12.0	39.3	36.9	120.9	1192	4.9	16.2	47.3	155.2
1093	11.9	39.1	33.9	111.2	1193	5.0	16.4	44.2	144.9
1095	11.9	39.1	30.8	101.0	1194	0.9	2.9	44.2	144.9
1101	11.6	38.0	51.1	167.7	1195	0.8	2.6	41.2	135.1
1102	10.9	35.8	49.5	162.3	1196	5.0	16.2	41.2	135.2
1103	10.2	33.5	48.2	158.0	1197	7.1	23.3	35.1	115.3
1104	9.6	31.6	47.0	154.0	1157	0.3	1.1	33.4	109.5
1105	8.8	28.9	45.2	148.4	1159	0.3	1.1	36.3	119.2
1106	8.4	27.7	44.2	144.9	1160	0.4	1.2	38.1	124.9
1107	7.6	24.9	42.6	139.7	1177	11.4	37.5	31.6	103.7
1108	7.1	23.4	41.2	135.2	1178	9.5	31.2	31.7	103.9
1109	6.5	21.3	39.8	130.6	1179	7.9	25.8	31.6	103.8
1110	6.0	19.7	38.4	126.1	1180	6.7	21.9	31.6	103.8
1111	5.5	18.2	37.0	121.5					

Table A.5 - Foam depth measurement point coordinates for Runs 5 and 12 in Barn B, pump-out port B. See Figure 4.11 for a schematic of these points and the origin defined.

Point	X		Y		Point	X		Y	
	(m)	*(ft)*	*(m)*	*(ft)*		*(m)*	*(ft)*	*(m)*	*(ft)*
2001	11.5	37.8	59.9	196.4	2028	0.9	3.0	41.4	135.7
2002	7.3	23.8	59.8	196.1	2029	0.4	1.3	39.1	128.1
2003	4.9	16.2	59.8	196.2	2030	0.9	3.1	39.1	128.2
2004	0.9	3.0	59.8	196.3	2031	1.5	5.1	39.1	128.2
2005	0.9	3.1	56.3	184.8	2032	3.4	11.0	39.0	128.1
2006	5.0	16.4	56.3	184.6	2033	4.7	15.3	39.0	128.1
2007	7.3	23.9	56.3	184.7	2034	6.4	20.9	39.1	128.3
2008	11.4	37.3	56.3	184.7	2035	7.7	25.3	39.1	128.2
2009	11.3	37.1	53.3	175.0	2036	9.0	29.4	39.1	128.2
2010	7.3	23.9	53.4	175.0	2037	10.7	35.0	39.1	128.2
2011	4.9	16.2	53.3	175.0	2038	12.1	39.5	39.1	128.1
2012	0.9	3.0	53.4	175.2	2039	0.7	2.1	38.4	126.0
2013	0.8	2.8	50.3	164.9	2040	1.3	4.4	37.9	124.4
2014	4.9	16.0	50.0	164.1	2041	2.0	6.5	37.2	121.9
2015	7.4	24.2	50.2	164.8	2042	2.6	8.5	36.5	119.6
2016	11.4	37.5	50.2	164.7	2043	4.1	13.4	34.9	114.4
2017	11.4	37.3	47.3	155.1	2044	5.5	18.0	33.5	110.0
2018	7.3	24.0	47.3	155.0	2045	7.1	23.2	31.8	104.3
2019	5.0	16.4	47.3	155.2	2049	0.4	1.3	38.7	127.0
2020	0.9	2.9	47.3	155.1	2050	0.4	1.2	38.2	125.4
2021	0.8	2.7	44.3	145.3	2051	0.4	1.2	37.7	123.6
2022	5.0	16.4	44.3	145.4	2052	0.4	1.2	36.1	118.5
2023	7.3	24.1	44.3	145.3	2053	0.4	1.2	34.6	113.4
2024	11.4	37.4	44.3	145.3	2054	0.4	1.1	33.0	108.1
2025	11.3	37.2	41.4	135.7	2055	0.4	1.2	31.4	103.1
2026	7.4	24.2	41.4	135.7	2060	11.4	37.3	34.2	112.2
2027	5.0	16.2	41.3	135.6					

Table A.6 - Foam depth measurement point coordinates for Runs 6 and 13 in Barn B, pump-out port D. See Figure 4.12 for a schematic of these points and the origin defined.

Point	X		Y		Point	X		Y	
	(m)	*(ft)*	*(m)*	*(ft)*		*(m)*	*(ft)*	*(m)*	*(ft)*
2061	12.0	39.3	22.1	72.4	2087	5.4	17.6	14.6	47.8
2062	11.4	37.3	22.0	72.2	2088	3.8	12.5	13.1	43.0
2063	10.8	35.5	22.0	72.2	2089	2.2	7.3	11.6	38.0
2064	9.5	31.0	22.0	72.2	2090	0.7	2.1	10.2	33.4
2065	7.7	25.4	22.0	72.2	2091	1.6	5.2	17.1	56.2
2066	6.3	20.8	22.0	72.3	2092	6.8	22.4	10.9	35.7
2067	4.7	15.3	22.0	72.2	2093	11.4	37.2	7.8	25.6
2068	3.3	10.8	22.0	72.2	2094	7.4	24.2	7.8	25.4
2069	1.6	5.2	22.0	72.2	2095	5.0	16.3	7.7	25.4
2070	0.4	1.4	22.0	72.1	2096	0.9	3.1	7.7	25.3
2071	11.9	39.1	21.7	71.2	2097	0.9	3.1	4.6	15.1
2072	12.0	39.2	21.0	68.9	2098	4.9	16.2	4.6	15.1
2073	12.0	39.4	20.5	67.2	2099	7.3	24.0	4.6	15.2
2074	12.0	39.3	18.9	62.1	2100	11.4	37.2	4.7	15.3
2075	12.1	39.6	17.2	56.3	2101	11.4	37.4	1.5	5.0
2076	12.0	39.2	15.8	51.8	2102	7.4	24.4	1.5	4.9
2077	12.0	39.3	14.2	46.6	2103	5.0	16.4	1.5	4.8
2078	12.0	39.3	12.7	41.6	2104	1.0	3.2	1.5	4.8
2079	12.0	39.2	11.3	36.9	2046	8.5	27.8	30.2	99.0
2080	12.0	39.3	9.7	31.9	2047	10.0	32.9	28.6	94.0
2081	11.6	38.2	21.2	69.4	2048	11.6	38.1	26.9	88.3
2082	11.0	36.2	20.7	67.7	2056	0.4	1.2	29.9	97.9
2083	10.4	34.1	19.8	64.8	2057	0.4	1.1	28.5	93.5
2084	9.8	32.0	19.3	63.2	2058	0.4	1.1	27.2	89.3
2085	8.3	27.1	17.7	58.0	2059	5.6	18.3	27.2	89.3
2086	6.8	22.3	16.1	52.7					

Table A.7 - Foam depth measurement point coordinates for Run 7 in Barn C, pump-out port D. See Figure 4.13 for a schematic of these points and the origin defined.

Point	X		Y		Point	X		Y	
	(m)	*(ft)*	*(m)*	*(ft)*		*(m)*	*(ft)*	*(m)*	*(ft)*
6061	15.0	49.2	7.4	24.3	6113	8.9	29.2	13.5	44.2
6063	14.5	47.5	7.4	24.3	6115	7.6	25.0	14.7	48.2
6065	13.6	44.6	7.4	24.2	6117	5.9	19.4	16.4	53.9
6067	12.1	39.8	7.4	24.1	6120	3.7	12.0	19.2	63.0
6069	11.1	36.4	7.4	24.2	6142	14.5	47.5	27.8	91.0
6071	9.8	32.3	7.4	24.2	6143	9.0	29.4	27.8	91.1
6073	8.0	26.2	7.4	24.2	6144	6.4	20.9	27.7	91.0
6075	6.5	21.2	7.4	24.1	6145	0.9	2.9	27.8	91.0
6077	4.1	13.5	7.4	24.2	6146	0.8	2.6	24.5	80.2
6080	0.4	1.3	7.4	24.3	6147	6.4	20.9	24.5	80.2
6081	15.0	49.3	7.7	25.4	6148	8.9	29.3	24.5	80.3
6083	15.0	49.3	8.3	27.1	6149	14.5	47.6	24.5	80.2
6085	15.0	49.3	9.1	30.0	6150	6.4	21.0	21.1	69.2
6087	15.0	49.3	10.3	33.9	6151	0.8	2.7	21.1	69.3
6089	15.1	49.4	11.6	38.0	6152	11.4	37.4	17.8	58.5
6091	15.1	49.4	12.8	41.9	6153	6.4	21.0	11.6	37.9
6093	15.1	49.5	14.7	48.2	6154	0.9	2.9	11.6	37.9
6095	15.1	49.5	16.5	54.0	6155	14.5	47.4	5.0	16.3
6097	15.1	49.4	18.6	60.9	6156	9.0	29.5	4.9	16.2
6100	15.1	49.4	22.2	72.9	6157	6.4	21.0	4.9	16.1
6101	14.7	48.2	7.9	26.0	6158	0.9	2.8	5.0	16.2
6103	14.2	46.6	8.3	27.1	6159	0.9	2.8	1.6	5.4
6105	13.6	44.5	8.9	29.3	6160	6.4	21.0	1.6	5.3
6107	12.5	41.0	10.0	32.8	6161	9.0	29.4	1.6	5.3
6109	11.4	37.4	11.1	36.3	6162	14.5	47.6	1.6	5.4
6111	10.3	33.9	12.1	39.7					

Table A.8 - Foam depth measurement point coordinates for Run 10 in Barn A, pump-out port A. See Figure 4.14 for a schematic of these points and the origin defined.

Point	X		Y		Point	X		Y	
	(m)	*(ft)*	*(m)*	*(ft)*		*(m)*	*(ft)*	*(m)*	*(ft)*
1097	11.9	39.1	27.6	90.6	1161	0.8	2.6	9.7	31.9
1099	11.9	39.2	24.7	80.9	1162	1.4	4.7	11.1	36.5
1100	11.9	39.1	23.1	75.9	1163	2.0	6.7	12.5	41.0
1116	2.4	7.7	30.1	98.7	1164	2.8	9.2	13.9	45.7
1117	1.9	6.1	28.7	94.2	1165	4.0	13.1	15.5	50.8
1118	1.3	4.2	27.3	89.5	1166	4.2	13.7	16.7	54.7
1119	0.5	1.7	25.9	85.1	1167	4.9	16.1	18.1	59.3
1120	6.0	19.5	25.9	85.1	1168	5.5	18.0	19.5	63.8
1131	0.4	1.3	8.7	28.5	1169	5.9	19.3	20.7	67.9
1132	1.8	5.8	8.7	28.6	1170	6.7	22.1	22.1	72.5
1133	2.9	9.5	8.5	28.0	1171	7.4	24.3	23.5	77.0
1134	4.5	14.6	8.7	28.4	1172	8.2	26.8	24.9	81.7
1135	5.6	18.3	8.7	28.6	1173	8.8	29.0	26.3	86.1
1136	6.8	22.4	8.7	28.5	1174	9.8	32.3	26.9	88.2
1137	8.0	26.3	8.7	28.5	1175	10.2	33.4	28.9	94.7
1138	9.1	29.7	8.5	28.0	1176	10.9	35.8	30.4	99.8
1139	10.3	33.9	8.5	27.9	1198	3.3	10.9	23.0	75.4
1140	11.8	38.8	8.5	27.9	1199	9.5	31.1	19.8	65.0
1141	0.4	1.4	9.1	29.7	1200	11.5	37.7	16.8	55.2
1143	0.4	1.2	12.0	39.2	1201	7.3	23.9	16.9	55.3
1145	0.3	1.0	15.0	49.0	1202	11.4	37.4	12.5	41.0
1147	0.4	1.1	18.1	59.2	1203	7.3	24.0	12.5	41.0
1149	0.4	1.2	21.2	69.6	1204	11.4	37.4	3.3	10.8
1151	0.3	1.1	24.2	79.2	1205	7.3	24.1	3.3	10.9
1153	0.4	1.1	27.3	89.5	1206	5.0	16.4	3.3	10.9
1155	0.3	1.1	30.2	99.2	1207	1.0	3.2	3.3	10.9

Table A.9 - Foam depth measurement point coordinates for Run 14 in Barn C, pump-out port B. See Figure 4.15 for a schematic of these points and the origin defined.

Point	X		Y		Point	X		Y	
	(m)	*(ft)*	*(m)*	*(ft)*		*(m)*	*(ft)*	*(m)*	*(ft)*
6001	0.4	1.1	51.3	168.2	6051	5.3	17.4	46.4	152.1
6003	1.0	3.1	51.3	168.3	6053	6.5	21.3	44.8	147.0
6005	1.9	6.2	51.3	168.2	6055	8.3	27.1	43.1	141.3
6007	3.4	11.0	51.2	168.1	6057	10.2	33.3	41.2	135.1
6009	4.3	14.2	51.3	168.2	6121	14.6	47.7	56.8	186.4
6011	5.6	18.3	51.3	168.2	6122	9.0	29.4	56.8	186.4
6013	7.4	24.3	51.3	168.1	6123	6.4	21.0	56.8	186.4
6015	9.5	31.1	51.3	168.1	6124	0.8	2.6	56.8	186.5
6017	11.5	37.7	51.3	168.3	6125	0.8	2.5	53.7	176.2
6020	15.0	49.2	51.3	168.2	6126	6.4	21.0	53.7	176.1
6021	0.4	1.2	50.9	167.1	6127	9.0	29.4	53.7	176.1
6023	0.4	1.1	50.2	164.8	6128	14.5	47.6	53.7	176.2
6025	0.4	1.2	49.5	162.5	6129	14.7	48.3	47.1	154.5
6027	0.3	1.1	48.3	158.5	6130	9.0	29.4	47.1	154.5
6029	0.4	1.2	47.1	154.5	6131	3.9	12.9	40.8	134.0
6031	0.4	1.1	45.9	150.6	6132	9.0	29.5	37.5	123.1
6033	0.4	1.1	44.0	144.3	6133	14.5	47.6	37.5	123.1
6035	0.3	1.1	42.2	138.5	6134	14.6	47.9	34.2	112.2
6037	0.4	1.1	40.0	131.1	6135	8.9	29.3	34.2	112.2
6040	0.4	1.1	36.5	119.6	6136	6.4	21.0	34.2	112.1
6041	0.7	2.2	50.9	167.1	6137	0.8	2.8	34.2	112.2
6043	1.1	3.4	50.4	165.4	6138	0.8	2.8	30.9	101.3
6045	1.9	6.1	49.5	162.5	6139	6.4	21.0	30.9	101.4
6047	2.9	9.4	48.7	159.7	6140	9.0	29.4	30.9	101.4
6049	3.9	12.8	47.6	156.2	6141	14.6	47.8	30.9	101.4

Table A.10 - Foam depth measurement point coordinates for Run 15 in Barn A. See Figure 4.16 for a schematic of these points and the origin defined.

Point	X		Y		Point	X		Y		Point	X		Y		Point	X		Y	
	(m)	*(ft)*	*(m)*	*(ft)*		*(m)*	*(ft)*	*(m)*	*(ft)*		*(m)*	*(ft)*	*(m)*	*(ft)*		*(m)*	*(ft)*	*(m)*	*(ft)*
1301	7.2	23.6	29.1	95.3	1339	6.7	22.0	33.2	109.0	1377	0.4	1.1	38.4	126.1	1415	6.8	22.2	21.6	70.7
1302	7.5	24.6	29.1	95.3	1340	6.8	22.3	33.7	110.7	1378	2.9	9.6	41.4	135.8	1416	6.8	22.1	20.8	68.4
1303	7.9	25.8	29.1	95.3	1341	6.7	22.1	34.1	111.7	1379	1.7	5.7	44.4	145.5	1417	6.8	22.1	20.2	66.1
1304	8.1	26.5	29.0	95.3	1342	6.7	22.1	34.4	113.0	1380	0.36	1.1811	46.76	153.412	1418	6.8	22.2	19.5	63.9
1305	8.4	27.5	29.0	95.3	1343	6.7	22.1	34.8	114.1	1381	7.2	23.5	29.4	96.5	1419	6.8	22.2	18.8	61.6
1306	8.7	28.5	29.0	95.2	1344	6.7	22.0	35.1	115.2	1382	7.7	25.2	29.8	97.7	1420	6.8	22.2	18.1	59.3
1307	9.0	29.6	29.1	95.3	1345	6.7	22.0	35.5	116.4	1383	7.9	25.8	30.1	98.6	1421	6.8	22.2	17.4	57.1
1308	9.5	31.0	29.1	95.3	1346	6.7	22.0	35.8	117.5	1384	8.0	26.2	30.4	99.8	1422	6.8	22.2	16.7	54.7
1309	9.7	32.0	29.1	95.3	1347	6.7	22.1	36.2	118.7	1385	8.4	27.6	30.7	100.9	1423	6.8	22.1	16.0	52.5
1310	10.0	32.9	29.0	95.2	1348	6.8	22.3	36.5	119.8	1386	8.7	28.6	31.1	102.1	1424	6.7	22.0	15.1	49.6
1311	10.3	33.9	29.0	95.3	1349	6.8	22.1	36.9	121.0	1387	9.0	29.6	31.5	103.2	1425	6.8	22.1	14.5	47.4
1312	10.6	34.9	29.0	95.2	1350	6.7	22.1	37.2	122.0	1388	9.7	31.9	32.2	105.5	1426	6.7	22.1	13.8	45.1
1313	11.0	36.0	29.0	95.2	1351	6.7	22.0	37.6	123.2	1389	10.1	33.0	32.5	106.6	1427	6.8	22.2	13.0	42.7
1314	11.3	37.0	29.0	95.2	1352	6.7	22.0	37.9	124.4	1390	10.3	33.8	32.8	107.7	1428	6.8	22.2	12.4	40.6
1315	11.6	38.1	29.0	95.2	1353	6.8	22.1	38.2	125.4	1391	10.6	34.9	33.2	108.9	1429	6.8	22.2	11.7	38.2
1316	12.0	39.2	29.0	95.2	1354	6.8	22.2	38.6	126.5	1392	11.4	37.5	34.0	111.6	1430	6.8	22.2	11.0	36.0
1317	6.5	21.3	29.1	95.3	1355	6.7	22.1	38.9	127.8	1393	12.1	39.5	34.6	113.5	1431	6.8	22.2	10.3	33.7
1318	5.8	19.2	29.0	95.3	1356	6.8	22.1	39.3	128.9	1394	9.7	31.8	36.0	118.0	1432	6.8	22.2	9.6	31.4
1319	5.2	17.1	29.1	95.3	1357	6.8	22.2	39.8	130.6	1395	6.5	21.2	29.4	96.5	1433	12.0	39.2	9.5	31.3
1320	4.8	15.7	29.0	95.3	1358	6.8	22.2	40.2	131.7	1396	5.8	19.1	30.1	98.7	1434	9.6	31.6	13.9	45.6
1321	4.2	13.6	29.0	95.2	1359	6.8	22.1	40.5	132.9	1397	5.1	16.8	30.8	101.0	1435	11.9	38.9	17.9	58.6
1322	3.6	11.7	29.1	95.3	1360	6.8	22.1	40.8	134.0	1398	4.4	14.4	31.5	103.2	1436	9.5	31.1	19.8	65.0
1323	2.9	9.5	29.0	95.2	1361	6.8	22.2	41.2	135.1	1399	3.6	11.9	32.2	105.5	1437	0.4	1.3	9.6	31.3
1324	2.3	7.7	29.0	95.3	1362	6.8	22.2	41.6	136.3	1400	2.8	9.2	32.9	107.9	1438	2.8	9.2	13.9	45.6
1325	1.7	5.6	29.0	95.2	1363	6.7	22.1	41.9	137.4	1401	2.0	6.5	33.7	110.7	1439	0.4	1.3	16.9	55.3
1326	1.1	3.6	29.0	95.3	1364	6.8	22.1	42.2	138.6	1402	1.3	4.2	34.4	113.0	1440	2.9	9.5	19.8	65.0
1327	0.4	1.2	29.0	95.2	1365	6.8	22.3	42.6	139.8	1403	0.4	1.2	35.3	115.8	1441	7.9	25.8	28.0	91.8
1328	6.8	22.3	29.4	96.5	1366	6.8	22.2	43.0	140.9	1404	3.6	11.8	36.2	118.8	1442	9.1	29.7	26.8	87.9
1329	6.8	22.2	29.7	97.5	1367	6.8	22.2	43.3	142.1	1405	6.8	22.3	28.7	94.2	1443	10.3	33.9	25.5	83.8
1330	6.8	22.3	30.1	98.7	1368	6.8	22.2	44.0	144.4	1406	6.8	22.3	28.0	91.8	1444	11.3	37.0	24.7	80.9
1331	6.8	22.2	30.4	99.8	1369	6.8	22.3	44.7	146.6	1407	6.8	22.2	27.3	89.5	1445	12.0	39.2	23.8	78.0
1332	6.8	22.2	30.8	101.0	1370	6.8	22.3	45.4	148.9	1408	6.8	22.2	26.6	87.3	1446	8.9	29.1	22.3	73.0
1333	6.8	22.2	31.1	102.1	1371	6.8	22.2	46.1	151.2	1409	6.8	22.2	25.9	85.0	1447	5.7	18.7	28.0	91.8
1334	6.8	22.2	31.4	103.1	1372	6.8	22.1	46.8	153.4	1410	6.8	22.3	25.2	82.7	1448	4.2	13.6	26.8	87.8
1335	6.8	22.2	31.8	104.4	1373	11.9	39.1	46.8	153.4	1411	6.7	22.0	24.3	79.9	1449	2.8	9.0	25.6	83.9
1336	6.8	22.2	32.2	105.6	1374	10.6	34.9	44.3	145.4	1412	6.8	22.3	23.6	77.6	1450	1.7	5.6	24.7	81.0
1337	6.8	22.2	32.5	106.7	1375	9.5	31.0	41.4	135.7	1413	6.8	22.3	23.0	75.4	1451	0.3	1.1	23.6	77.5
1338	6.8	22.2	32.9	107.8	1376	12.0	39.3	38.4	126.0	1414	6.8	22.2	22.2	72.9	1452	3.5	11.4	22.1	72.5

Appendix B: Zone Radii and Area

Table B.1 – Measurement zone radii and areas for Runs 1 through 14.

Zone	Radius		Run 1 Area		Run 2 Area		Run 3 Area		Run 4 Area		Run 5 Area		Run 6 Area		Run 7 Area	
	(m)	(ft)	(m^2)	(ft^2)	(m^2)	(ft^2)	(m^2)	(ft^2)	(m^2)	(ft^2)	(m^2)	(ft^2)	(m^2)	(ft^2)	(m^2)	(ft^2)
1	1.0	3.3	1.6	16.9	1.6	16.9	1.6	16.9	1.6	16.9	1.6	16.9	1.6	16.9	1.6	16.9
2	3.0	9.8	12.6	135.2	12.6	135.3	12.6	135.3	12.6	135.3	12.6	135.3	12.6	135.1	12.6	135.2
3	5.0	16.4	25.1	270.5	25.1	270.5	25.1	270.5	25.1	270.5	25.1	270.5	25.1	270.3	25.1	270.5
4	7.0	23.0	37.7	405.8	37.7	405.8	37.7	405.7	37.7	405.7	37.7	405.8	37.7	405.8	37.7	405.6
5	9.0	29.5	48.8	525.3	49.8	536.1	48.8	525.4	48.8	525.4	49.4	531.9	49.1	528.7	44.7	481.0
6	11.0	36.1	51.4	553.3	52.7	567.1	51.4	553.1	51.4	553.1	52.1	560.6	51.7	556.4	47.7	513.6
7	13.0	42.7	51.4	553.3	52.4	563.9	51.4	553.7	51.4	553.7	51.9	559.0	51.6	556.0	53.7	577.5
8	15.0	49.2			34.4	369.8	33.6	361.3	33.6	361.3	34.0	365.7	33.7	363.2	59.4	639.9
9	17.0	55.8			27.8	299.0	27.8	299.1	27.8	299.1	27.8	299.1	27.8	299.0	48.8	525.2
10	19.0	62.3			26.8	288.7	26.8	288.7	26.8	288.7	26.8	288.7	26.8	288.7	36.3	390.4
11	21.0	68.9			26.3	282.6	26.2	282.2	26.2	282.2	26.3	282.6	26.3	282.6	34.9	375.5
12	23.0	75.5			19.5	210.4	21.6	233.0	21.6	233.0	20.7	222.7	21.4	230.0	27.8	299.3
13	25.0	82.0			4.8	51.3	6.5	69.9	6.5	69.9	5.5	59.6	6.1	65.3	15.4	166.0

Zone	Radius		Run 8 Area		Run 9 Area		Run 10 Area		Run 11 Area		Run 12 Area		Run 13 Area		Run 14 Area	
	(m)	(ft)	(m^2)	(ft^2)	(m^2)	(ft^2)	(m^2)	(ft^2)	(m^2)	(ft^2)	(m^2)	(ft^2)	(m^2)	(ft^2)	(m^2)	(ft^2)
1	1.0	3.3	1.6	16.9	1.6	16.9	1.6	16.9	1.6	16.9	1.6	16.9	1.6	16.9	1.6	16.9
2	3.0	9.8	12.6	135.3	12.6	135.3	12.6	135.3	12.6	135.3	12.6	135.3	12.6	135.1	12.6	135.2
3	5.0	16.4	25.1	270.5	25.1	270.5	25.1	270.5	25.1	270.5	25.1	270.5	25.1	270.3	25.1	270.5
4	7.0	23.0	37.7	405.8	37.7	405.7	37.7	405.8	37.7	405.7	37.7	405.8	37.7	405.8	37.6	404.4
5	9.0	29.5	49.8	536.1	48.8	525.4	49.8	536.1	48.8	525.4	49.4	531.9	49.1	528.7	41.9	450.6
6	11.0	36.1	52.7	567.1	51.4	553.1	52.7	567.1	51.4	553.1	52.1	560.6	51.7	556.4	46.5	500.8
7	13.0	42.7	52.4	563.9	51.4	553.7	52.4	563.9	51.4	553.7	51.9	559.0	51.6	556.0	52.3	563.1
8	15.0	49.2	34.4	369.8	33.6	361.3	34.4	369.8	33.6	361.3	34.0	365.7	33.7	363.2	58.3	627.8
9	17.0	55.8	27.8	299.0	27.8	299.1	27.8	299.0	27.8	299.1	27.8	299.1	27.8	299.0	47.6	512.4
10	19.0	62.3	26.8	288.7	26.8	288.7	26.8	288.7	26.8	288.7	26.8	288.7	26.8	288.7	36.7	394.8
11	21.0	68.9	26.3	282.6	26.2	282.2	26.3	282.6	26.2	282.2	26.3	282.6	26.3	282.6	34.9	375.5
12	23.0	75.5	19.5	210.4	21.6	233.0	19.5	210.4	21.6	233.0	20.7	222.7	21.4	230.0	31.3	337.2
13	25.0	82.0	4.8	51.3	6.5	69.9	4.8	51.3	6.5	69.9	5.5	59.6	6.1	65.3	20.1	216.9

Table B.2 – Measurement zone radii and areas for Run 15.

Zone	Radius		Run 1 Area	
	(m)	(ft)	(m^2)	(ft^2)
1	1.0	3.3	3.1	33.8
2	3.0	9.8	25.1	270.5
3	5.0	16.4	50.3	540.9
4	7.0	23.0	65.3	702.8
5	9.0	29.5	56.7	610.1
6	11.0	36.1	52.8	568.2
7	13.0	42.7	51.3	552.7
8	15.0	49.2	50.6	544.5
9	17.0	55.8	50.1	539.6
10	19.0	62.3	49.8	536.4
11	21.0	68.9	49.6	534.2
12	23.0	75.5	49.5	532.6
13	25.0	82.0	49.4	531.4
14	27.0	88.6	49.3	530.4
15	29.0	95.1	50.0	537.8
16	31.0	101.7	40.1	431.5

Appendix C: Supplementary Results Figures and Tables

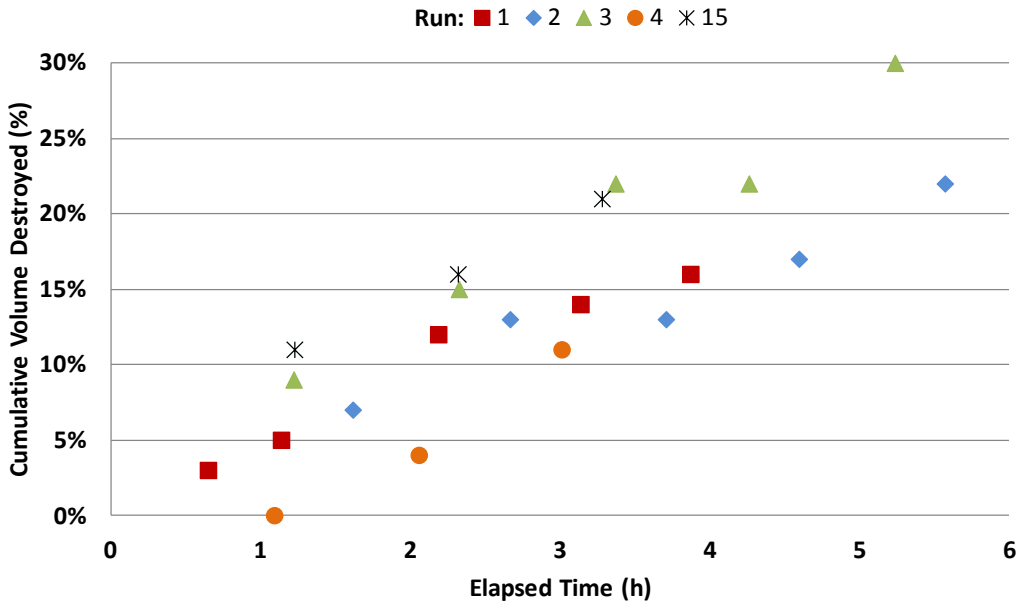

Figure C.1 - Cumulative percent of initial foam volume destroyed in Zone 3 over time elapsed since device start up for continuous runs in Barn A with initial foam depths >0.200 m (7.9 in). Runs 1 through 4 featured the device installed in a pump-out port, while in Run 15 the device was installed inside Barn A. Refer to Table C.7.

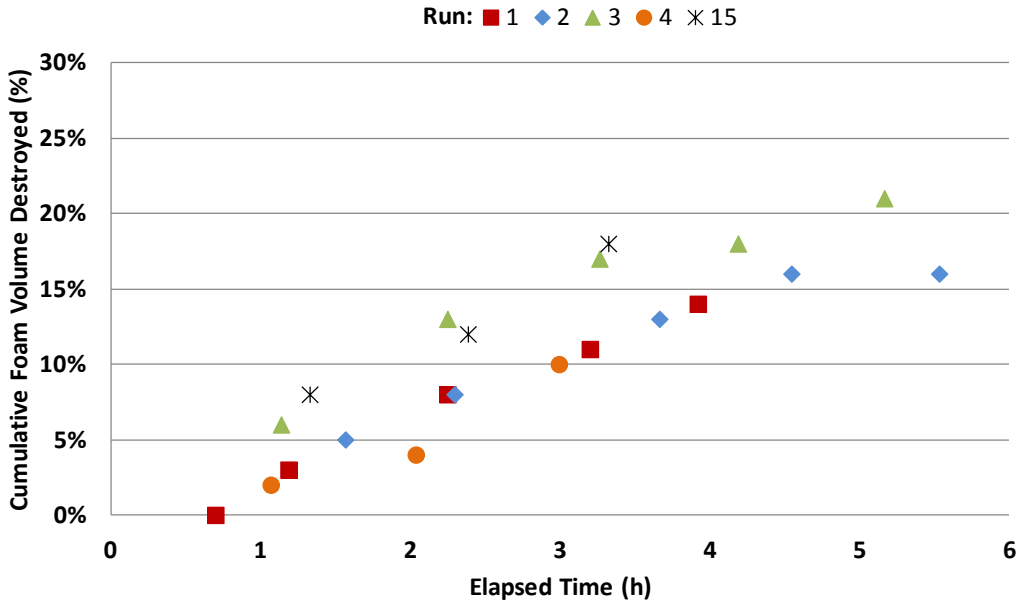

Figure C.2 - Cumulative percent of initial foam volume destroyed in Zone 6 over time elapsed since device start up for continuous runs in Barn A with initial foam depths >0.200 m (7.9 in). Runs 1 through 4 featured the device installed in a pump-out port, while in Run 15 the device was installed inside Barn A. Refer to Table C.8.

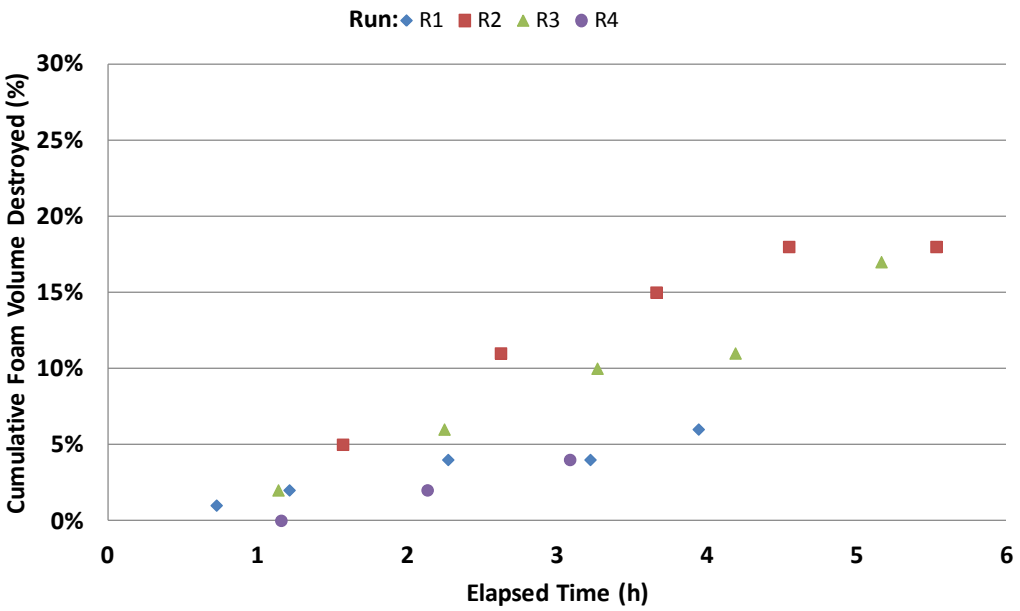

Figure C.3 - Cumulative percent of initial foam volume destroyed in Zone 7 over time elapsed since device start up for continuous runs in Barn A with initial foam depths >0.200 m (7.9 in). Runs 1 through 4 featured the device installed in a pump-out port, while in Run 15 the device was installed inside Barn A. Refer to Table C.9.

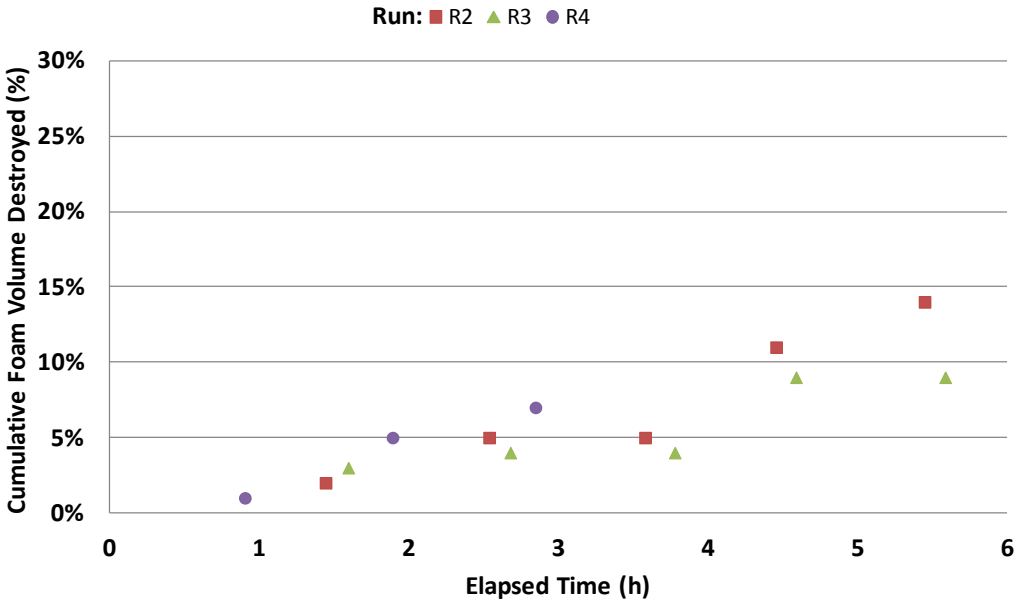

Figure C.4 - Cumulative percent of initial foam volume destroyed in Zone 12 over time elapsed since device start up for continuous runs in Barn A with initial foam depths >0.200 m (7.9 in). Runs 1 through 4 featured the device installed in a pump-out port, while in Run 15 the device was installed inside Barn A. Refer to Table C.10.

Table C.1 - Run 5 summary calculations. In this run the device was installed in pump-out port B of Barn B (Figure 4.2) and was operated continuously.

	t_e[1]	Δt_s[2]	$V_{f,s}$		Δd_s		$\Delta d_s / \Delta t_s$		ΔV_s			$\Delta V_s / \Delta t_s$ (sFDR)			sFDR / $d_{i,s}$		
	(h)	(h)	(m^3)	(f^3)	(m)	(f)	(m/h)	(f/h)	(m^3)	(f^3)	%	m^3/h	f^3/h	%/h	m^2/h	f^2/h	%/h-m
Time Series 1	1.2	1.2	34.34	1212.6	0.000	0.00	0.000	0.00	-0.11	-3.9	0%	-0.10	-3.4	0%	-1.04	-11.2	-3%
Time Series 2	2.1	1.0	33.62	1187.3	0.002	0.01	0.002	0.01	0.72	25.4	2%	0.74	26.3	2%	8.08	87.0	24%
Time Series 3[3]	3.0	0.9	34.34	1212.9	-0.002	-0.01			-0.72	-25.6	-2%						
Run 5 Summary								Mean	0.7[4]	25.4[4]	2%[4]	0.32	11.5	1%	3.52	37.9	10%
								SD				0.59	21.0	2%	6.45	69.4	19%
								Min				-0.10	-3.4	0%	-1.04	-11.2	-3%
								Max				0.74	26.3	2%	8.08	87.0	24%

[1] Time elapsed since device start up

[2] Series final mean device operation time minus series initial mean device operation time

[3] Time series 3 not used in run summary calculations

[4] Sum of column, negative values treated as zero when adding

Table C.2 - Run 6 summary calculations. In this run the device was installed in pump-out port D of Barn B (Figure 4.2) and was operated continuously.

	t_e[1]	Δt_s[2]	$V_{f,s}$		Δd_s		$\Delta d_s / \Delta t_s$		ΔV_s			$\Delta V_s / \Delta t_s$ (sFDR)			sFDR / $d_{i,s}$		
	(h)	(h)	(m^3)	(f^3)	(m)	(f)	(m/h)	(f/h)	(m^3)	(f^3)	%	m^3/h	f^3/h	%/h	m^2/h	f^2/h	%/h-m
Time Series 1	1.2	1.2	27.56	973.3	0.000	0.00	0.000	0.00	0.13	4.5	0%	0.11	3.9	0%	1.48	16.0	5%
Time Series 2	2.3	1.2	26.15	923.5	0.004	0.01	0.003	0.01	1.41	49.8	5%	1.19	42.0	4%	15.94	171.6	58%
Time Series 3[3]	3.6	1.3	25.84	912.6	0.001	0.00			0.31	10.9	1%						
Run 6 Summary								Mean	1.9[4]	65.2[4]	6%[4]	0.6	22.9	2%	8.71	93.8	32%
								SD				0.8	26.9	3%	10.23	110.1	37%
								Min				0.1	3.9	0%	1.48	16.0	5%
								Max				1.2	42.0	4%	15.94	171.6	58%

[1] Time elapsed since device start up

[2] Series final mean device operation time minus series initial mean device operation time

[3] Time series 3 not used in run summary calculations

[4] Sum of column

Table C.3 - Run 7 summary data. In this run the device was installed in pump-out port D of Barn C (Figure 4.2) and was operated continuously.

	t_e[1]	$V_{f,s}$		Δd_s		$\Delta d_s / \Delta t_s$		ΔV_s			$\Delta V_s / \Delta t_s$ (FDR)			FDR / $d_{i,s}$		
	(h)	(m^3)	(f^3)	(m)	(f)	(m/h)	(f/h)	(m^3)	(f^3)	%	m^3/h	f^3/h	%/h	m^2/h	f^2/h	%/h-m
Run 7	2.9	22.52	795.3	0.002	0.01	0.001	0.00	0.7	24.3	3%	0.24	8.5	1%	4.61	49.6	20%

[1] Time elapsed since device start up

Table C.4 - Run 12 summary calculations. In this run the device was installed in pump-out port B of Barn B (Figure 4.2) and operated on a duty cycle of 1 h on: 1 h off.

	t_e[1]	Δt_s[2]	$V_{f,s}$		Δd_s		$\Delta d_s / \Delta t_s$		ΔV_s			$\Delta V_s / \Delta t_s$ (sFDR)			sFDR / $d_{i,s}$		
	(h)	(h)	(m^3)	(f^3)	(m)	(f)	(m/h)	(f/h)	(m^3)	(f^3)	%	m^3/h	f^3/h	%/h	m^2/h	f^2/h	%/h-m
Time Series 1	0.8	0.8	35.70	1260.8	0.001	0.00	0.002	0.01	0.51	18.1	1%	0.60	21.3	2%	6.19	66.6	17%
Time Series 2[3]	3.2	1.3	34.23	1208.7	0.004	0.01			1.47	52.0	4%						
Run 12 Summary									2.0[4]	70.1[4]	5%[4]	0.60	21.3	2%	6.19	66.6	17%

[1] Time elapsed since device start up

[2] Series final mean device operation time minus series initial mean device operation time

[3] Time series 2 not used in run summary calculations

[4] Sum of column

Table C.5 - Run 13 summary calculations. In this run the device was installed in pump-out port D of Barn B (Figure 4.2) and operated on a duty cycle of 1 h on: 1 h off.

	t_e[1]	Δt_s[2]	$V_{f,s}$		Δd_s		$\Delta d_s / \Delta t_s$		ΔV_s			$\Delta V_s / \Delta t_s$ (sFDR)			sFDR / $d_{i,s}$		
	(h)	(h)	(m^3)	(f^3)	(m)	(f)	(m/h)	(f/h)	(m^3)	(f^3)	%	m^3/h	f^3/h	%/h	m^2/h	f^2/h	%/h-m
Time Series 1	1.0	1.0	25.99	918.0	0.000	0.00	0.000	0.00	-0.15	-5.3	-1%	-0.16	-5.5	-1%	-2.23	-24.0	-9%
Time Series 2[3]	3.8	1.0	26.17	924.1	0.000	0.00			-0.12	-4.1	0%						
Run 13 Summary									0[4]	0[4]	0[4]	-0.16	-5.5	-1%	-2.23	-24.0	-9%

[1] Time elapsed since device start up

[2] Series final mean device operation time minus series initial mean device operation time

[3] Time series 2 not used in run summary calculations

[4] Sum of column, negative values treated as zero

Table C.6 - Run 14 summary data. In this run the device was installed in pump-out port B of Barn C (Figure 4.2) and operated on a duty cycle of 1 h on: 1 h off.

	t_e[1]	t_{op}[2]	$V_{f,s}$		Δd_s		$\Delta d_s / \Delta t_s$		ΔV_s			$\Delta V_s / \Delta t_s$ (FDR)			FDR / $d_{i,s}$		
		(h)	(m^3)	(f^3)	(m)	(f)	(m/h)	(f/h)	(m^3)	(f^3)	%	m^3/h	f^3/h	%/h	m^2/h	f^2/h	%/h-m
Run 14	3.5	2.3	25.42	897.7	0.007	0.02	0.003	0.01	3.15	111.4	11%	1.39	49.1	5%	21.74	234.0	76%

[1] Time elapsed since device start up

[2] Total device operation time

Table C.7 - Cumulative percent foam volume destroyed in zone 3 for Runs 1 through 4 and Run 15. In these runs the device was operated continuously (Figure C.1). Runs 1 through 4 featured the device installed in a pump-out port in Barn A while Run 15 had the device installed inside Barn A.

		Time Series				
		1	2	3	4	5
R1	t_e (h)[1]	0.6	1.1	2.2	3.1	3.9
	ΔV %[2]	3%	5%	12%	14%	16%
R2	t_e (h)[1]	1.6	2.7	3.7	4.6	5.6
	ΔV %[2]	7%	13%	13%	17%	22%
R3	t_e (h)[1]	1.2	2.3	3.4	4.3	5.2
	ΔV %[2]	9%	15%	22%	22%	30%
R4	t_e (h)[1]	1.1	2.1	3.0		
	ΔV %[2]	0%	4%	11%		
R15	t_e (h)[1]	1.2	2.3	3.3		
	ΔV %[2]	11%	16%	21%		

[1] Time elapsed since start of run

[2] Cumulative percent initial volume destroyed

Table C.8 - Cumulative percent foam volume destroyed in zone 6 for Runs 1 through 4 and Run 15. In these runs the device was operated continuously (Figure C.2). Runs 1 through 4 featured the device installed in a pump-out port in Barn A while Run 15 had the device installed inside Barn A.

		Time Series				
		1	2	3	4	5
R1	t_e (h)[1]	0.7	1.2	2.2	3.2	3.9
	ΔV %[2]	0%	3%	8%	11%	14%
R2	t_e (h)[1]	1.6	2.3	3.7	4.5	5.5
	ΔV %[2]	5%	8%	13%	16%	16%
R3	t_e (h)[1]	1.1	2.2	3.3	4.2	5.2
	ΔV %[2]	6%	13%	17%	18%	21%
R4	t_e (h)[1]	1.1	2.0	3.0		
	ΔV %[2]	2%	4%	10%		
R15	t_e (h)[1]	1.3	2.4	3.3		
	ΔV %[2]	8%	12%	18%		

[1] Time elapsed since start of run

[2] Cumulative percent initial volume destroyed

Table C.9 - Cumulative percent foam volume destroyed in zone 7 for Runs 1 through 4 and Run 15. In these runs the device was operated continuously (Figure C.3Figure C.2). Runs 1 through 4 featured the device installed in a pump-out port in Barn A while Run 15 had the device installed inside Barn A.

		Time Series				
		1	2	3	4	5
R1	t_e (h)[1]	0.7	1.2	2.3	3.2	3.9
	ΔV %[2]	1%	1%	2%	0%	2%
R2	t_e (h)[1]	1.6	2.6	3.7	4.5	5.5
	ΔV %[2]	5%	6%	4%	3%	0%
R3	t_e (h)[1]	1.1	2.2	3.3	4.2	5.2
	ΔV %[2]	2%	4%	4%	1%	6%
R4	t_e (h)[1]	1.2	2.1	3.1		
	ΔV %[2]	0%	2%	2%		
R15	t_e (h)[1]					
	ΔV %[2]					

[1] Time elapsed since start of run

[2] Cumulative percent initial volume destroyed

Table C.10 - Cumulative percent foam volume destroyed in zone 12 for Runs 1 through 4 and Run 15. In these runs the device was operated continuously (Figure C.4Figure C.2). Runs 1 through 4 featured the device installed in a pump-out port in Barn A while Run 15 had the device installed inside Barn A.

		Time Series				
		1	2	3	4	5
R1	t_e (h)[1]					
	ΔV %[2]					
R2	t_e (h)[1]	1.4	2.5	3.6	4.5	5.5
	ΔV %[2]	2%	3%	0%	6%	3%
R3	t_e (h)[1]	1.6	2.7	3.8	4.6	5.6
	ΔV %[2]	3%	1%	0%	5%	0%
R4	t_e (h)[1]	0.9	1.9	2.8		
	ΔV %[2]	1%	4%	2%		
R15	t_e (h)[1]					
	ΔV %[2]					

[1] Time elapsed since start of run

[2] Cumulative percent initial volume destroyed